Implementation of Multi-Capillary Column-Ion Mobility Spectrometry (MCC-IMS) for Medical and Biological Applications

Zur Erlangung des akademischen Grades eines

Doctor rerum naturalium
(Dr. rer. nat.)

von der Fakultät Bio- und Chemieingenieurwesen
der Technischen Universität Dortmund

genehmigte Dissertation

vorgelegt von

M.Sc. Chandrasekhara B Hariharan

aus
Madurai, Indien

Tag der mündlichen Prüfung : 17th February 2012

1. Gutachter : PD Dr. Jörg Ingo Baumbach
2. Gutachter : Prof. Dr. Andreas Schmid

Dortmund, 2012

.... make things as simple as possible, but not simpler

- Albert Einstein

Acknowledgements

First and foremost, I would like to thank PD Dr. Jörg Ingo Baumabch for having provided me the opportunity to do my doctoral thesis at ISAS. I appreciate his constant guidance throughout this period. I would also like to thank my second examiner Prof.-Dr. Andreas Schmid for his ideas during the writing.

No words can express my gratitude to Dr. Wolfgang Vautz who had been guiding me at every step during this work. I take this opportunity to appreciate his constant availability, support and enthusiasm. I would like to thank the lab technicians Mrs. Stephanie Güssgen, Mrs. Susanne Krois and most importantly Mrs. Luzia Seifert for having helped me out with the experiments.

I take this opportunity to thank Dr. Glenn Spangler, who has accepted to study the quantum modeling of ion-neutral collisions after my talk at Thun, Switzerland. I am humbled by the fact that such a veteran readily accepted to remodel the ion-neutral collisions which has been standing for almost 30 years. I would also like to thank the fruitful discussions with Dr. Gary Eiceman and Dr. Herb Hill at the ISIMS conferences.

I would like to appreciate the support of my group colleagues Dr. Jürgen Nolte, Mrs. Rita Fobbe, Mr. Rolf Bandur, Sonja Vosbeck, Bertram Bödecker, Alexander Bunkowski and Rafael Slodzynski for their support and encouragement. I also appreciate Mr. Jürgen Lozynski and his team at the work shop for having helped me out with the instrumental constructions by understanding my poor German.

Special regards to Dr. Johnathan West, Dr. Jean-Phillipe Frimat, Dr. Brendan Holland, Ann-Katrin Stark, Dr. Joanna Stewart and most importantly to Anja Schmalfuss for their moral support over the last three years.

Last but not the least, I would like to thank my parents, brother and all my friends for their support and encouragement throughout this period.

Abstract

The complexity of samples measured and analysed with a Multi Capillary Column-Ion Mobility Spectrometer (MCC-IMS) has increased multi-fold since the advent of the 21st century. Even with its multiple advantages such as rapid separation, high resolution, reproducibility, femtomole sensitivity, etc. the MCC-IMS faced two major problems, namely; identification of a detected analyte from the output chromatogram and the peak clusters encountered when analysing these samples.

For the first time ever, a linear relation between the inverse reduced ion mobility and the number of carbon atoms seen within homologous series of compounds is used to predict the reduced ion mobilities of other compounds in the same series. The empirical prognosis of eighteen aliphatic compounds, later verified with measurements using a MCC-IMS, has an overall accuracy greater than 99.5 %. This innovative technique spares the need for the time consuming and costly reference measurements with other systems such as Gas chromatography-Mass Spectrometry (GC-MS), which are currently being employed to identify the detected compounds in an IMS chromatogram.

The regression equations obtained from the empirical prediction were then generalised into one reduced ion mobility equation and compared to the existing Mason-Schamp equation and also proved inconsistency in the 30 year old latter. To resolve the inconsistency, the single collision cross section term in the Mason-Schamp equation had to be split into two different terms namely; the mass dependent and the radical dependent cross sections. This modified Mason-Schamp equation can hence, completely describe the ion-neutral collisions that take place in a drift tube.

In the final part of this study, a novel drift is presented which enables variation in drift length due to a modular design. This resulted in a 40 % increase in the resolving power of individual peaks detected in an IMS chromatogram. Peak cluster formations usually encountered between medically important substances have been largely avoided with the new drift tube. This state of the art design for drift tubes aids in custom made IMS systems to suit every individual application. Furthermore, the fact that these drift tubes can be altered in length thereby providing a wide range of electric fields, opens up new research options in the realm of ion motions in an electric field.

Zusammenfassung

Die Komplexität der mittels Ionenmobilitätsspektrometern in Kopplung mit Multi-Kapillarsäulen analysierten Proben hat sich seit Beginn des 21. Jahrhunderts enorm erhöht. Trotz der zahlreichen Vorteile der Methode, wie die schnelle Trennung, die hohe Auflösung, die Empfindlichkeit im Femtomol-Bereich u.v.m., steht die MCC-IMS zwei grundlegenden Problemen gegenüber: zum einen der erforderlichen Identifikation eines detektierten Analyten aus dem gemessenen Chromatogramm und zum anderen der Clusterbildung, wie sie bei der Analyse derartiger Proben auftritt.

Erstmalig wurde in dieser Arbeit ein linearer Zusammenhang zwischen der inversen reduzierten Ionemobilität und der Anzahl der Kohlenstoffatome innerhalb einer homologen Reihe von Substanzen gezeigt und schließlich zur Vorhersage der reduzierten Ionenmobilität anderer Substanzen aus der gleichen Reihe genutzt. Die empirische Prognose, welche mit 18 aliphatischen Komponenten durchgeführt und mittels MCC-IMS Messungen validiert wurde, zeichnet sich durch eine sehr hohe Genauigkeit von über 99,5 % aus. Diese innovative Technik reduziert den Aufwand für zeitraubende und kostenintensive Referenzmessungen mittels anderer Methoden, wie der Gaschromatographie gekoppelt mit Massenspektrometrie, die derzeit verwendet wird um unbekannte Signale im IMS Chromatogramm zu identifizieren, signifikant.

Die aus der empirischen Vorhersage entwickelten Regressionsgleichungen wurden anschließend generalisiert in eine einzige Gleichung für die reduzierte Ionenmobilität, die dann mit der herkömmlichen Mason-Schamp-Gleichung verglichen wurde. Dabei zeigten sich Unstimmigkeiten in dieser 30 Jahre alten Gleichung. Um diese aufzulösen wurde der den Stoßquerschnitt beschreibende Term in zwei unterschiedliche, die Massen- und die Radikalabhängigkeit beschreibende Terme, aufgespalten. Die derart modifizierte Mason-Schamp-Gleichung beschreibt nun die in der Driftstrecke stattfindenden Stöße zwischen geladenen und ungeladenen Molekülen vollständig.

Im abschließenden Kapitel dieser Studie wird eine neuartige Driftstrecke vorgestellt, deren modularer Aufbau eine Variation der Länge erlaubt. Damit konnte die Auflösung der mittels IMS detektierten Signale um bis zu 40 % gesteigert werden. Zudem konnte die Clusterbildung in der Driftstrecke, beispielsweise bei medizinisch relevanten Substanzen, weitgehend vermieden werden. Dieses moderne Design erleichtert die maßgeschneiderte Anpassung von IMS-Systemen an die jeweilige individuelle Anwendung. Dies wird noch dadurch verstärkt, dass neben einer Variation der Länge der

Driftstrecke auch die Driftspannung innerhalb eines sehr großen Bereichs eingestellt werden kann, was neue Forschungsoptionen bezüglich der Bewegung von Ionen im elektrischen Feld erschließt.

Contents

Chapter 1

Introduction

Over the past few decades, Ion Mobility Spectrometry has evolved into an inexpensive and powerful analytical technique for the detection of gas phase samples in the lower ng·L^{-1} (ppb$_v$) down to pg·L^{-1} (ppt$_v$) levels at ambient pressures and temperatures. This instrument was initially used by the military establishments of the U.S.A and the United Kingdom to detect human activities in the jungles of Vietnam. In the late 1970s and early 1980s, several research and development programmes were started at universities, government organisations and small companies with the IMS to develop the instrumentation of this analytical device which proved attractive with its advantages such as lower detection limits, ruggedness, reasonable selectivity and the potential for miniaturisation [1].The first uses of the Ion Mobility Spectrometer (IMS) were to detect specific compound classes such as chemical warfare agents and drugs of abuse and in process control [1], [2]. This analytical instrument came in with many advantages including high sensitivity, rapid separation, reproducibility, information density, relatively low technical costs, ruggedness and ability to operate at normal temperature and pressure conditions. Chapter 2 in this thesis describes the working principle and the construction of a Multi Capillary Column-Ion Mobility Spectrometer. It elucidates the functionality of the various parts of the instrument and the science behind reactant and product ion formation.

Till the end of the twentieth century, IMS was used to detect specific target analytes like drugs, alcohol or explosives with known reduced ion mobility. However, in recent years, the instrument is increasingly in demand for new applications specifically on biological samples (cells, fungi, bacteria) [3–12], in medicine (diagnosis, therapy and medication control e.g. from breath analysis) [13–22]. For the analysis of these complex mixtures, the ion mobility alone will not be sufficient for the identification of analytes in the mixture. Several analytes have similar or even the same mobility.

Therefore, additional rapid pre-separation techniques like Gas Chromatography (GC) or Multi-Capillary Column (MCC) are applied. Ergo, for every analyte, there is a specific ion mobility value and the time it takes to elute out from the pre-separation column, known as the retention time, which are the characteristics of the particular analyte at a specific temperature, pressure, column length, polarity and flow rate. Providing this database of relevant analytes for every analysis enables the identification of compounds in a sample.

During the analysis of complex sample matrices, e.g. human breath, volatile organic compounds from bacteria, fungi etc., there are many unknown peaks in the IMS chromatogram due to the voluminous amount of substances in the sample matrix . Identifying all the detected substances is one of the major problems. There are a huge number of possible analytes emanating from these matrices which could be the detected peak in the chromatogram. Measuring each and every possible substance as a reference and probing to identify the detected analyte is a very time consuming process. Most applicable solution is the additional sampling on adsorption materials and analysis by Gas chromatography/Mass Spectrometry (GC/MS). From such analysis, substances possibly responsible for the unknown signals could be proposed. This proposal has to be validated by IMS measurements of the reference analyte. Obviously, such a procedure is time consuming and expensive as well. Thus, additional tools for the identification of unknown analytes would be very helpful. There have been earlier attempts to calculate the ion mobility of analytes directly from the molecular structure using computational neural networks and multiple linear regression analysis [23], [24]. But, these methods are seemingly complex, lack accuracy, require a comprehensive database for the calculations, extensive modeling and validation of the ion structure resulting in an assumed ion mobility value and hence cannot be used for online characterisation of complex mixtures.

In this study, a new, simple and a very accurate method to see trends within the homologous series of polar aliphatic compounds between the ion mobility and the number of carbon atoms in the analyte is used to predict the ion mobilities of other unmeasured analytes in that particular homologous series directly. Chapter 3 presents the linear trend seen in homologous series namely, primary alcohols, secondary alcohols, primary aldehydes and ketones and the empirical prediction and the verification of the prognosis accuracy.

To analyse the science behind the empirical predicion, in Chapter 4, a generalised ion mobility equation for polar aliphatic organic compounds is empirically derived from the different series of compounds analysed in Chapter 3 and its validity is discussed by comparing with the existing mathematical Mason-Schamp equation for ion mobility and the various models describing it.

With increasing complexity of the sample matrices, the number of substances detected by the IMS increases and hence the chances that two or more substances having very close retention times through pre-separation and ion mobilities, thus resulting in peak clusters on the output chromatogram, are high. Under these conditions, identification and quantification of individual peaks can be very difficult and sometimes even impossible. An optimised change in the instrument was necessary to increase the resolution without changing any other influential parameters or the reference database. Chapter 5 describes how this problem of peak clusters was solved by designing and constructing a novel and optimised drift tube which could be useful in laboratorial as well as clinical conditions to negate peak clusters.

In short, the two major problems that the Ion Mobility Spectrometer encounters in medical and biological applications, namely, the inability to identify unknown peaks in a complex and humid sample matrix directly and the peak clusters encountered during these measurements have been addressed in this study and the results are concisely summarised and discussed in Chapter 6.

Chapter 2

Ion Mobility Spectrometry

The science of ion formation in ambient air has been known since the end of the nineteenth century [25]. In the early twentieth century, Paul Langevin, a famous physicist, studied the motion of ions in an electric field [26], [27]. These results later proved to be the governing principles of Ion Mobility Spectrometry. The instrumentation, however, took almost 70 years to be first developed under the name of Plasma Chromatography, a gas phase electrophoretic analytic technique [2], [28]. In this section, the underlining principles involved in ion motion in an electric field, the various components involved in an ion mobility spectrometer along with the theory of ion formation in gases, ion mobility at molecular level and the various ion models used to describe the motion are elucidated. This chapter also describes the IMS settings employed with the various data acquisition and analysis softwares used in this study.

2.1   Principle of Ion Mobility Spectrometry

The working principle of an Ion Mobility Spectrometer (IMS) is based on the distinct velocities attained by accelerating ions in an electric field. Depending on their mass and/or structure different ions, in a swarm, reach different velocities under the influence of a constant electric field in a counter-flowing neutral drift gas [1]. Ion acceleration, along with permanent collisions between the ions in the swarm and neutral gas molecules, leads to an average ion velocity over a certain path length [29]. The average velocity attained by the accelerating ions (v_D) over the drift length (l_D) is determined by the number of collisions made by the ion swarm with the neutral drift gas and, in homogeneous low field strengths, it is directly proportional to the electric field strength E (V·cm^{-1}). The constant of proportionality is defined as the ion mobility K [1], [30].

The time spent by an ion swarm "drifting" along the drift tube is known as the drift time t_D.

$$v_D \ \propto \ E \tag{2.1}$$

$$v_D = K \cdot E \tag{2.2}$$

In equation 2.2, K, a combined property of the ion and the drift gas, is represented in $cm^2 \cdot V^{-1} \cdot s^{-1}$. Since the drift velocity is the ratio between the drift length(l_D) and drift time (t_D); the electric field is the voltage applied (V) across the drift length, Equation 2.2 can be rewritten as,

$$\frac{l_D^2}{t_D} = K \cdot V \tag{2.3}$$

This ion mobility value is a function of the gas density and therefore is usually normalized to the standard gas density of 2.687 x 10^{19} molecules·cm^{-3} at standard temperature, T_0 (273 K), and pressure, P_0 (101325 Pascal), conditions and is reported as the reduced ion mobility, K_0 ($cm^2 \cdot V^{-1} \cdot s^{-1}$) [30], [29].

$$K_0 = K \left(\frac{P}{P_0} \right) \left(\frac{T_0}{T} \right) \tag{2.4}$$

In equation 2.4, P and T are the actual pressure and temperature values during the measurement.

The measured drift time is used to calculate the reduced mobility K_0 as per equation 2.4. Since the drift time, the measured parameter, is inversely proportional to the mobility, K (equation 2.3), implying;

$$t_D \propto \frac{1}{K_0} \tag{2.5}$$

Hence, $1/K_0$ in V·s·cm^{-2} is used as the reporting value for ion mobilities during the visualization and correlation of IMS spectra.

2.2   Components of the state of the art MCC/IMS

A basic IMS consists of a sample inlet system, an ionization source, a reaction region, an ion gate, a drift region and an ion collector. Additionally, a voltage supply is necessary to create the electric field. Furthermore, a shutter controller, clean sources of carrier and drift gases, temperature and pressure sensors, fast electrometers and a data acquisition and analysis system are required for its complete functioning. Besides these components, the IMS may also be coupled to a gas chromatographic column (GC) or a multi-capillary column (MCC) to pre-separate complex and humid sample mixtures before it enters the drift tube [30].
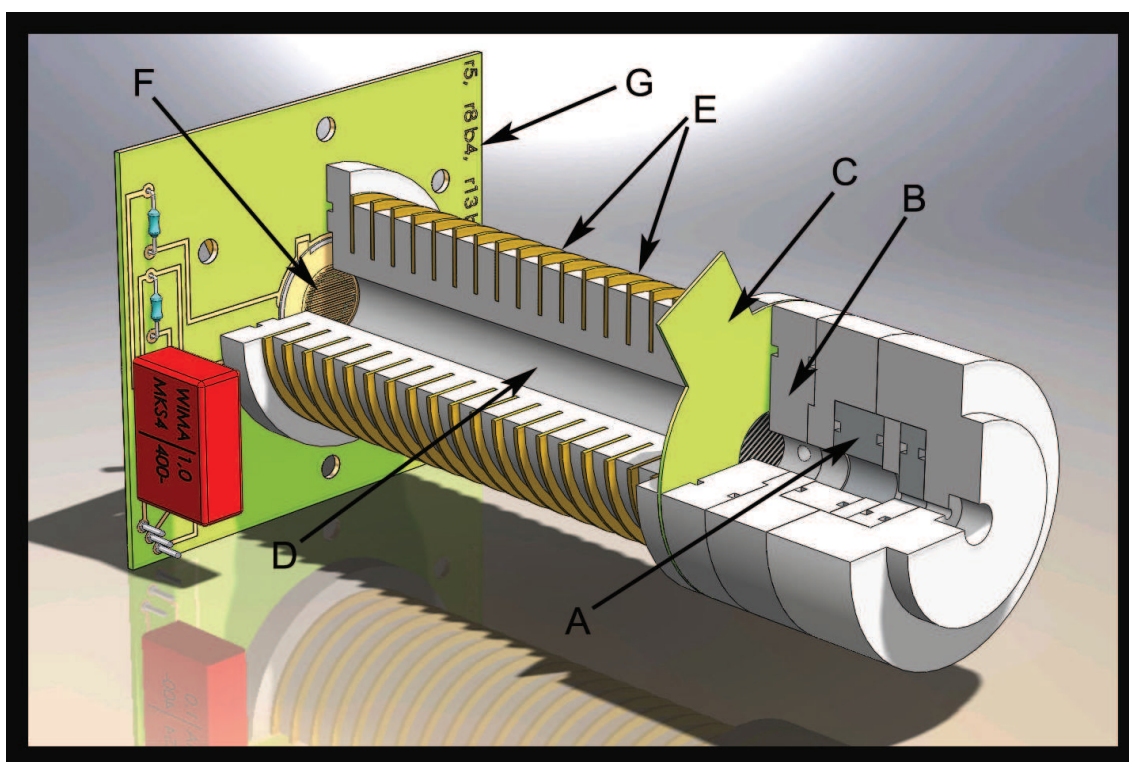

Figure 2.1: Three dimensional illustration of an ion mobility spectrometer. A - ionization source, B - ionization region, C - shutter grid, D - drift region, E - drift rings, F - aperture grid, G - Faraday plate

2.2.1   Sample inlet systems

Depending on the physical state and volatility of the sample, analytical chemists have followed several techniques for introducing sample into the IMS. These include sample wire probe [31], syringe injection [32], exponential dilution flasks [33], permeation

tubes [34], diffusion tubes [35], thermal desorption techniques [36], laser desorption [37] and suction of ambient/sample air into the instrument either directly or using an membrane inlet [38], [30].

2.2.1.1 Gas Calibration System - HOVACAL

At the ISAS labs, a new gas calibration system, HOVACAL (HovaCAL 3834SP-VOC, IAS, Frankfurt, Germany) is used to provide calibration gases of known liquid samples at specific concentrations. Vautz *et al.* have published the complete details of its functioning to provide vapour samples in ppb_v and ppt_v concentrations and is shown in Figure 2.2 [39]. For analysis of human breath, sampling is done under human control or automated control with sensors [15].
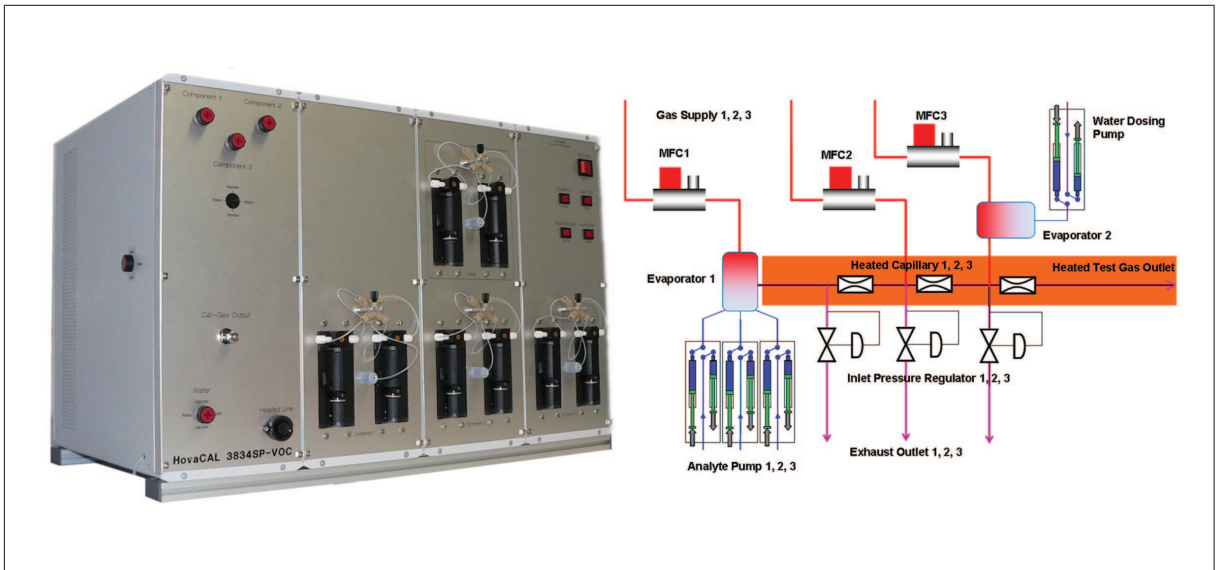

Figure 2.2: Photograph and the flowchart describing the functioning of the calibration gas system [39]

2.2.1.2 Pre-separation system

Complex volatiles, which are usually the samples measured with the IMS, are pre-separated using a gas chromatographic column (GC) before entering the IMS. In this study, a Multi Capillary Column (MCC), which is an altered GC, is used. This column was purchased from Multichrom, Novosibirsk, Russia. The MCC consists of a bundle of approximately 1000 quartz capillaries, coated with 95 % dimethylpolysiloxane and 5 % diphenyl, Figure 2.3. The length of the column is commonly 20 cm and is usually

maintained at a constant elevated temperature with an electronic heating device to obtain concordant values. The time taken for a substance to elute out from the MCC is hence termed as the retention time (R_T). The advantage of using such a multi-capillary column in place of a GC is the allowability to use higher flow rates (upto 200 mL·min^{-1}). This aids in faster pre-separation times (around 10 minutes) combined with higher sensitivity and humidity separation.

When pre-separation techniques are used to couple a MCC with the IMS, a carrier gas is required to transport the sample gas into the pre-separation system. A six port valve, figure 2.4 is used to regulate the inlet of the sample from a sample loop (8 mL in volume). The sample loop, made out of Teflon or stainless steel, is maintained at an elevated temperature like the MCC to avoid condensation of the sample.

2.2.2   Ionization and drift regions

The drift tube in an IMS is spatially divided into two sections, the ionization/reaction region and the drift region. The ionization region is the area where the sample molecules enter the IMS to be ionized. After ionization, the ionized molecules, as swarms move into the drift region where they drift along and reach a constant velocity due to the acceleration by the surrounding electric field countered by the deceleration due to collisions with the neutral gas molecules and thus get separated and detected. Though classically, the regions in a drift tube are divided into the two main sections, ionization and ion drift occurs all over the drift tube. These effects are very weak and are hence negligible.

2.2.3   Ionization sources

One of the earliest and the most common source of ionization in the IMS is the use of radioactive ^{63}Ni [2], [28]. ^{63}Ni emits β particles with average energies of 6.7 x 10^4 eV [40] and a half life of 85 years [29]. The advantage of using ^{63}Ni is the low particle energy, production of small number of ion pairs per disintegration thereby minimizing fluctuations in ion current and hence noise levels. It also has the advantage of high temperature operational stability (400 °C) [30].
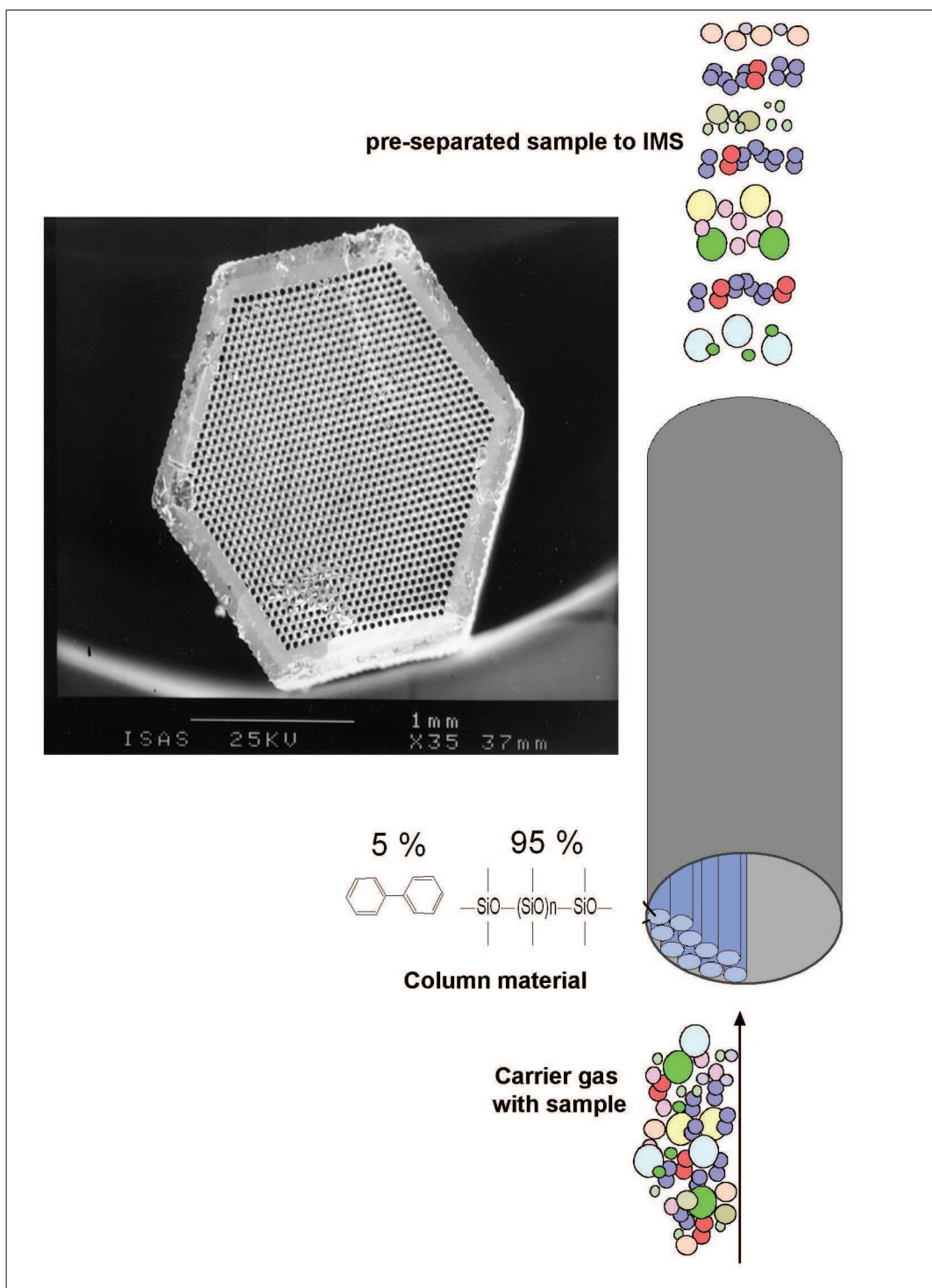
Figure 2.3: Schematic representation of a Multi-capillary Column as a pre-separation system optionally coupled with an IMS. The photograph on the left shows the cross section of the Multi-capillary Column (MCC) viewed through a microscope. Each 'hole' seen in the hexagonal cross section is a capillary

Figure 2.4: Schematic representation of the two positions which a 6 port valve may assume. The loading position is A and position B charges the column with the sample [21].

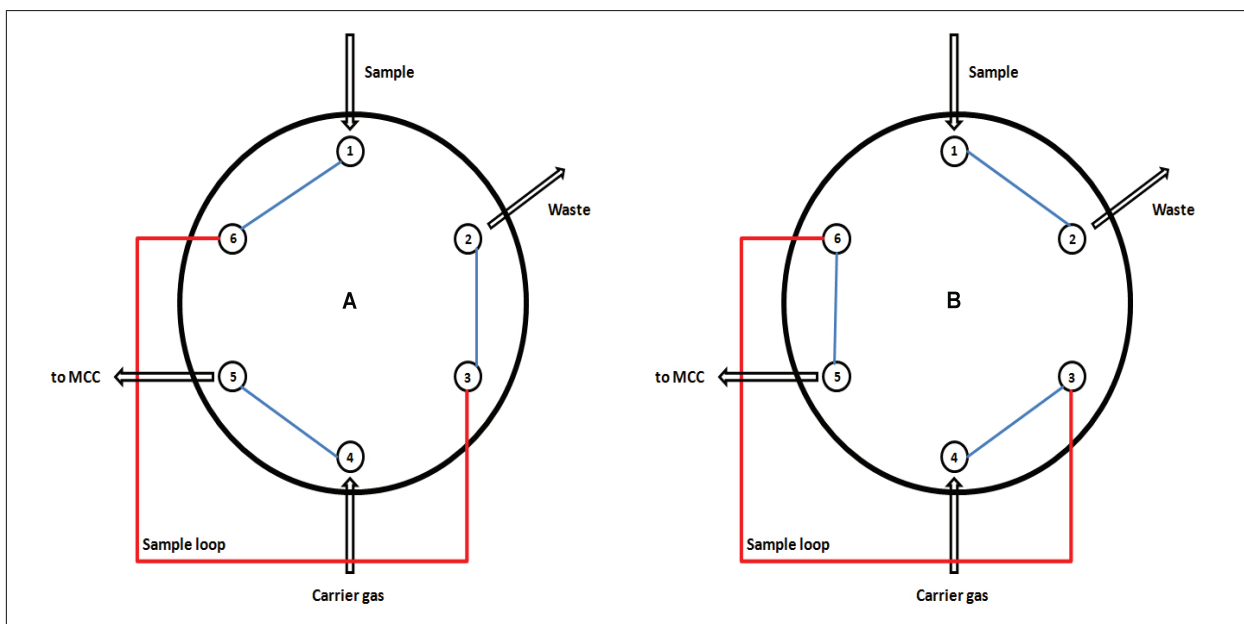Depending on the physical state of the sample matrix, there are other sources of ionization. They include; radioactive sources like ^{272}Am (α particles), ^{3}T (β particles), discharge sources like corona, plasma, dielectric barrier, pulsed corona discharges, photo ionization sources like UV lamps, lasers, MALDI, hollow cathode, electro spray ionization, pneumatic sources like sonic spray ionization and desorption sonic spray ionization, paper spray ionization, surface ionization techniques and penning ionization techniques like DART (Direct analysis in real time).

2.2.4   Ion gates

The ion gate is the part of the IMS which allows the ion swarm into the drift region. There are two different systems of ion gates, The Bradbury-Nielson gate and the Tyndall gate. Both the techniques involve creating an electric field between the fine wires strung across the drift tube. The gates are opened by removing the gate field, thus allowing the wires to assume the potential of their location in the drift field [30].

In the Bradbury-Nielson gate, which is the most common one and used in the IMS for this study, the ions are passed in a single plane of the drift field. The gate consists of a single grid of widely spaced wire, alternate wires being biased positive and negative to the gates' reference voltage, creating an orthogonal gate field to the drift field [41]. The gate field is usually three times the drift field, directing the ions into the wires where they are neutralized [30].

The Tyndall gate on the other hand consists of two independent wire grids separated by a minimal distance ($\approx$ 1 cm) composed of finely spaced wires. The gate is closed by applying a voltage across the grids which reverses the drift field in the vicinity of the gates [42], [30].

2.2.5   Drift field

Ions entering the drift region through the ion gate are directed towards the detector by an electric field created by the voltage difference between a repeller plate and the grounded collector. This electric field is maintained and protected from other stray fields by enclosing the drift region within a cylindrical tube (in this study, Teflon tube) composed of identical, equally spaced brass guard rings. Voltages suitable to the rings' position within the field are applied by soldering a string of resistors (1 MΩ), connected

in series down the length of the tube.

Uniformity in such systems has been previously studied [31]. The field uniformity is a function of c/h, where c is the inner radius of the guard ring and h is the distance between the centers of the gaps of successive rings. Field uniformity can be improved by increasing the value of c/h (c/h of the IMS used in this study is 3) [30].

2.2.6 Aperture grid

To maintain the spectral resolution in single-scan or single averaged spectral collection, an aperture grid must be placed approximately 1 mm prior to the ion collector (in this study, a Faraday plate) [30], [29]. This provides a capacitive decoupling between the arriving ions and the detector. Without the aperture grid, the ion swarm is coulombicly felt by the collector several millimeters prior to its arrival resulting in decreased signal intensity and peak broadening hence spectral resolution.
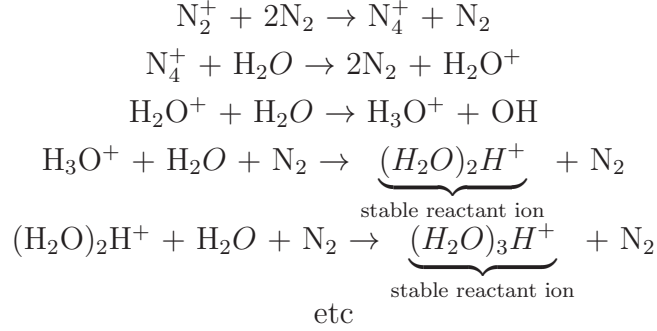
2.3 Ion formation

The ions formed in an IMS depends on the ionization technique used during the measurement. Since ^{63}Ni is used in this study, this section deals in detail about the chemistry of formation of reactant and product ions when radioactive ^{63}Ni is used as an ionization source.

2.3.1 Formation of Reactant ions

The drift gas circulating in the IMS, in our study synthetic air (20.5 % O_2, 79.4 % N_2 and < 2 ppb$_v$ water), is responsible for the formation of the reactant ions. The β particles in ^{63}Ni lose energy during collisions with the drift gas. The average energy released per collision is 35 eV. Nitrogen ionizes as long as the energy of the radiation is higher than 15.58 eV [43].

$$N_2 + \beta \rightarrow N_2^+ + \beta' + e^-$$

This β' is a β particle of reduced energy following the reaction and the e^- is the electron produced upon ionization of N_2. The N_2^+ initiates a chain of reactions leading to the formation of the positive reactant ion species.

$$N_2^+ + 2N_2 \rightarrow N_4^+ + N_2$$
$$N_4^+ + H_2O \rightarrow 2N_2 + H_2O^+$$
$$H_2O^+ + H_2O \rightarrow H_3O^+ + OH$$
$$H_3O^+ + H_2O + N_2 \rightarrow \underbrace{(H_2O)_2H^+}_{\text{stable reactant ion}} + N_2$$
$$(H_2O)_2H^+ + H_2O + N_2 \rightarrow \underbrace{(H_2O)_3H^+}_{\text{stable reactant ion}} + N_2$$
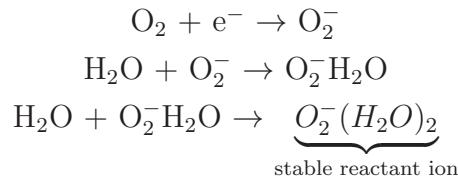$$\text{etc}$$

There are other possible product ions like $(H_2O)_yNO^+$ and $(H_2O)_xNH_4^+$ [44], [29]. But at the flow rates under 1400 mL/min, $(H_2O)_xH^+$ predominates [30]. The number of water clusters, x, in the reactant ion, $(H_2O)_xH^+$, is a function of the temperature and partial pressure of water in the gas.

In the negative mode, high energy electrons from ^{63}Ni are rapidly thermalized at ambient pressure conditions through,

$$N_2 + \beta \rightarrow N_2^+ + \beta' + e^-$$
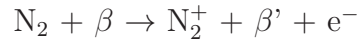
In pure nitrogen, or other inert gases, these electrons are the reactive species for ionizing the sample and can be observed as free electrons in the mobility spectrum [1]. When air is used as the surrounding gas, these electrons attach to oxygen and hydrate through the following reactions [45], [46],

$$O_2 + e^- \rightarrow O_2^-$$
$$H_2O + O_2^- \rightarrow O_2^-H_2O$$
$$H_2O + O_2^-H_2O \rightarrow \underbrace{O_2^-(H_2O)_2}_{\text{stable reactant ion}}$$

The number of water molecules which define a stable reactant ion is dependent on the ambient pressure and temperature conditions. Traces of $(H_2O)OH^-$, Cl^-, NO_2^-, CO_4^- and CN^- though, have also been identified depending on the gas and its purity used during the measurements [47].
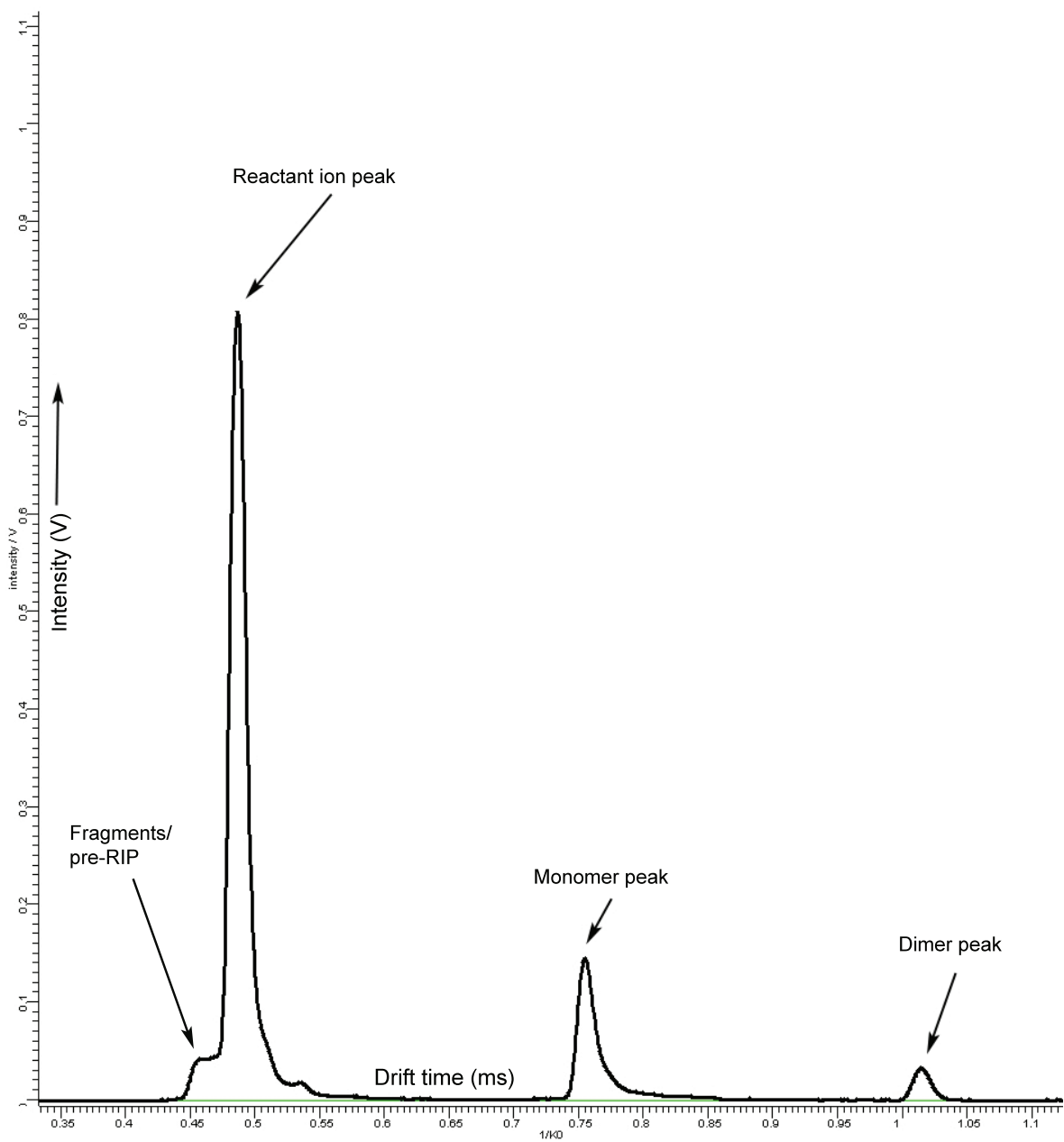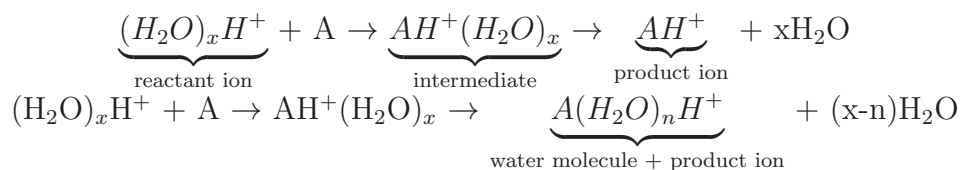
Figure 2.5: IMS spectrum showing the reactant ion peak (RIP), fragment peak (pre-RIP) along with a monomer peak and a dimer peak of an introduced sample in positive ionization mode with synthetic air.
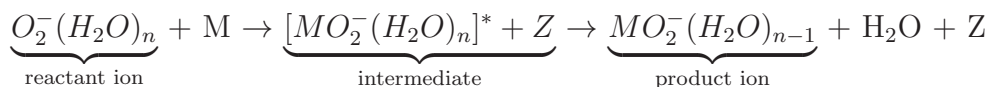
2.3.2 Formation of Product ions

The formation of product ions from the reactant ions is based on proton transfer and depends on the proton affinity of the substance to be ionized. These proton transfer reactions can only occur if the proton affinity of the molecules to be ionized (A) areis greater than the reactant ion (in this study, water).

$$\underbrace{(H_2O)_xH^+}_{\text{reactant ion}} + \text{A} \rightarrow \underbrace{AH^+(H_2O)_x}_{\text{intermediate}} \rightarrow \underbrace{AH^+}_{\text{product ion}} + \text{xH}_2\text{O}$$

$$(H_2O)_x\text{H}^+ + \text{A} \rightarrow AH^+(H_2O)_x \rightarrow \underbrace{A(H_2O)_nH^+}_{\text{water molecule + product ion}} + \text{(x-n)H}_2\text{O}$$

Since the proton affinity of water is relatively low (7.22 eV) [48], the positive reactant ions of water ionizes almost all possible organic compound classes. These include alkenes, alcohols, ethers, aldehydes, ketones, carboxylic acids, esters, thiols, sulfides, nitriles, amines etc. When the concentration of the sample substance is high dimerization and in some cases trimerization also occurs as follows [1].

$$\underbrace{A(H_2O)_xH^+}_{\text{monomer}} + \text{A} \rightarrow \underbrace{A_2(H_2O)_nH^+}_{\text{dimer ion}} + \text{(x-n)H}_2\text{O}$$
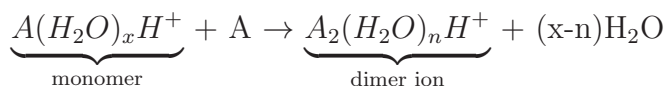
The formation of product ions in negative polarity occurs by the formation of an adduct in the first step [1], [49],

$$\underbrace{O_2^-(H_2O)_n}_{\text{reactant ion}} + \text{M} \rightarrow \underbrace{[MO_2^-(H_2O)_n]^*}_{\text{intermediate}} + Z \rightarrow \underbrace{MO_2^-(H_2O)_{n-1}}_{\text{product ion}} + \text{H}_2\text{O} + \text{Z}$$

The adduct is stabilized by collision with a third body, Z, and the product ion is a stable hydrated ion between M and O_2^-. Sometimes, reactions by charge transfer (formation of $M^-(H_2O)_n$) or proton abstraction (formation of $(M\text{-}1)^-(H_2O)_n$) might occur as well [1].
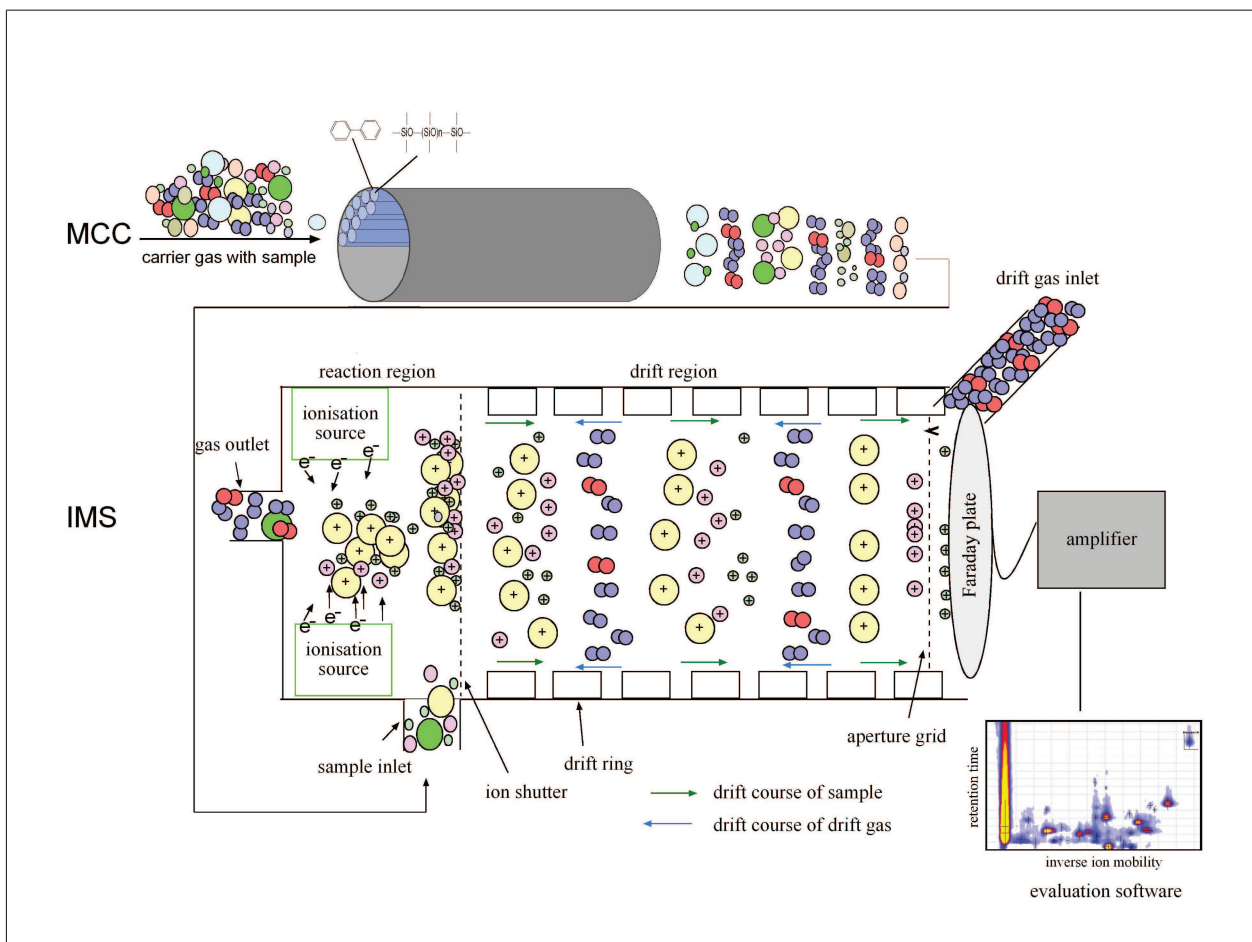
Figure 2.6: Schematic representation of the drift tube with ions (after pre-separation through MCC) and neutral molecules [17]

2.4 Ion mobility at molecular level

A localized ion cloud in a gas of uniform temperature and total pressure will be dispersed through the gas by the process of diffusion. The diffusive flow is in the direction opposite to the gradient concentration and is directly proportional to its magnitude [50]. This law is known as the Fick's law of diffusion and the constant of proportionality is D. The ionic flux density J is hence given by,

$$J = -D\nabla n \tag{2.6}$$

The magnitude of J is equal to the number of ions flowing in unit time through unit area normal to the direction of the flow [51]. The negative sign indicates the direction of the flow and n is the number density of the ions. As diffusive velocity flow can be given as [51],

$$J = nv \tag{2.7}$$

Fick's law can be rewritten as,

$$v = -\frac{D}{n}\nabla n \tag{2.8}$$

2.4.1 Einstein relation

The relationship between the defined variables D and zero-field value K depends on the relating current, concentration gradient and the linear electric field [51], [52]. With the linearity in flux density in presence of a concentration gradient and electric field, J is given by,

$$J = -D\nabla n + nKE \tag{2.9}$$

This is a general equation and we can consider a special case assuming equilibrium where J = 0, wherein ∇n can be found from equilibrium statistical mechanics. This condition is given by the Boltzmann expression as [51],

$$\frac{dn}{n} = \frac{eEdz}{kT} \tag{2.10}$$

or in three dimensions,

$$\nabla n = \frac{ne}{kT}E \tag{2.11}$$

Substituting the equilibrium conditions to Equation 2.9,

$$K = \frac{eD}{kT} \tag{2.12}$$

The main condition for this equation is the low field regions in a drift section (E/p < 2 V·cm^{-1}·Torr^{-1}) [30]. Equation 2.12 is known as the Einstein equation and sometimes referred to as the Nernst-Townsend relationship.

Mason et al. [51] have published many reviews on the ion mobility of gases at molecular level as a combined property of the ion and the neutral counter flowing drift gas. This is famously known as the Mason-Schamp equation [53], [54]. At the molecular level, considering a free-flight of the ion swarm, the mobility of an ion is described by the Mason-Schamp equation [30].

$$K = \frac{3q}{16N} \left(\frac{2\pi}{\mu kT}\right)^{1/2} \frac{1 + \alpha}{\Omega_D} \tag{2.13}$$

Where, q is the ionic charge (1.602 x 10^{-19} C), N; the number density of the drift gas (molecules.cm^{-1}), k; the Boltzmann constant (1.381 x 10^{-23} J.K^{-1}), T; the temperature in Kelvin, μ; the reduced mass: μ = mM/(m+M), m; the ion mass, M; the mass of neutral the drift gas, α is a mass dependent correction term and Ω_D; the ion collision cross section which is derived through a series of integrations of the ion-neutral cross sections over all possible scattering angles. For spherically symmetric systems, the integrations are as follows,

$$\Omega_D(T) \quad = \quad 1/2(kT)^{-3} \int_0^\infty Q_D(\epsilon) exp(-\epsilon/kT)\epsilon^2 d\epsilon \tag{2.14}$$

$$Q_D(\epsilon) \quad = \quad 2\pi \int_0^\pi (1 - cos\theta)s(\theta, \epsilon)sin\theta d\theta \tag{2.15}$$

where, ϵ is the relative kinetic energy of a collision and s(θ,ϵ) is the differential cross section for a scattering through an angle θ when the collision energy is ϵ [30], [1]. From Equation 2.13 it is seen that q/$\mu^{1/2}\Omega_D$ is the quantity which is measured during an IMS experiment. For small ions, the mobility is governed by the reduced mass and for

larger ions the reduced mass is essentially equal to M, the mass of the neutral drift gas.

Mason and coworkers have solved the above integral where the collision cross section is given by [1], [51], [55],

$$\Omega_D = \pi r_m^2 (1,1) * (T^*) \tag{2.16}$$

where $\Omega(1,1) * (T^*)$ is a good approximation of the dimensionless collision integral that depends on ion-neutral interaction potential and is a function of the dimensionless temperature, $T^* = kT/\epsilon_0$ [51]. Where, ϵ_0 is the depth of the minimum in the potential surface and r_m is the position of this minimum.

2.4.2   Ion-Neutral collision models

There are three main models which describe the collisions that happen in a drift tube between the ion cloud and the neutral drift gas molecules. They are the Rigid-sphere model, the polarization limit model and the 12,4-hard core potential model. Out of these, the simplest model is the rigid sphere model [1] where the basic assumption is that upon collision between the ion and the neutral gas molecule, the ion is equally likely to be scattered in any direction. This model treats both ions and neutral gas molecules as rigid spheres and hence the collision cross section is given by,

$$\Omega_D = \pi d^2 \tag{2.17}$$

where d is the sum of the radii of the ion and the neutral molecule [55].

The second model is the polarization limit model which assumes that the neutral gas molecules have no permanent dipole or quadrapole moment and no ion-neutral repulsive forces. The interaction between the two, according to this model, is solely due to the ion induced dipole interaction which is the function of the polarizability of the neutral molecule, α_p. The interaction potential varies as a function of the distance, r, between the ion and the neutral molecule, [1]

$$V_{pol}(r) = \epsilon^2 \alpha_p / (2r^4) \tag{2.18}$$

In this model, the repulsive forces are completely neglected, hence the third model, which is the 12,4 hard-core potential model was formulated. This considers the short range repulsive term to the interaction potential when the ion and the neutral molecules come very close to one another.

$$V(r) = (\epsilon_0/2) \left\{ \left[(r_m - a)/(r - a) \right]^{12} - 3 \left[(r_m - a)/(r - a) \right]^4 \right\} \tag{2.19}$$

Though all the 3 models cannot describe the ion-neutral collision that happen completely, [1], the 12,4 hard-core potential model is currently the most approximate one.

2.5 Signal Processing

2.5.1 Spectra acquisition

The signals detected in the Faraday plate are collected in several ways. Single scan technique, signal averaging and Fourier transform method are the most common ways to acquire the signal. Single scan method is the technique used in this study. Every single spectrum detected by the Faraday plate, when the gate is open, is collected and stored. Total data collection time (50 ms - 100 ms) can be used to monitor concentration variations with time [30]. This method requires extremely fast electrometers (rise time$\leq$ 0.1 ms). The other methods to acquire the signal are signal averaging technique, Fourier transform method [56], moving second gate and a method based on nonlinear electric fields [57].

2.5.2 Resolution

Generally ion mobility spectrometrists have measured separation power of the IMS by using a single peak quotient [58], called the resolving power (R_p),

$$R_p = t_D/w_h \tag{2.20}$$

Where t_D is the ion drift time and w_h is the ion pulse duration at the detector measured at the half of the maximal intensity. Mason and Revercomb developed an expression for measured peak width for IMS where only the initial pulse width and the broadening due to normal diffusion are important [53].
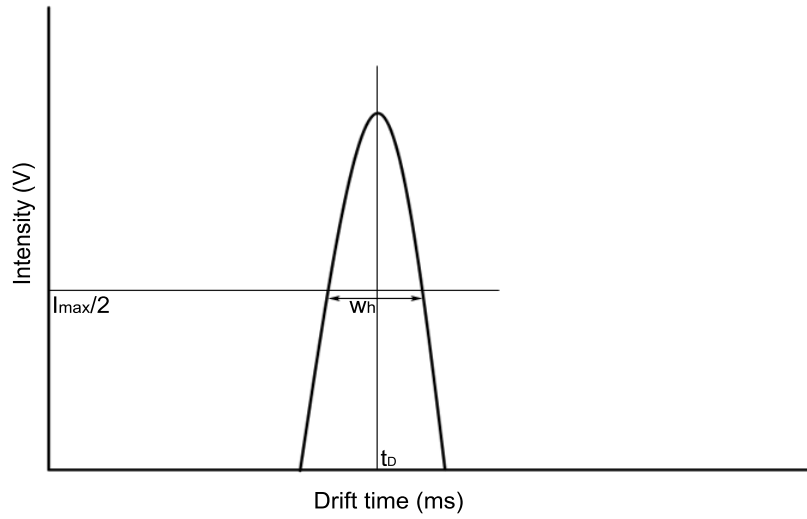
Figure 2.7: Illustration describing the parameters, the drift time (t_D) and the full width at half maximum (FWHM - w_h), defining Resolving power (R_p) of a peak

$$w_h^2 = t_g^2 + \left(\frac{16kTln2}{Vez} \right) + t_D^2 \tag{2.21}$$

Where t_g is the initial ion pulse width, V is the voltage potential across the drift length and z is the number of charges on the ion.
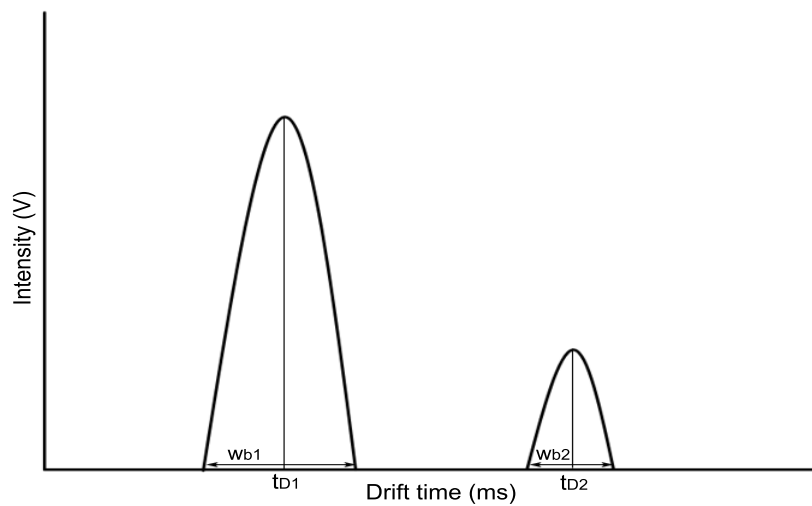

Figure 2.8: Illustration describing the parameters, the drift time (t_D) and the base width (w_h), defining Resolution (R) between two peaks

Resolution in IMS is a function of both the efficiency of the separation and the selectivity of the separation [59]. The standard two peak definition of resolution is,

21

$$R = \left(\frac{t_{D2} - t_{D1}}{w_{bavg}} \right) \qquad (2.22)$$

Where t_{D2} and t_{D1} are the drift times of the second and the first peaks and w_{bavg} is the average base width of the two peaks.

2.6 IMS operational procedure

The spectrometer used in this study is a small table top instrument connected to a 220 V/50 Hz power supply. When the power is on, the desired electric field can be set by applying the high-voltage (up to 10 kV as used in this study). Parallelly, the shutter grid opening time and the drift times can be set. Once that is done, the gas flows, the drift gas, carrier gas and the sample gas flow rates are controlled. With the various sample inlet systems described in section 2.2.1, the required sample is then washed for a specific period of time in the sample loop and when the measurement starts, the 6-port valve changes to position B (Figure 2.4) and the sample is sent into the MCC with the help of the carrier gas where by differential adsorption and desorption rates, it is pre-separated and enters the drift tube. Reference substances are usually measured alongside 2-Nonanone as a standard substance. Upon entering the drift tube the pre-separated sample gets ionized by proton transfer or electron transfer with the reactant ions, thus forming product ions which are then periodically let into the drift region by the shutter. Depending on the polarity of the electric field, the positive ions or the negative ions pass through the shutter into the drift region where they attain different velocities and are separated and detected by the Faraday plate at the end of the drift tube. The signals are amplified and sent to a computer where the software records the data. This data acquisition as comma separated value (.csv) file, is achieved by a software (qIMS) developed at ISAS. This format has been describe in detail by *Vautz et al.* [60]. Figure 2.9 shows the screen shot of this data acquisition software.

The *.csv* data file which is obtained during the measurement is visualized and analysed using another JAVA based software developed at ISAS. Bödecker et al. have published the complete details about the functioning of this analysis software [61]. The output from this analysis is a three dimensional chromatogram depicting the retention time (R_T), the drift time expressed as ($1/K_0$) and the intensity representing the concentration of the ions. A sample output (screen shot) of this analysis software is shown in Figure 2.11 and Figure 2.10.
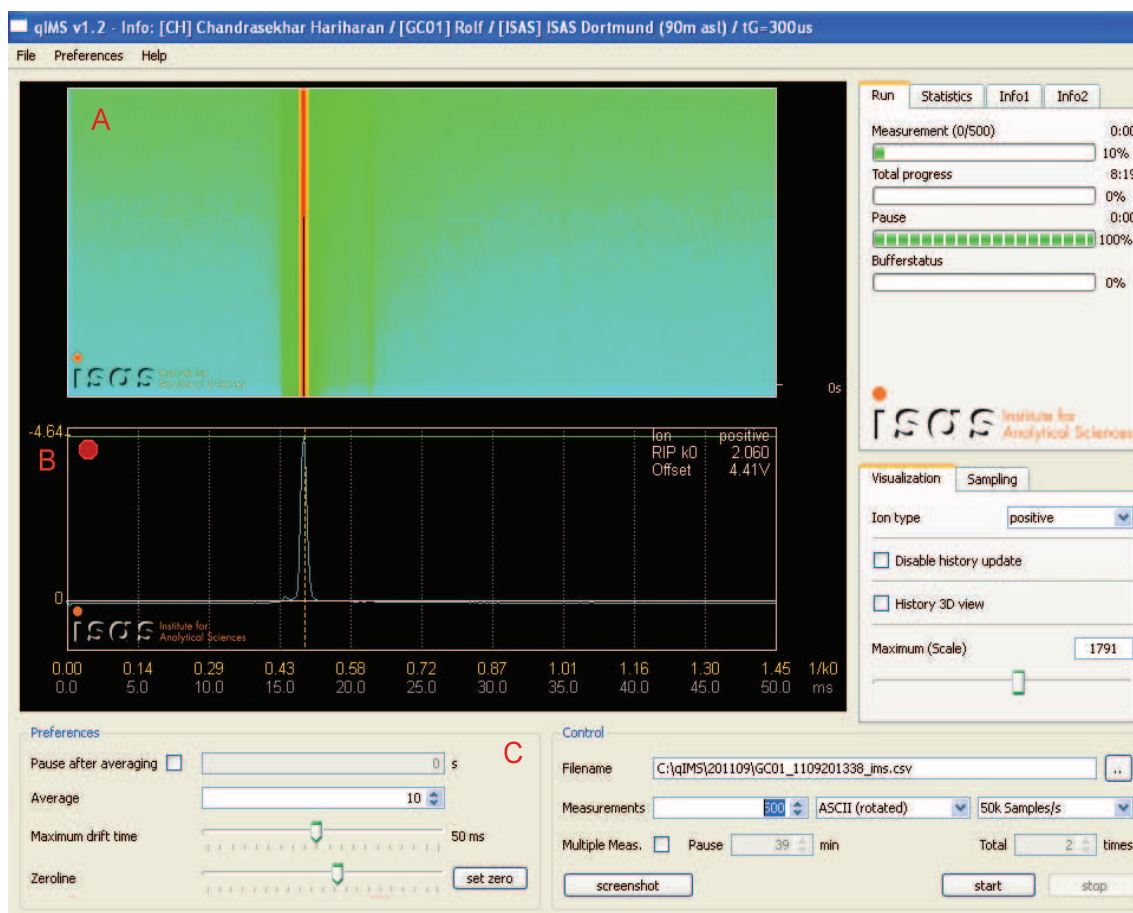
Figure 2.9: Screen shot of the data acquisition software developed at ISAS labs. A - real time 3-D output of the measurement, B- real time spectra visualization window, C-control parameters

Table 2.1: Standard operating parameters of MCC- ^{63}Ni IMS in this study

Ionization source	β radiation (^{63}Ni, 550 MBq)
Voltage polarity	Positive mode
Grid opening time	300 μs
Spectral length/sample interval	100 ms
Spectral resolution	40 kHz
Drift length	120 mm
Drift voltage	4 kV
Electric field intensity	330 V·cm^{-1}
Drift gas and carrier gas	Synthetic air
	(20.5 % O$_2$, 79.4 % N$_2$, <2 ppb$_v$ water)
	(Air Liquide GmbH, Germany)
Drift gas flow	100 mL·min^{-1}
Carrier gas flow	150 mL·min^{-1}
Pre-separation type	MCC-OV-5, 20 cm
Pre-separation temperature	40 °C
Sample loop volume and temperature	8 mL and 40 °C
Operating temperature and pressure	room temperature and ambient pressure

2.6.1 Exemplar applications of MCC/IMS for biological and medical purposes

Over the past decade, IMS has been widely used in the field of biology and medicine. The metabolites of any organism are increasingly subjected to investigations as they are a carrier of information about the state of the organism itself, about the influences of the environment on the organism and about the synergistic effects [62], [4]. They could be cells, bacteria, fungi, plants, animals and human beings as well. Feasibility studies have been successfully carried out at ISAS, including the detection of bacteria, fungi and metabolites of cells and in human breath [4].

2.6.1.1 Analytical pre-requisites in biological and medical samples

Biological and medical samples are vastly diverse and huge. It is therefore absolutely important to utilize the MCC as a pre-separation unit to provide a three dimensional separation along with the ion mobility and intensity to obtain high resolution analytics. Biological and medical samples also require fast, high resolution and accurate analysis as minor errors can sometimes be life threatening. The use of the MCC avoids negative influences especially when analysing humid samples. If humidity enters the ionisation
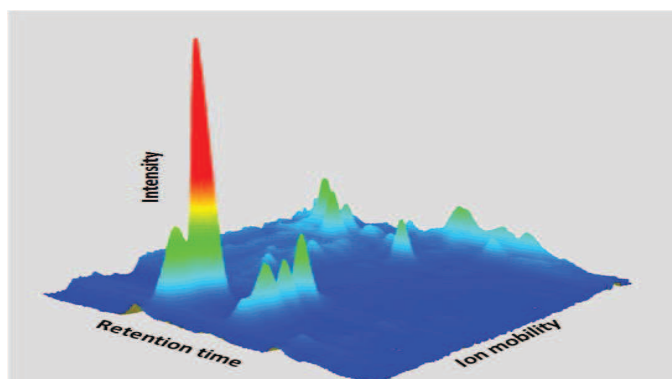
Figure 2.10: A sample 3-D output of a chromatogram from an IMS measurement with the retention time, drift time and intensity. The biggest peak seen is the reactant ion peak (RIP)

region together with the analyte, water clusters are formed with the product ions which would make identification tough or even impossible [1]. Hence, when using a MCC as a pre-separation unit, the water molecules and the analytes entering the ionisation region are well separated thereby having no negative influence on the measurements. This technique also helps analysing 100 % humid samples which are often the case in the field of biology and medicine.

Bacteria and viruses have affected humans for centuries and mortality is usually due to late and/or inaccurate diagnostics of the infecting micro organism. With the advantage of the ^{63}Ni-MCC-IMS, it is possible to detect and identify patterns of several bacteria and fungi cultured from human breath thereby giving an opportunity for an early and accurate medication [5].

As the starting step towards early diagnosis of diseases like lung cancer, the metabolites of the cancer cell lines were detected in the head space of a cell culture by the ^{63}Ni-MCC-IMS and compared to the medium of growth and a non-cancer cell line as well [3].

Human breath has been measured and various metabolites and VOCs responsible for several diseases have been detected and identified. They include acetone, a well known marker for diabetes mellitus [63], [4]. Human breath has also been measured to identify other diseases like sarcoidosis and lung cancer [15], [3].
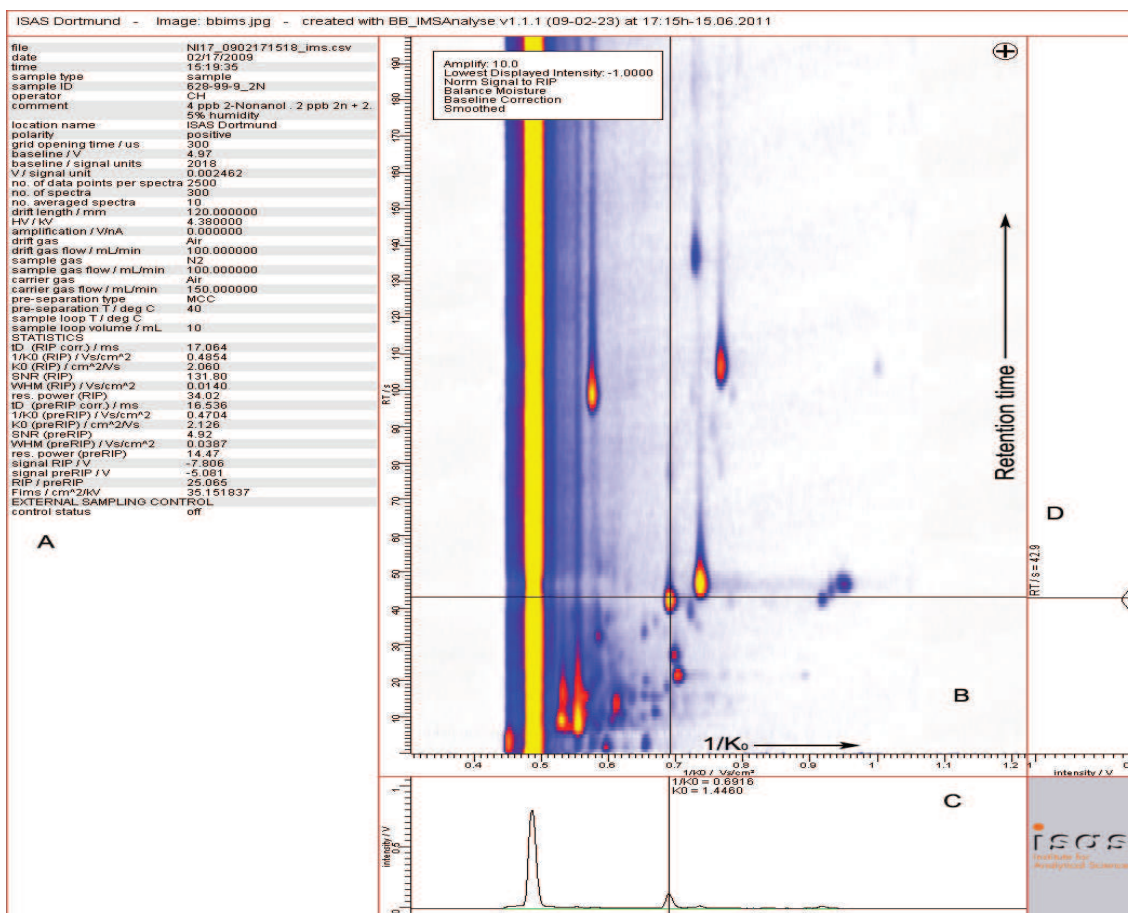
Figure 2.11: Screen shot of the JAVA based analysis software developed at ISAS to visualize the IMS data. A- window showing the various experimental parameters, B- IMS chromatogram, the intensity is colour coded, C- single spectrum selected at a particular retention time, D- single chromatogram at a particular ion mobility.
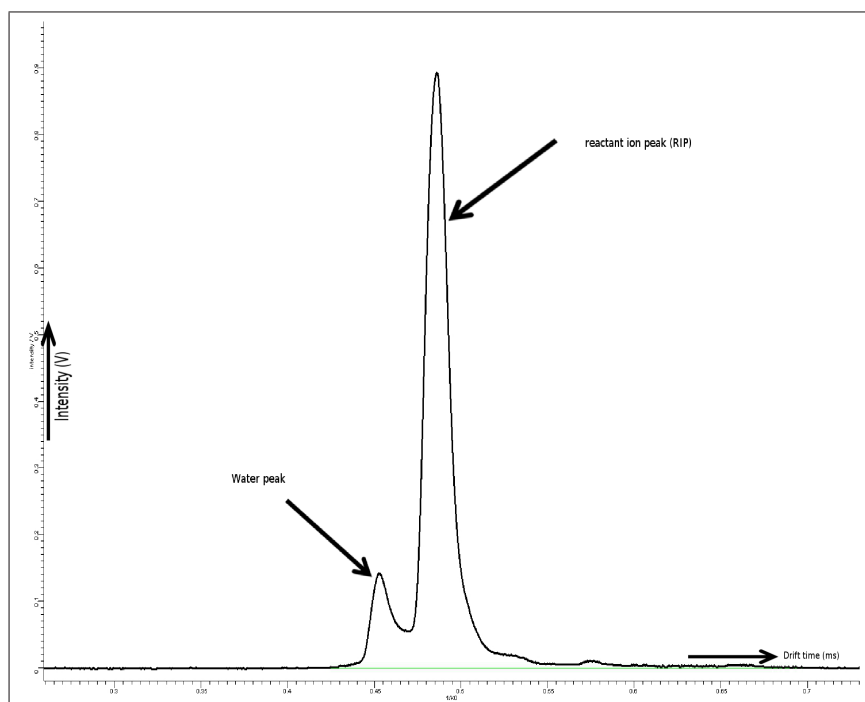
Figure 2.12: The advantage of using a MCC as a pre-separation unit. The water in the sample is removed and the protonated water cluster ion is seen resolved, thereby negating any influences on the product ion formation

The above mentioned biological and medical samples are hugely complex and require both qualitative and quantitative analysis. In this doctoral thesis, a new and accurate method for qualitative identification of the detected peaks has been described. Additionally, a state-of-the-art drift tube has been constructed to resolve the complex peaks that are usually encountered when measuring these samples.

Chapter 3

Empirical Prediction of Reduced Ion Mobilities

Till recently, IMS have been used to detect specific target analytes with known reduced ion mobility. For the analysis of complex mixtures, the reduced mobility alone will not be sufficient for the identification of analytes in the mixture [1]. Several analytes have similar or even the same mobility [4]. Hence, additional rapid pre-separation techniques are applied. The time taken by an analyte to elute out of the Multi-capillary column (MCC) is termed as the retention time (R_T) of the analyte. Thus, for every analyte, there is a specific reduced ion mobility value and a retention time which are the characteristics of a particular analyte at a specific temperature, column length and flow. Providing such a database of ion mobilities and retention time of relevant analytes for every analysis enables the identification of compounds in an unknown complex mixture.

---

[1]The results published in this chapter are the work solely carried out by the author with opinions and suggestions from Dr. Vautz and Dr. Baumbach. This work presented has been published in parts in the following publications

- Hariharan C, Baumbach J I, Vautz W (2009), Empirical prediction of reduced ion mobilities of secondary alcohols, Int. J. Ion Mob. Spec., 12:59-63

- Hariharan C, Baumbach J I, Vautz W (2010), Linearized equations for the reduced ion mobilities of polar aliphatic organic compounds, Anal. Chem., 82:427-31

The work was also presented at the 18 [th] Annual conference on Ion Mobility Spectrometry, July 2009, Thun, Switzerland.

3.1 General peak identification techniques

During the analysis of complex mixtures, e.g. human breath, volatile organic compounds from bacteria etc., there are many unknown peaks in the IMS chromatogram. Identifying them is one of the major problems. It is evident that, to identify the peaks obtained from an IMS chromatogram, we need databases of reference substances for the identification. If a peak is detected by an IMS that is not included in the database, there are a huge number of analytes available from which one could select, measure and identify the unknown peak. Parallel measurements with other mass spectrometric methods may be carried out to explore the composition of the sample matrix. Most applicable solution is the additional sampling on adsorption materials and analysis by GC/MS. From such analysis, substances possibly responsible for the unknown signals could be proposed. This proposal has to be validated by IMS measurements of the reference analyte. Obviously, such a procedure is time consuming and expensive. Statistical alignment tools are also used for peak identification by aligning the GC retention times to the IMS retention times and the reactant ion peak (RIP) to the reduced mobility [64], [61], [65], [60]. Thus, additional tools for the identification of unknown analytes would be very helpful.

There have been earlier attempts to calculate the ion mobility of analytes directly from the molecular structure using computational neural networks and multiple linear regression analysis [23], [24]. But, these methods are seemingly complex and require extensive modeling of the ion structure, resulting in an assumed mobility value and hence cannot be used for online characterisation of complex mixtures.

In this study, a rather simple method to see regression trends within a homologous series of substances between the inverse reduced ion mobility and the number of carbon atoms in the analyte is used to predict the reduced ion mobilities of other unmeasured analytes in that particular homologous series directly.

3.2 Mass mobility correlations in homologous series

From the database of analytes available at the Leibniz-Institute for Analytical Sciences - ISAS- Dortmund, Germany, the homologous series of primary alcohols, secondary alcohols, primary aldehydes and ketones were chosen for this study. The substances were sorted into the four homologous series' and from this data, the inverse reduced

ion mobility values were plotted against the number of carbon atoms (Figure 3.1).
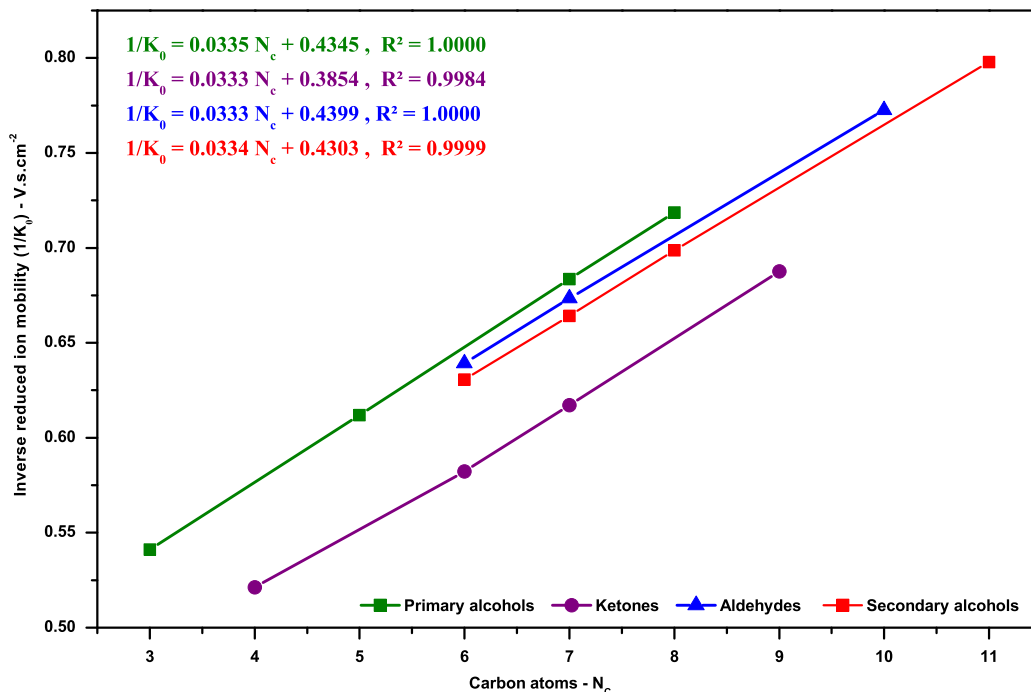

Figure 3.1: Linear trend between the number of carbon atoms (N_C) and the inverse reduced ion mobility for four different homologous series

From Figure 3.1 we see that there is a linear trend between the number of carbon atoms in a substance and its inverse reduced ion mobility. The regression lines were plotted using Microsoft Office 2003, Figure 3.1, and the linear equations obtained were read off from the plot.

- primary alcohols : $1/K_0 = 0.0355 \ N_C + 0.4345$ ($R^2 = 1.0000$)

- secondary alcohols : $1/K_0 = 0.0334 \ N_C + 0.4303$ ($R^2 = 0.9999$)

- aldehydes : $1/K_0 = 0.0333 \ N_C + 0.4399$ ($R^2 = 1.0000$)

- ketones : $1/K_0 = 0.0333 \ N_C + 0.3854$ ($R^2 = 0.9984$)

3.3 Empirical prediction and validation

Using the linear equations obtained from Figure 3.1, the inverse reduced ion mobility values of other analytes in the same homologous series were empirically predicted. To validate the quality of this empirical prediction, the analytes prognosed were individually measured with a [63]Ni-MCC-IMS using the same experimental parameters as used during the database creation. Table 3.1 gives the details of the results.

From Table 3.1, it is obvious that the accuracy in this empirical prediction is higher than 99.5 % on an average. Figure 3.3 shows the accuracy by comparing the predicted and the measured mobility values of the substances in the four series'. The fact that the correlation is linear proves that we need minimal number of data points in a homologous series to predict the mobility values of other substances in the same series. Figure 3.4 shows the same with high correlation coefficients for the series of substances considered.
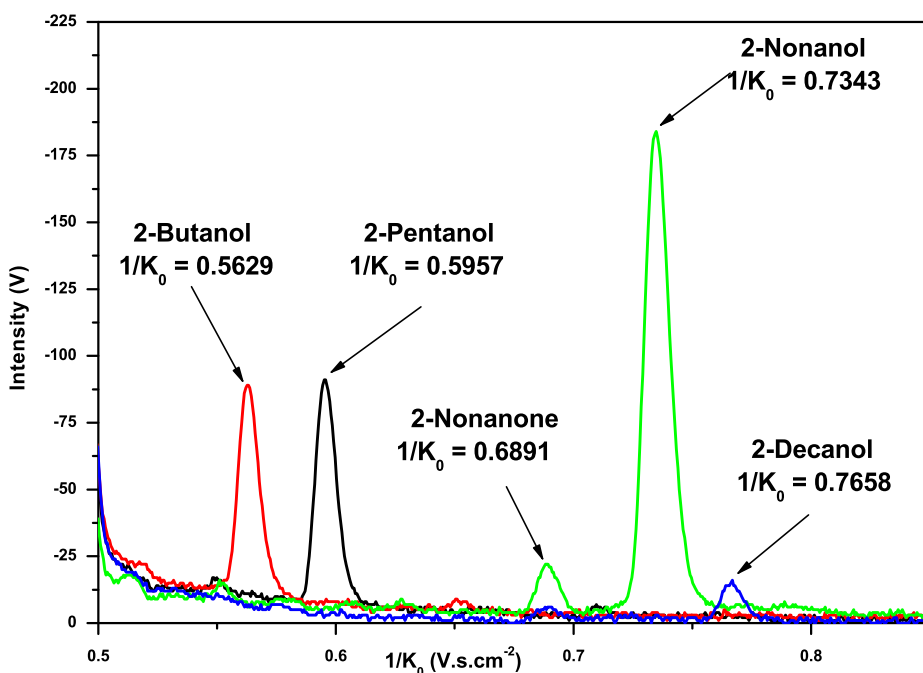

Figure 3.2: Spectra of the validation measurements of the four predicted secondary alcohols with 2-Nonanone as a reference substance. The other spectra and a comprehensive database of the ion mobilities of analytes are available at ISAS.

Table 3.1: Measured, predicted and validated $1/K_0$ values of the four homologous series

| Analyte	No. carbon atoms N_c	Predicted $1/K_0$ (V·s·cm^{-2})	Measured/validated $1/K_0$ (V·s·cm^{-2})	Accuracy (%)
primary alcohols				
$1/K_0 = 0.0355\ N_C + 0.4345$				
1-Propanol	3		0.5412	
1-Butanol	4	0.5765	0.5765	100.0
1-Pentanol	5		0.6120	
1-Hexanol	6	0.6475	0.6472	99.95
1-Heptanol	7		0.6835	
1-Octanol	8		0.7137	
1-Nonanol	9	0.7540	0.7542	99.97
1-Decanol	10	0.7895	0.7893	99.34
secondary alcohols				
$1/K_0 = 0.0334\ N_C + 0.4303$				
2-Butanol	4	0.5639	0.5629	99.82
2-Pentanol	5	0.5973	0.5957	99.73
2-Hexanol	6		0.6306	
2-Heptanol	7		0.6642	
2-Octanol	8		0.6988	
2-Nonanol	9	0.7309	0.7343	99.54
2-Decanol	10	0.7643	0.7658	99.80
2-Dodecanol	11		0.7979	
aldehydes				
$1/K_0 = 0.0333\ N_C + 0.4399$				
Butanal	4	0.5731	0.5788	99.02
Pentanal	5	0.6064	0.6087	99.62
Hexanal	6		0.6392	
Heptanal	7		0.6734	
Octanal	8	0.7063	0.7098	99.50
Nonanal	9	0.7396	0.7373	99.69
Decanal	10		0.7726	
Undecanal	11	0.8062	0.7957	98.69
ketones				
$1/K_0 = 0.0333\ N_C + 0.3854$				
2-Butanone	4		0.5212	
2-Pentanone	5	0.5519	0.5494	99.55
2-Hexanone	6		0.5823	
2-Heptanone	7		0.6172	
2-Octanone	8	0.6518	0.6529	99.83
2-Nonanone	9		0.6876	
2-Decanone	10	0.7184	0.7221	99.48
2-Undecanone	11	0.7517	0.7553	99.52
2-Dodecanone	12	0.7850	0.78990	99.34
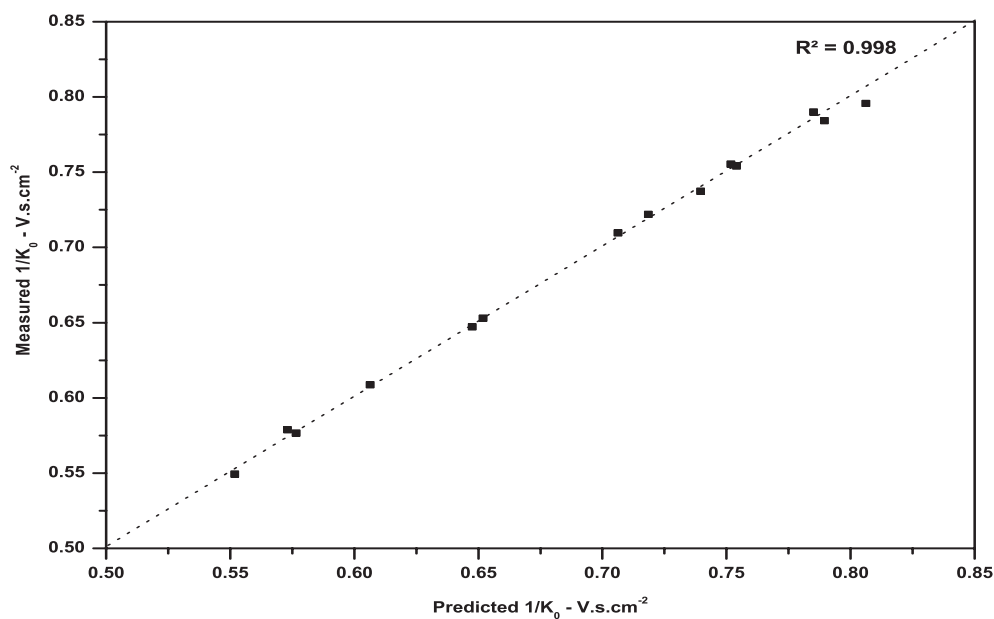
Figure 3.3: Comparison chart of the measured and the predicted $1/K_0$ values of the 18 compound from the four different series
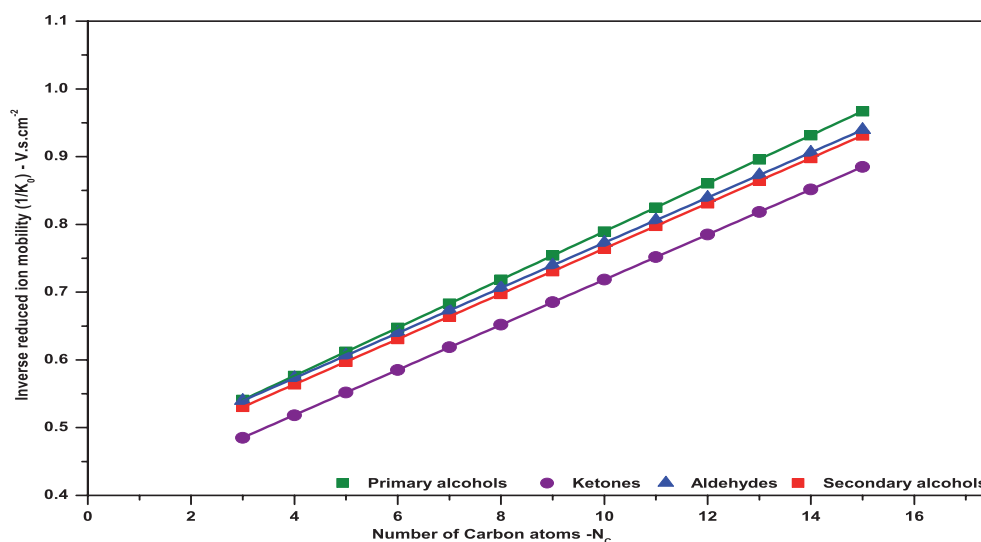

Figure 3.4: Linear correlations seen with the measured $1/K_0$ values of the four homologous series of substances in this study. The correlation coefficients are, primary alcohols - 0.9995; secondary alcohols - 0.9998; aldehydes - 0.9984 ; ketones - 0.9995. The almost linear correlations between the inverse reduced mobilities and the number of carbon atoms implies the necessity of only few data points in a series to predict the trend for the prognosis of the mobility values of other compounds in the series.

This highly accurate (> 99.5 %) empirical prediction method would be a considerable facilitation for a preliminary identification of unknowns and development of databases. This can also be extended to all other homologous series with minimal number of susbtances to determine the linear equations and predict the mobility values of the other substances in the series.

3.4 Global IMS database trends

This empirical prediction presented in this chapter can be used for any database of ion mobilities. This can be seen in Figure 3.5 which shows the linear trends of the some homologous series used in the study but measured with a different IMS at the Eiceman Group, New Mexico State University and published as a reference database of ion mobilities of substances [1]. The linear trends seen in the global IMS database proves that the prognosis method to identify unknown peaks in an IMS chromatogram can be used in any database of homologous series of substances.
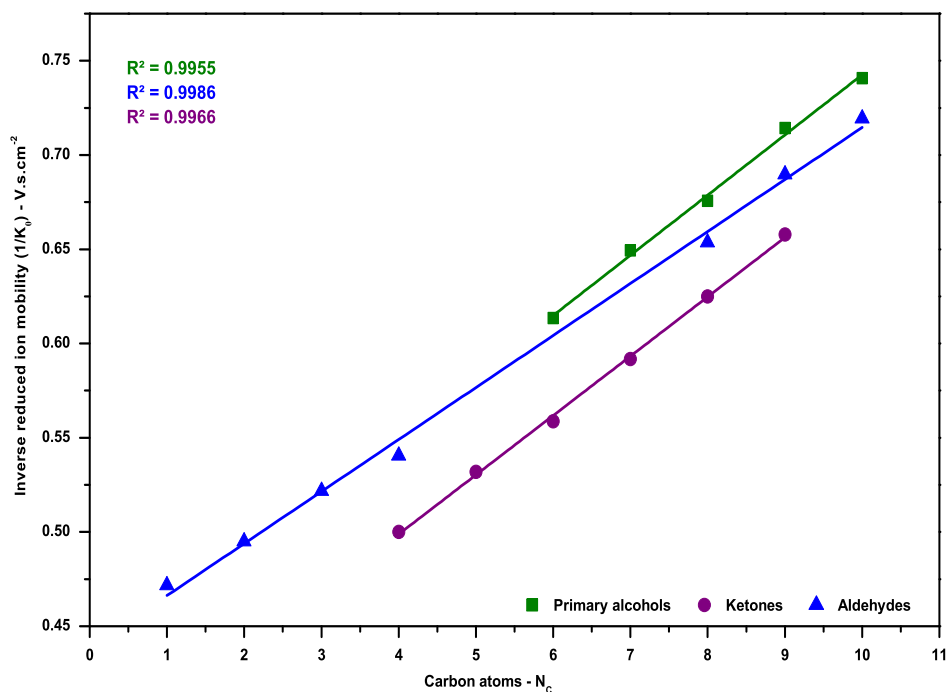

Figure 3.5: Linear trends of alcohols, aldehydes and ketones from the IMS database of New Mexico State University, U.S.A

34

Chapter 4

Linearized Ion Mobility Equations

The empirical prognosis technique presented in Chapter 3 provided a highly accurate method to identify unknown peaks in an IMS chromatogram. This empirical trend can be extended for many other series of compounds to increase the reference database. However, the theoretical correlation of the presented approach to the molecular structure of the analyte and to the behaviour of its ions in the drift tube under the influence of an electric field required further investigation. In this chapter[1], further investigation has been carried into the existing Mason Schamp equation 2.13 and compare it with the linear equations obtained from the prognosis to shed light into the validity of the method and the various existing ion models.

4.1 General reduced mobility equation

The four linear equations obtained empirically in Chapter 3 are

- primary alcohols : $1/K_0 = 0.0355 \ N_C + 0.4345 \ (R^2 = 1.0000)$

- secondary alcohols : $1/K_0 = 0.0334 \ N_C + 0.4303 \ (R^2 = 0.9999)$

- aldehydes : $1/K_0 = 0.0333 \ N_C + 0.4399 \ (R^2 = 1.0000)$

- ketones : $1/K_0 = 0.0333 \ N_C + 0.3854 \ (R^2 = 0.9984)$

---

[1]The results published in this chapter are the work solely carried out by the author with opinions and suggestions from Dr. Vautz and Dr. Baumbach. This work presented has been published in-Hariharan C, Baumbach J I, Vautz W (2010), Linearized equations for the reduced ion mobilities of polar aliphatic organic compounds, Anal. Chem., 82:427-31. The proposed model is currently being mathematically validated by Dr. Glenn Spangler, Technispan, United States. The work was also presented at the 18 th Annual conference on Ion Mobility Spectrometry, July 2009, Thun, Switzerland.

The four empirically obtained linear equations can be written in a general form with variables as shown,

$$\frac{1}{K_0} = \epsilon N_C + \delta \qquad (4.1)$$

Where, ϵ is the slope of the equation and δ the intercept. This represents the general form of a first order linear equation, y = mx + c, and the intercept term (δ) in Equation 4.1 is a mass independent term and has a characteristic value for every homologous series of compounds. The ion mobility equation is now compared to the Mason-Schamp equation, 2.13, for detailed interpretation into this empirical prediction.

4.2 Comparison with Mason-Schamp equation

The Mason-Schamp equation for ion mobility and the pressure and temperature correction equations, Equations 2.4 and 2.13,

$$K_0 = K \left(\frac{P}{P_0}\right) \left(\frac{T_0}{T}\right) \qquad (4.2)$$

$$K = \frac{3q}{16N} \left(\frac{2\pi}{\mu kT}\right)^{1/2} \frac{1+\alpha}{\Omega_D} \qquad (4.3)$$

when combined together yields,

$$K_0 = \left(\frac{3q}{16N}\right) \left(\sqrt{\frac{2\pi}{kT}}\right) \left(\frac{1}{\sqrt{\mu}}\right) \left(\frac{1+\alpha}{\Omega_D}\right) \left(\frac{P}{P_0}\right) \left(\frac{T_0}{T}\right) \qquad (4.4)$$

where μ represents the reduced mass of the drift gas and the ion. Rearranging the terms we get,

$$K_0 = \underbrace{\left(\frac{3q}{16N}\right) \left(\sqrt{\frac{2\pi}{kT}}\right) \left(\frac{P}{P_0}\right) \left(\frac{T_0}{T}\right)}_{\frac{1}{\psi}} \left(\frac{1}{\sqrt{\mu}}\right) \left(\frac{1+\alpha}{\Omega_D}\right) \qquad (4.5)$$

The braced terms, marked $1/\psi$, are constants when the experimental and ambient conditions remain unaltered. Hence the equation can be rewritten as,

$$K_0 = \left(\frac{1}{\psi}\right)\left(\frac{1}{\sqrt{\mu}}\right)\left(\frac{1+\alpha}{\Omega_D}\right) \tag{4.6}$$

$$\Rightarrow \left(\frac{1}{K_0}\right) = (\psi)(\sqrt{\mu})\left(\frac{\Omega_D}{1+\alpha}\right) \tag{4.7}$$

Equation 4.1 has been mathematically validated in Chapter 3. The two equations which now represent $1/K_0$, equations 4.1 and 4.6, are mathematically different though. Equation 4.6 represents a linear trend with a nonzero intercept unlike equation 4.1. For further insights into this divergence, equation 4.6 has to be written in a linear form for comparison. Linearizing the equation is possible only by splitting a term in the numerator. The reduced mass term and the collection of constants, ψ, are non reducible. hence, the collision integral (Ω) term is split into two, Ω_C and Ω_S.

$$\frac{1}{K_0} = \frac{\psi\sqrt{\mu}}{1+\alpha} * (\Omega_C + \Omega_S) \tag{4.8}$$

$$\Rightarrow \frac{1}{K_0} = \left(\frac{\psi\Omega_C\sqrt{\mu}}{1+\alpha}\right) + \left(\frac{\psi\Omega_S\sqrt{\mu}}{1+\alpha}\right) \tag{4.9}$$

4.3   Proposed ion-neutral collision model

The Mason-Schamp equation, rewritten by splitting the collision integral into two terms, equation 4.9, can now be compared to the empirically obtained equation 4.1. On comparison, one of the adduct terms in equation 4.9 should be a mass-dependent term and the second one should be a mass-independent but a series-dependent term.

The reduced mass term $\mu^{1/2}$ in the Mason-Schamp equation can be approximated to M [30], [1], as m $\gg$ M, is true for all the ions in this study. Hence, a valid reason for series-dependent and mass dependent collisions taking place between the ions and neutral molecules will validate this study. Let us consider any class of homologous series and the ions of the compounds formed. The part of the molecule where the charge is located (the ionic head) is the same throughout the series, independent of the mass or size of the compound. This means that the neutral molecules from the drift gas that strike the ion may encounter two types of collision cross-sections: One, on the ionic head which is the same in any homologous series giving the series dependent collision (Ω_S), and the other on the tail of the ion giving rise to the mass-dependent collision integral (Ω_C), Figure 4.2.
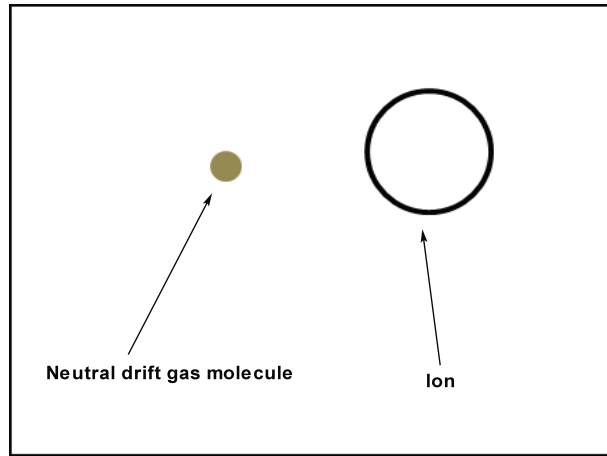
Figure 4.1: Illustration of the traditional collision model between the neutral drift gas molecule and the drifting ion collision. Both the ion and the neutral drift gas molecule are considered spherical.
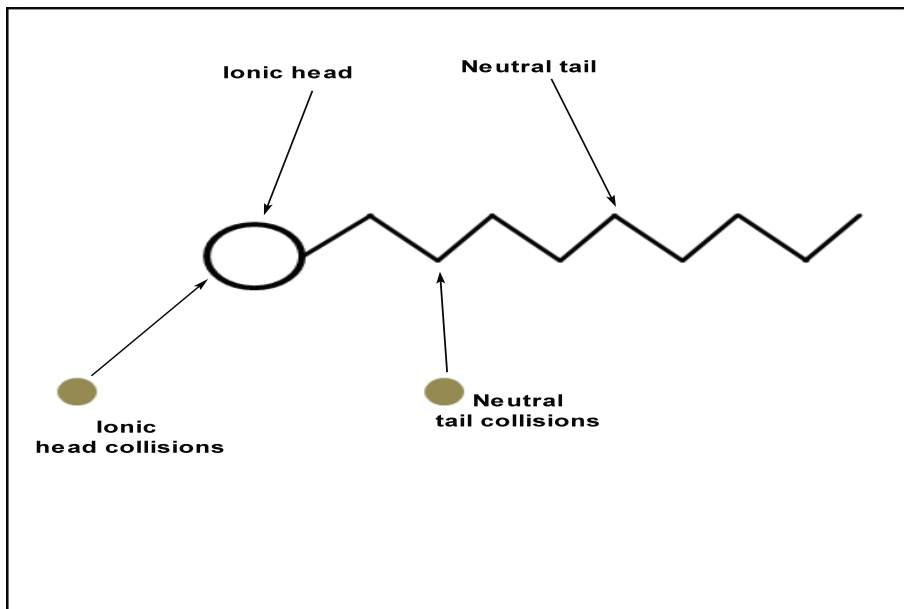

Figure 4.2: Pictorial representation of the proposed model of the collisions between the neutral drift gas molecule and the drifting ion collision. The picture shows the occurrence of two types of collisions, namely the neutral-ion head collisions and the neutral tail collisions.

At a more scientific level, the Boltzmann equation that is used to solve the collision cross-section of molecules is a linear differential equation used for calculations of the collision integral [66] and should, in principle, allow the collision cross-section to be broken up into linear components associated with independent force fields. Hence, by splitting the collision integral term in the Mason-Schamp equation, the empirical linear equation obtained in this study is plausible. The mass dependent term (ϵN_C) is due to the neutral gas collisions occurring at the non ionic part of the compound, and the series dependent term (δ) is due to the neutral gas collisions taking place in the ionic head.

Chapter 5

Novel design of drift tubes for optimized peak cluster resolution

With increasing complexity of the sample matrices, the number of substances detected by the IMS increases and hence the chances that two or more substances having very close retention times and drift times, thus resulting in peak clusters are high. Under these phenomena, identification and quantification of individual peaks can be difficult even when comprehensive databases and prediction tools are available as the substances compete against each other for protons. An optimized change in the instrument is necessary to increase the resolution without changing any influential parameters like drift gas, shutter grid size or temperature and pressure conditions [1]. Care should also be taken to make it suitable not just for laboratorial conditions but also for real time applications at clinics where the majority of our measurements take place.

---

[1]The results published in this chapter are the work solely carried out by the author with opinions and suggestions from Mrs. Luzia Seifert, Dr. Vautz and Dr. Baumbach. This work presented has been published in- Hariharan C, Seifert L, Baumbach J I, Vautz W(2011) Novel design for drift tubes in ion mobility spectrometry for optimised resolution of peak clusters, Int. J. Ion Mob. Spec, 14(1):31-38. The design for the drift tube is a joint idea by the author and Dr. Vautz and constructed at the workshop of the Leibniz- Institute for Analytical Sciences - ISAS- e.V., Dortmund , Germany. The work was also presented at the 20 [th] Annual conference on Ion Mobility Spectrometry, July 2011, Edinburgh, Scotland, U.K.

As a first step to resolve the peak clusters seen in the output chromatogram in an IMS measurement of a humid and complex sample, a 100 cm long Multi-capillary column was used for pre-separation in place of the 20 cm MCC. This column was purchased from Multichrom, Novosibirsk, Russia and attached to a heating device to maintain a constant temperature, Figure 5.1. The column design specifications required a flow rate of carrier gas to be a maximum of 100 mL·min^{-1}. The longer pre-separation column and smaller flow meant that the measurements took more time to complete and this negates the biggest advantage of an IMS namely, the fast measurement times, Figure 5.2.
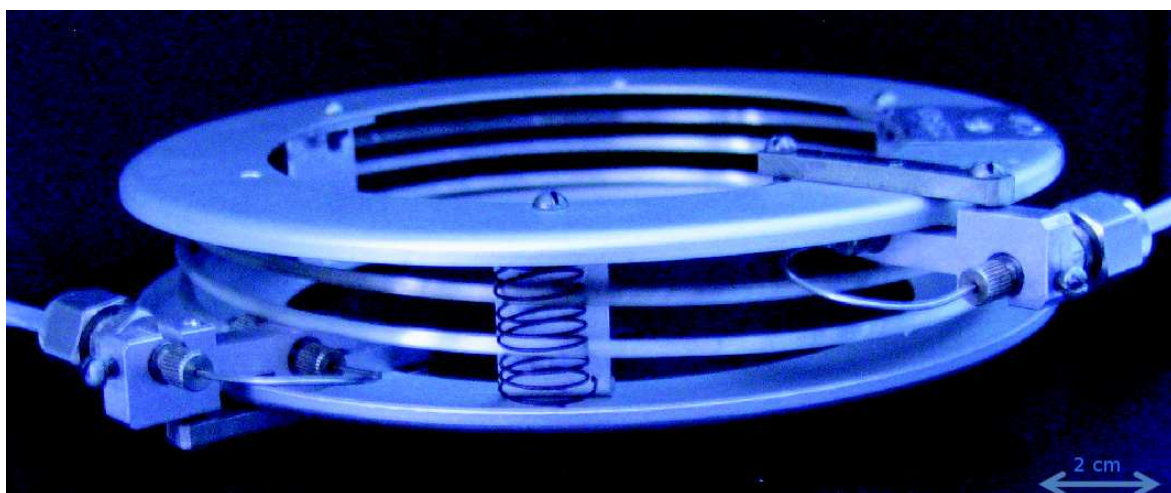

Figure 5.1: Photograph of the 100 cm spiral Multi-capillary column obtained from Multichrom, Novosibirsk, Russia

To hold on to the advantage of fast measurement times (≤ 500 s for human breath), it was optimal to change the drift length (increase) rather than the pre-separation, as even doubling the drift length would mean, a single scan would take 50 ms longer.

It is obvious that increasing the resolution of the instrument would resolve the peak cluster problems. Hence, for a higher resolution between those peaks found in human breath which lie close to one another, we constructed a drift tube whose length can be varied depending on the complexity and the demands of the sample matrix. This drift tube with variable length has a much high resolving power and resolution than the existing one which is used at ISAS for breath analysis. Studies have been carried out previously with similar kind of drift tubes but at higher pressures and temperatures [67]. In this study we present a variable length drift tube which can be used under ambient temperatures and pressure conditions. This drift tube is suitable not
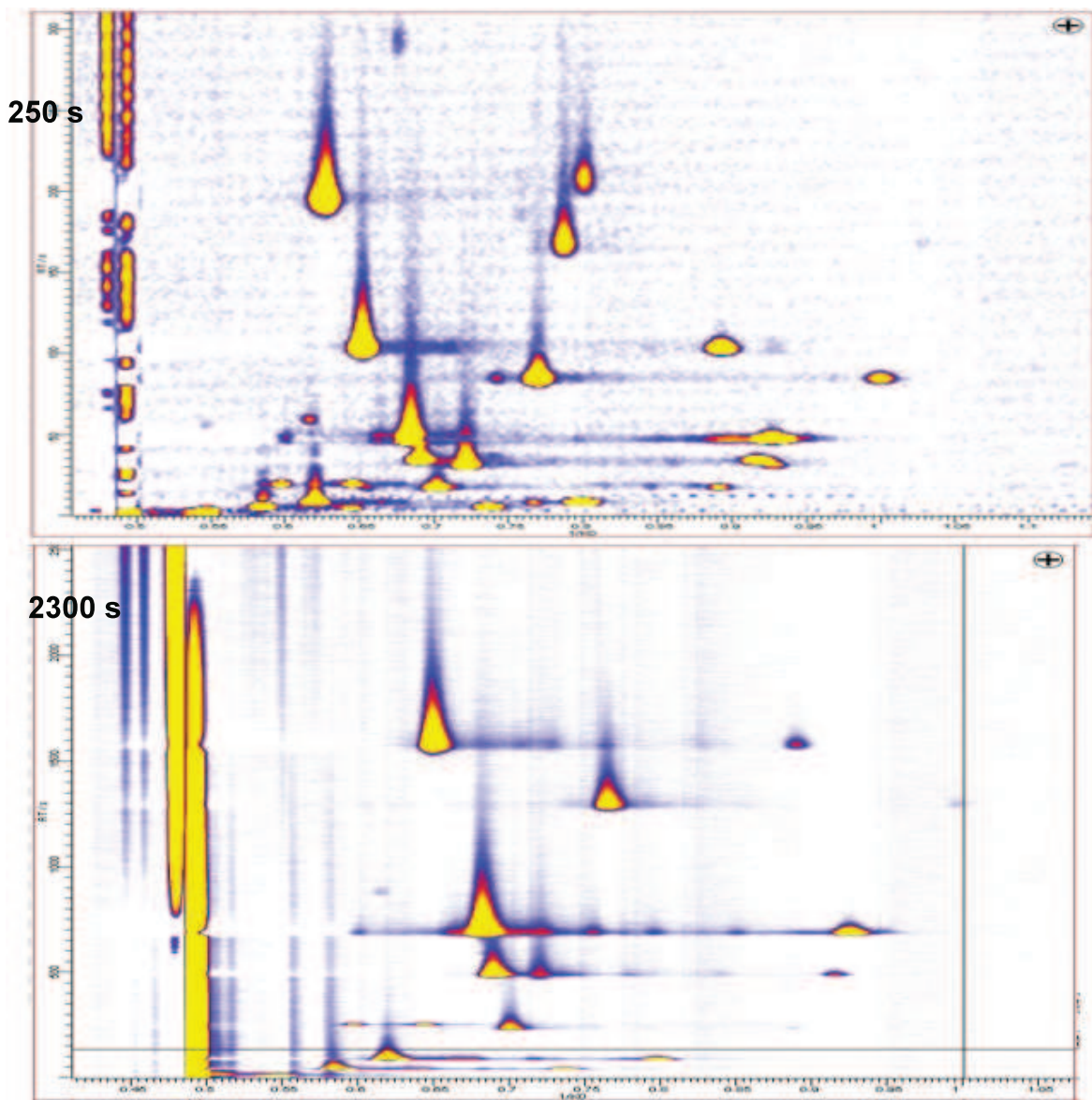
250 s

2300 s

Figure 5.2: A sixteen substance mixture, of compounds usually found in human breath, measured with the two different multi-capillary columns. The chromatogram on top shows the results from the 20 cm long column which takes 250 s to elute out and the 100 cm column, below, takes more than 2300 s to elute out. The list of substances are attached in the Appendix 1.

just under laboratorial conditions but also under clinical and commercial conditions to get better resolved peaks for clinical and medical diagnostics.

5.1   Drift tube design

The new drift tube presented in this study was made up of Teflon pieces, inner diameter 1.5 cm, fit externally with equally spaced brass drift rings connected by 1 MΩ resistors to provide the uniform electric field. Two 3 cm pieces, one 6 cm and one 12 cm piece of the drift tube were constructed which enabled the drift tube length to be varied up to 24 cm in 3 cm steps to suit the demands of the sample matrix. A special voltage supply unit was constructed to enable voltage supply up to 10 kV, Figure 5.3, to enable the same electric field as in the traditional drift tube. The aperture grid and the Faraday plate at the end of the detector remained the same as in the reference IMS.

In the first part of the study the peak characteristics of the RIP in the standard IMS was compared with the different RIPs obtained at various lengths and voltages applied on the high resolution IMS. In the second part of the study, substances which are potential markers of certain diseases found in human breath, which usually form clusters were measured with both the IMS' and their peak characteristics were compared.

5.2   Stability tests

To test out the stability of the new drift tube constructed, measurements of the RIP were carried out at different voltages and different lengths of the drift tube and the results obtained are summarised in, Figures 5.4- 5.6.

Figure 5.4 shows the influence of applied voltage and drift lengths on the drift time. It is obvious that with any particular electric field, the drift time is directly proportional to the drift length (Equation 2.2) and observing this tendency (Figure 5.4 and Figure 5.5) in the newly constructed drift tube made out of smaller pieces proves the stability and reproducibility of the drift tube and the homogeneity of the electric field within the drift region. This initial test also shows that the drift tube can be relied upon to vary the lengths and be used for further measurements of various analytes.
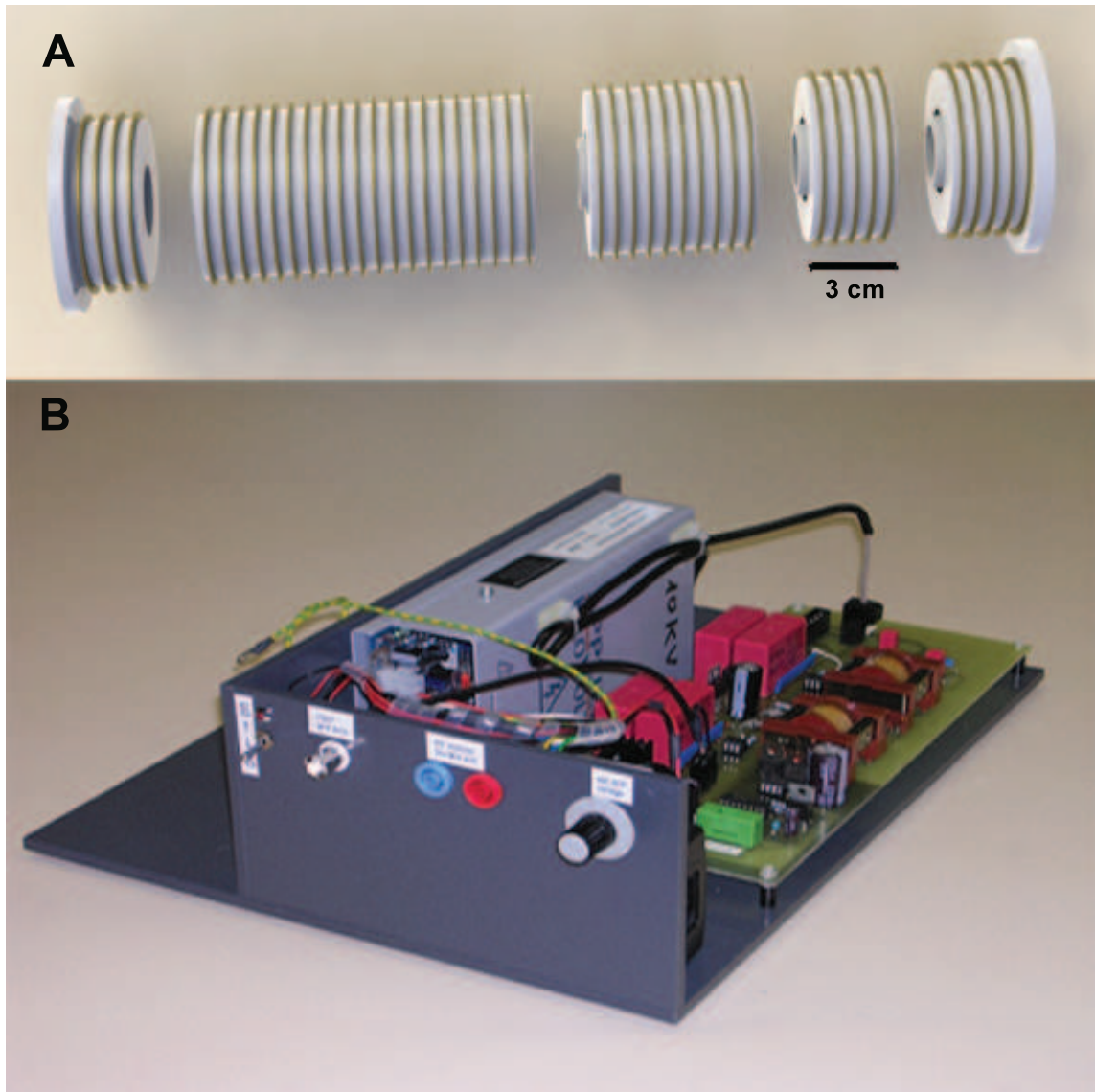
Figure 5.3: The variable length drift tube constructed at ISAS with drift pieces of different lengths, A, along with the electronic unit constructed to provide voltages up to 10.0 kV, B
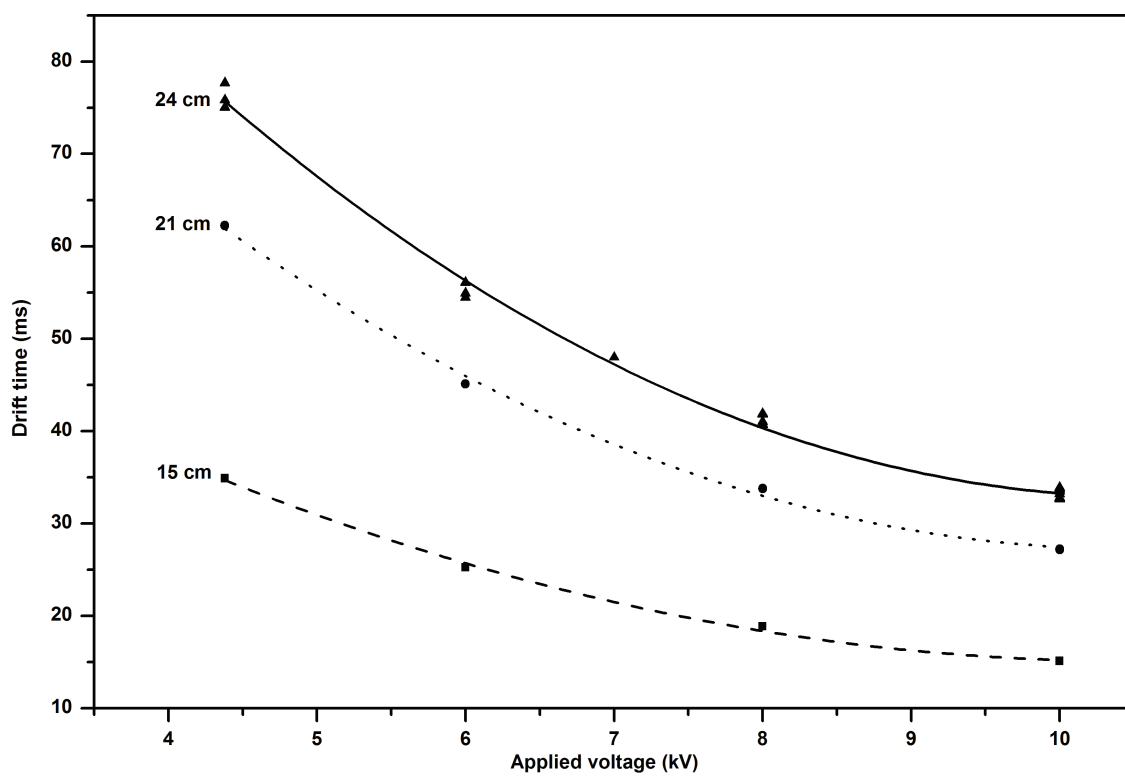
Figure 5.4: Dependency of drift time of the reactant ion peak at various applied voltages with different drift lengths
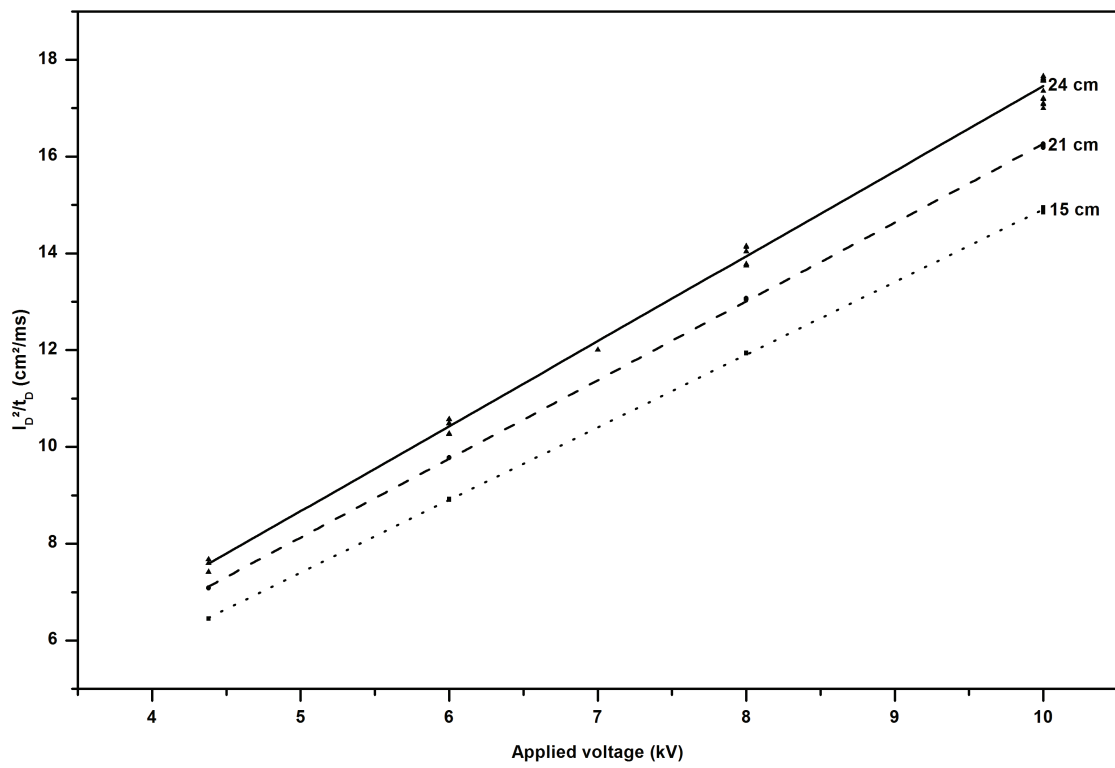
Figure 5.5: Behaviour of the fraction of the squared drift length and drift time to the applied voltage at various drift lengths

In Figure 5.5, we see the confirmation of Equation 2.2 proving the stability of the drift tube to various drift length changes. From Figure 5.4 and Figure 5.5 we have the confirmation that the drift tube made up of smaller drift sections is electrically and mechanically stable to vary the lengths and carry out analytical measurements. With this confirmation, we did one more test to find out the variation of the full width half maximum (FWHM) of the RIP with the applied electric field to establish the final proof of stability of these drift tubes.

The RIP peaks obtained at various drift lengths and electric fields were fit to a Gaussian peak by the Levenberg-Marquardt algorithm and from the fit peaks, the full width at half the maximum intensity (FWHM) was hence found out. It is seen from Figure 5.6 that the FWHM behaves asymptotically with a minimum value of $\cong 0.53$ ms with increasing electric field for the instrument depending on the other parameters of the instrument such as the opening time of the shutter grid, response time of the pre-amplifier which remained unaltered in the new drift tube. This also depends on other factors such as broadening by Coulomb repulsion between the ions in both the reaction region and the drift channel, ion-molecule and ion-ion interactions in the drift region, gate depletion, spatial broadening by diffusion of the ion packet during the drift temperature and pressure inhomogeneities within the spectrometer and capacitive cooling between the aperture grid and the collector [68], [69].

This is mathematically derived as [70],

$$R_d \equiv lim R \left(\frac{t_g}{t_D} \right) \to 0 = \sqrt{\frac{Vez}{16kTln2}} = 0.3\sqrt{\frac{Vez}{kT}} \qquad (5.1)$$

The ever increasing entries in the database of analytes, with their retentions times through the MCC and their characteristic drift time, represented as $1/K_0$, to aid us identify analytes in any chromatogram, any change in the drift length would alter the database completely. But representation of drift time using $1/K_0$ for the ions in the drift channel negates this problem as the RIP is kept constant at one particular $1/K_0$ (0.4854 V.s.cm^{-2} for synthetic air and 0.4950 V.s.cm^{-2} for nitrogen) and the scale thereby calibrated which makes all the analytes retain the same $1/K_0$ though they have different drift times at various drift lengths [71].
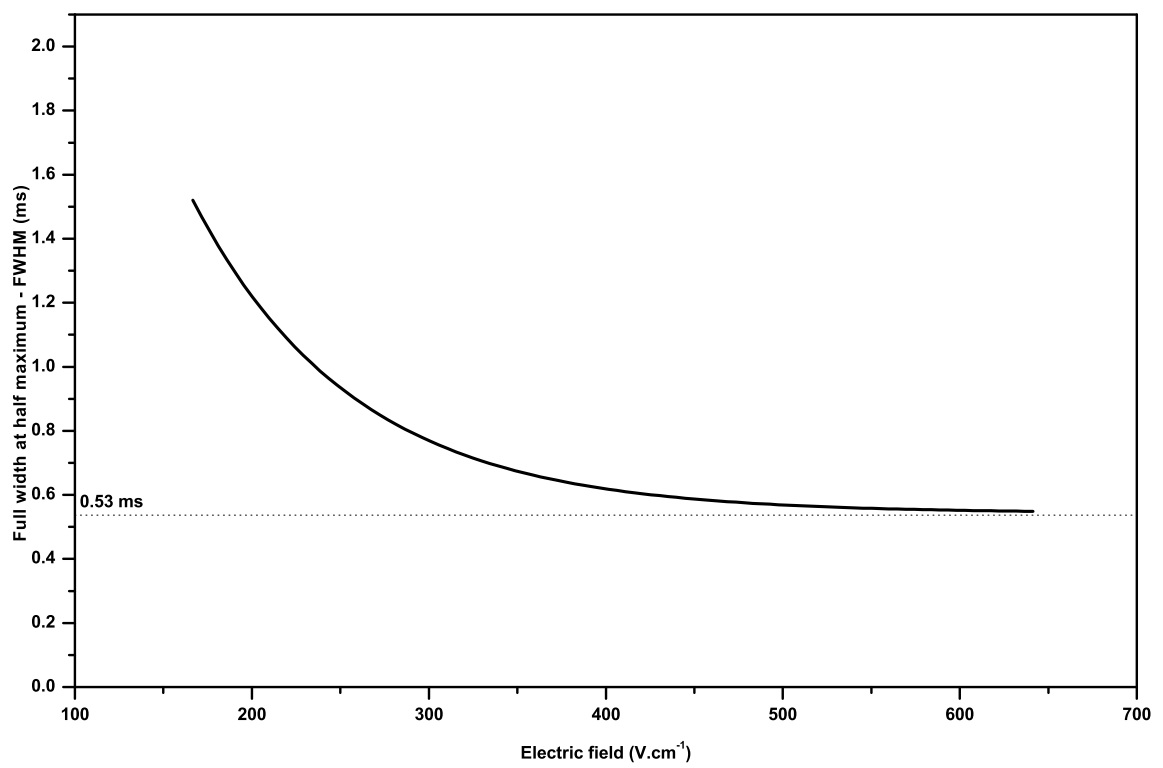
Figure 5.6: Variation of the full width at half maximum of the RIP with the applied electric field

5.3　Analytes resolution

In the next part of the study analytes usually detected in human breath and which tend to form clusters with other peaks were measured at the longest possible drift length at various voltages to find out the resolution.

Acetone (CAS Number 67-64-1), a substance commonly found in human breath in various health conditions, e.g diabetics, was our first substance of interest. The levels of acetone in a person's breath vary depending on their health condition and diet. Hence it is very important to quantify acetone found in the breath [16], [63]. The measurements carried out with the new drift tube at various electric fields are shown in Figure 5.7.
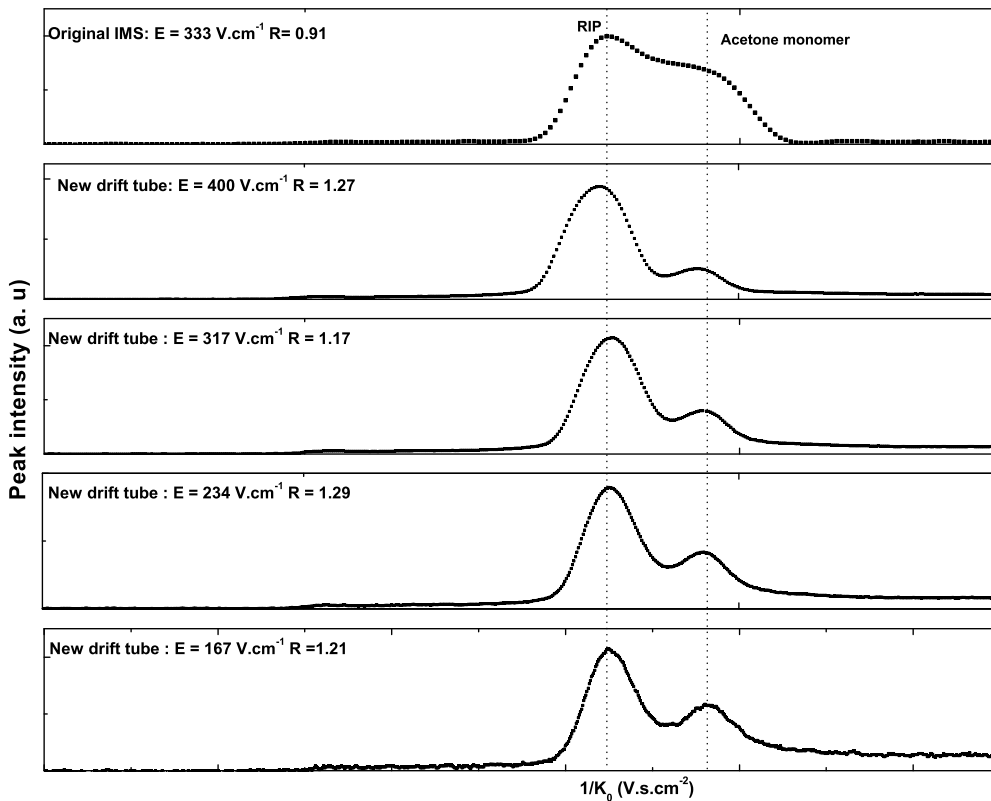
Figure 5.7: The RIP and the monomer peaks of acetone compared with the original IMS. The resolution (R) between the two peaks is shown in each spectrum alongside the corresponding electric field applied.

Figure 5.7 shows that the cluster usually seen between the RIP and the monomer peak of acetone has been resolved at longer drift lengths. The resolution between the two peaks is shown besides each spectrum and the maximum resolution is at E =

234 V·cm^{-1}. It should also be noted that the abscissa which represents $1/K_0$ has not changed for the different voltages as mentioned above, thus aiding in the retention of the existing database of substances to identify peaks in the chromatogram.
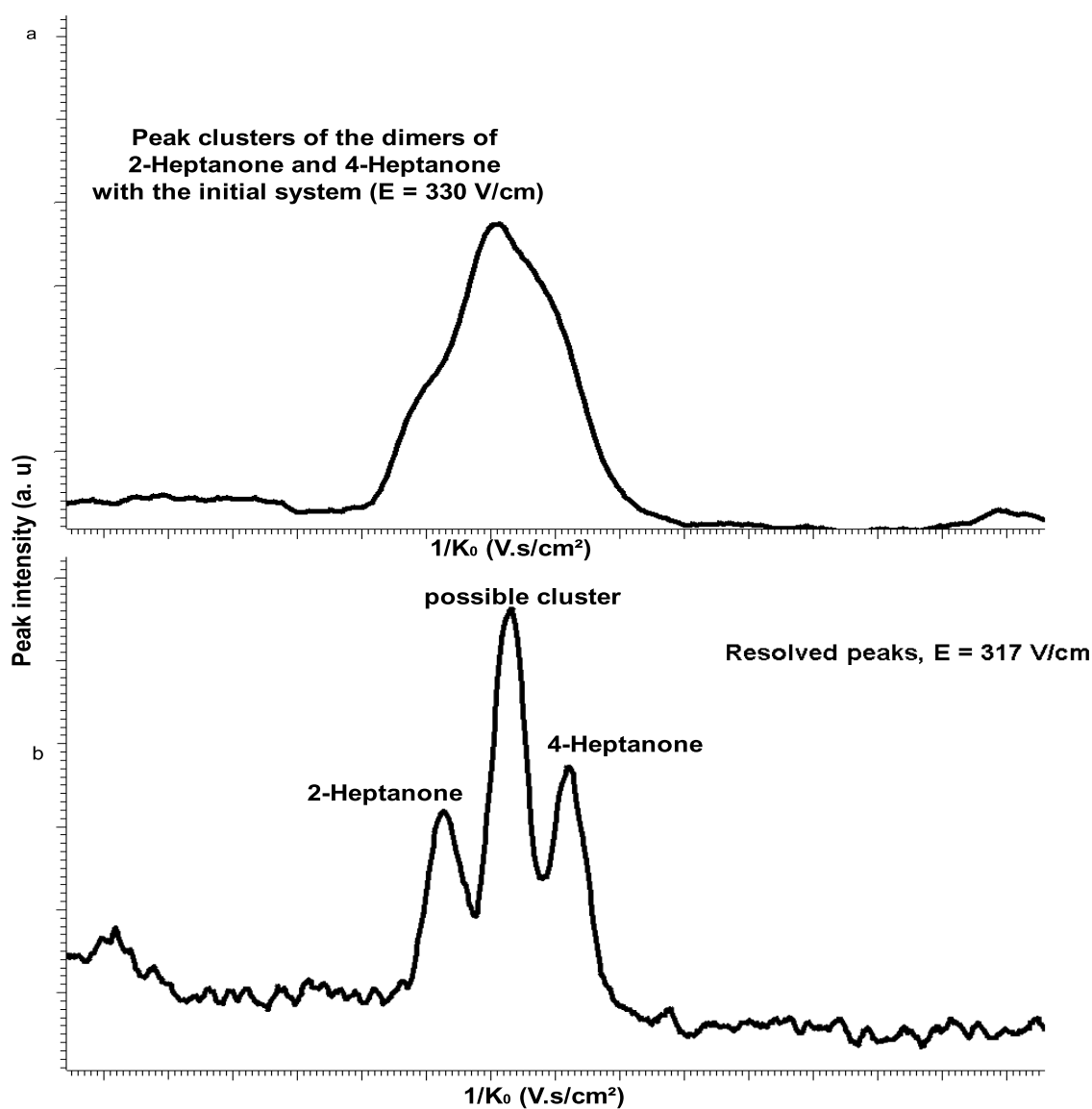

Figure 5.8: Dimer peaks of 2-Heptanone and 4-Heptanone comparison with (a) the traditional IMS and (b) with longer drift length

The next set of analytes used in this study was the dimer peaks of 2-Heptanone (CAS Number 110-43-0) and 4-Heptanone (CAS Number 123-19-3). The two analytes are common substances in human breath that are 'signs of life' which may help in locating trapped people. The analytes are also reported to be seen in urine samples [72], [73]. Furthermore, they are also used as chemical markers in petroleum products and markers for valporic acid therapy [74].

When a mixture of 2-Heptanone and 4-Heptanone is measured with the original IMS, the dimers of the two substances form a cluster which makes the identification of the two peaks almost impossible, Figure 5.8 a. Hence with a longer drift length but with similar electric fields, the substances were measured and the spectrum is shown in Figure 5.8b.

Figure 5.8 shows that the peak cluster seen when a mixture of 2-Heptanone and 4-Heptanone measured with the traditional IMS, Figure 5.8 a, is clearly resolved with the longer drift tube, Figure 5.8 b. A third peak which could be a cluster of one of the analytes is also seen in the spectrum.

Chapter 6

Summary and Outlook

Ion mobility spectrometry, a method time tested for its sensitivity, rapid separation, ruggedness, reproducibility, low costs and functionality at normal temperature and pressure conditions, has established a very strong foothold in the field of medical and biological applications over the past decade. Many clinics have started using this method for breath analysis to identify markers of various health conditions and particular diseases.

There are however, certain drawbacks associated with this technique. One of the major disadvantage is the complexity and humidity of the samples from the fields of biology and medicine. The Multi-Capillary Column, used as a pre-separation unit helps users negate humidity from the samples. The other major disadvantage of an IMS is the inability to directly identify the peaks detected during the measurement. With the IMS being used every day for newer applications, it was necessary to identify almost all the peaks detected by the instrument in the complex sample without time consuming and costly reference measurements. An unknown and a complex sample matrix could give a lot of unidentified peaks in the resultant IMS chromatogram.

A linear correlation between the number of carbon atoms with the inverse reduced ion mobilities of polar aliphatic organic compounds was used to predict inverse ion mobility values of other analytes in the same homologous series. This empirical prediction method proves that the inverse reduced mobilities of analytes in the IMS can be predicted very accurately from known values of the analytes in the same homologous series. The prognosis of compounds performed in this study, will considerably facilitate preliminary identification by reducing the possibility of unknown substances that could be associated with a peak in the IMS chromatogram without the costly and time consuming reference measurements currently employed. Similar mass mobility trends

are also observed in other classes of compounds such as amino acids and other groups of compounds of biological interest, and such an empirical method can be extended to these series, too.

This prognosis can be extended to other homologous series in order to develop a generalised equation for the prediction of the reduced ion mobility with different variables for every series depending on the molecular structure of the analyte. This would also lead to an extension of analytes' database with the predicted values from which the responsible analyte for any unknown peak in an IMS chromatogram could be identified. However, the theoretical correlation of the presented approach to the molecular structure of the analyte and to the behaviour of its ions in the drift gas under the influence of the electric field requires further investigations.

Such predictions will assist peak characterisations using Breit-Wigner-Functions and simulations of the shape of peaks in 3-D plots of IMS-chromatograms and allow forecast of peak positions within the drift time-retention time-intensity space. Furthermore, it could be helpful to reduce false alarms and to separate overlapping signals [75].

The splitting of the collision integral (Ω_D) into two terms (Ω_C, Ω_S), performed in this study (Chapter 4), was done empirically to draw comparisons with the linear equation for reduced ion mobilities obtained from the prognosis data and the Mason-Schamp equation and to get a better understanding of the same. Even though this study has not dealt deeply into the various forces that play a role during collisions, such as electrostatic and van der Waals forces, this opens up new insights into the behavioral trend seen in a homologous series. This will also give new inputs to the various models that describe the collisions taking place between the ion swarm and the neutral drift molecules in an electric field and find out if the size/volume increase in a compound/ion would have a direct relationship with the mobility data [76]. This in turn may also help in modeling the charge distribution within large organic ions and its effects on the mobility values which remains a void until now [1], [51].

This study has also shown the effects of drift length and voltage changes to resolve peak clusters without altering the database by using $1/K_0$ to represent ion mobility rather than drift time. The state of the art drift tube constructed for this study, can be varied in length depending on the complexity of the substance measured and a suitable voltage supply thus being applied. The stability of drift section made up of small drift pieces, could be used in research to effectively resolve clusters with a higher resolution.

Acetone, 2-Heptanone and 4-Heptanone are detected in every human breath at various concentration levels depending on the health condition of the subject. It is therefore very important to know the exact concentration of these substances in the human breath for any diagnosis. The peak clusters seen during the measurement of these substances have been resolved with the newly constructed drift tube in this study.

The first studies carried out in this article are just the onset of a new generation of drift tubes with variable lengths in ion mobility spectrometry. These drift tubes can be used in clinics where human breath is being measured and analysed for a multitude of markers for various diseases by tuning the drift tube suitably for the particular marker being searched for rather than having many different drift tubes/IMS for various health conditions. Further studies regarding the sensitivity of this high resolution instrument with change in drift lengths, water molecule fragments and clusters due to change in drift lengths and variation in peak parameters at constant electric fields by varying the voltage supply and length are areas which have to be studied more thoroughly to establish these drift tubes for high resolution ion mobility spectrometry in medical and biological applications.

6.1   Future Work

The IMS could be described as an "adolescent" in the field of medicine and biology. The complexity of the samples being analysed in these fields are increasing day by day. With increasing complexity, the science that can be incorporated into this field is enormous. The study carried out paves way for some interesting future work in the field of physics, chemistry and engineering.

The empirical prediction, as stated above, when extended to all possible series of compounds would give an exhaustive database of ion mobilities of substances which would ease the process of compound identification. This process will obviously reduce the time consuming compound identification process, like parallel Mass spectrometric measurements and thereby provide users an idea as to what the detected compound could be. This pre-identification process could also be made on-line where the compounds detected are immediately narrowed down for identification using their ion mobilities and retention time during data acquisition. This would also reduce the time consuming analysis done after every IMS measurement.

The two types of plausible collisions described in this study, Chapter 4, could finally provide a clear, correct and a complete ion-neutral collision model to describe the collisions in a drift tube. This work is already under way by Dr. Glenn Spanlger from the United States. When this model is complete, using quantum mechanics and classical mechanics, ion mobility spectrometrists can finally understand the collision cross section completely.

The state of the art drift tube engineered in this study could be used to create tailor made IMS suiting individual applications. This technology could also be the starting point for creating miniaturized and hand held IMS devices which could reach out the common man to test his breath for specific substances. This should envisage as a very vital breakthrough in the field of medicine and biology.

Bibliography

[1] G. A. Eiceman and Z. Karpas, *Ion Mobility Spectrometry*. 1995.

[2] F. W. Karasek, "The plasma chromatograph," *Research and Development*, vol. 21, pp. 34–37, 1970.

[3] J. I. Baumbach and M. Westhoff, "Ion mobility spectrometry to detect lung cancer and airway infections," *Spectroscopy Europe*, vol. 18, pp. 22–27, 2006.

[4] W. Vautz and J. I. Baumbach, "Exemplar applications of multi-capillary column ion mobility spectrometry for biological and medical purpose," *Internation Journal of Ion mobility spectromerty*, vol. 11, pp. 35–41, 2008.

[5] V. Ruzsanyi, J. I. Baumbach, and G. A. Eiceman, "Detection of the mold markers using ion mobility spectrometry," *International Journal of Ion Mobility Spectrometry*, vol. 6, pp. 53–57, 2003.

[6] S. Prasad, K. M. Pierce, H. Schmidt, J. V. Rao, R. Güth, S. Bader, R. E. Synovec, G. B. Smith, and G. A. Eiceman, "Analysis of bacteria by pyrolysis gas chromatography-differential mobility spectrometry and isolation of chemical components with a dependence on growth temperature.," *The Analyst*, vol. 132, no. 10, pp. 1031–9, 2007.

[7] S. Prasad, H. Schmidt, P. Lampen, M. Wang, R. Güth, J. V. Rao, G. B. Smith, and G. A. Eiceman, "Analysis of bacterial strains with pyrolysis-gas chromatography/differential mobility spectrometry," *The Analyst*, vol. 131, no. 11, p. 1216, 2006.

[8] W. Chaim, "New technology for diagnosis of bacterial vaginosis," *European Journal of Obstetrics & Gynecology and Reproductive Biology*, vol. 111, no. 1, pp. 83–87, 2003.

[9] Z. Karpas, "Determination of volatile biogenic amines in muscle food products by ion mobility spectrometry," *Analytica Chimica Acta*, vol. 463, no. 2, pp. 155–163, 2002.

[10] A. P. Snyder, D. B. Shoff, G. A. Eiceman, D. a. Blyth, and J. A. Parsons, "Detection of bacteria by ion mobility spectrometry," *Analytical Chemistry*, vol. 63, no. 5, pp. 526–529, 2002.

[11] P. B. Harrington, T. L. Buxton, and G. Chen, "Classification of Bacteria by Thermal Methylation Hydrolysis Ion Mobility Spectrometry Using SIMPLISMA and Multidimensional Wavelet Compression," *International Journal for Ion Mobility Spectrometry*, vol. 4, no. 2, pp. 148–151, 2001.

[12] M. Shnayderman, B. Mansfield, P. Yip, H. A. Clark, M. D. Krebs, S. J. Cohen, J. E. Zeskind, E. T. Ryan, H. L. Dorkin, M. V. Callahan, T. O. Stair, J. A. Gelfand, C. J. Gill, B. Hitt, and C. E. Davis, "Species-specific bacteria identification using differential mobility spectrometry and bioinformatics pattern recognition.," *Analytical chemistry*, vol. 77, no. 18, pp. 5930–7, 2005.

[13] M. Basanta, T. Koimtzis, and C. L. P. Thomas, "Sampling and analysis of exhaled breath on human subjects with thermal desorption- gas chromatography-differential mobility spectrometry," *International Journal for Ion Mobility Spectrometry*, vol. 9, pp. 45–49, 2006.

[14] M. Westhoff, V. Ruzsanyi, P. Litterst, L. Freitag, and J. I. Baumbach, "Ion mobility spectrometry - a new method for the fast detection of sarkoidose in human breath ?- preliminary results of a feasible study," *Journal of Physiology and Pharmacology*, vol. 58, pp. 739–751, 2007.

[15] W. Vautz, J. I. Baumbach, M. Westhoff, K. Züchner, E. T. H. Carstens, and T. Perl, "Breath sampling control for medical application," *International Journal for Ion mobility spectrometry*, vol. 13, p. 41, 2010.

[16] V. Ruzsanyi, J. I. Baumbach, S. Sielemann, P. Litterst, M. Westhoff, and L. Freitag, "Detection of human metabolites using multi-capillary columns couple to ion mobility spectrometers," *Journal of Chromatography A*, vol. 1084, pp. 145–151, 2005.

[17] S. Neuhaus, "Untersuchung von entzündungsmediatoren mittels multikapillarsäulen-ionenmobilitätsspektrometrie im murinen asthma-modell," *Ruhr-universität Bochum*, 2010.

[18] W. Vautz, J. Nolte, R. Fobbe, and J. I. Baumbach, "Breath analysis - performance and potential of ion mobility spectrometry," *Journal of Breath Research*, vol. 3, pp. 1–8, 2009.

[19] T. Perl, E. Carstens, A. Hirn, M. Quintel, W. Vautz, J. Nolte, and M. Junger, "Determination of serum propofol concentrations by breath analysis using ion mobility spectrometry," *British Journal of anaesthesia*, vol. 103, p. 822, 2009.

[20] J. I. Baumbach, W. Vautz, V. Ruzsanyi, and L. Freitag, *Early detection of lung cancer: Metabolic profiling of human breath with ion mobility spectrometer.* 2008.

[21] S. Sielemann, "Detektion flüchtiger organischer verbindungen mittels ionenmobilitätsspektrometrie und deren kopplung mit multi-kapillar-gaschromatographie," *Technische Universität Dortmund*, 1999.

[22] M. Junger, B. Boedeker, and J. I. Baumbach, "Peak assignment in multi-capillary column-ion mobility spectrometry using comparative studies with gas chromatography-mass spectrometry for voc analysis," *Analytical and Bioanalytical Chemistry*, vol. 396, pp. 471–482, 2009.

[23] M. D. Wesel, J. M. Sutter, and P. C. Jurs, "Prediction of reduced ion mobility constants of organic compounds from molecular structure," *Analytical Chemistry*, vol. 68, pp. 4237–4243, 1996.

[24] M. D. Wesel and P. C. Jurs, "Prediction of reduced ion mobility constants from structural information using multiple linear regression analysis and computational neural networks," *Analytical Chemistry*, vol. 66, pp. 2480–2487, 1994.

[25] W. C. Röntgen, "Eine neue art von strahlen," *Science*, vol. 3, p. 726, 1896.

[26] P. Langevin, "Une formule fondamentale de theorie cinnetique," *Ann. de Chim. et de Phys.*, vol. 5, pp. 245–288, 1905.

[27] P. Langevin, "Recombinaison et mobilites des ions dans les gaz," *Ann Chim Phys*, vol. 28, pp. 289–384, 1903.

[28] M. J. Cohen and F. W. Karasek, "Plasma chromatography - a new dimension for gas chromatography and mass spectrometry," *Journal of Chromatographic Science*, vol. 8, pp. 330–337, 1970.

[29] J. Stach and J. I. Baumbach, "Ion mobility spectrometry - basic elements and applications," *International Journal for Ion Mobility Spectrometry*, vol. 5, pp. 1–21, 2002.

[30] R. Louis and H. Hill, "Ion mobility spectrometry in analytical chemistry," *Analytical Chemistry*, vol. 21, pp. 321–355, 1990.

[31] G. E. Spangler and M. J. Cohen, *Instrument design and description in plasma chromatography.* 1984.

[32] M. M. Metro and R. A. Keller, "Fast scan ion mobility spectra of diethyl, dipropyl and dibutyl ethers as determined by the plasma chromatograph," *Journal of Chromatography Science*, vol. 11, p. 520, 1973.

[33] G. E. Spangler and P. A. Lawless, "Ionization of nitrotoluene compounds in negative plasma chromatography," *Analytical Chemistry*, vol. 50, p. 884, 1978.

[34] A. E. O'Keefe and G. C. Ortman, "Primary standards for trace gas analysis," *Analytical Chemistry*, vol. 38, p. 760, 1966.

[35] R. L. Grob, *Modern practices of gas chromatography.* 1977.

[36] A. A. Nanji, A. H. Lawrence, and N. Z. Mikhael, "Use of skin surface sampling and ion mobility spectrometry as a preliminary screening method for drug detection in an emergency room," *Clinical Toxicology*, vol. 25, p. 501, 1987.

[37] S. D. Huang, L. Kolaitis, and D. M. Lubman, "Detection of explosives using laser desorption in ion mobility spectrometry/mass spectrometry," *Applied Spectroscopy*, vol. 41, p. 1371, 1987.

[38] G. E. Spangler and C. I. Collins, "Reactant ions in negative ion plasma chromatography," *Analytical Chemistry*, vol. 47, p. 393, 1975.

[39] W. Vautz and M. Schmäh, "Hovacal - a generator for multi component humid calibration gases," *International Journal for ion mobility spectrometry*, vol. 12, pp. 139–147, 2009.

[40] R. C. Weast, *CRC handbook of chemistry and physics.* 1972.

[41] N. E. Bradbury and R. A. Nielson, "Absolute values of the electron mobility in hydrogen," *Physics reviews*, vol. 49, p. 388, 1936.

[42] A. M. Tyndall, *The mobility of positive ions in gases.* 1938.

[43] E. D. Pellizzari, "Electron capture detection in gas chromatography," *Journal of Chromatography*, vol. 98, p. 323, 1974.

[44] A. Good, D. A. Dunder, and P. Kebarle, "Ion-molecule reactions in pure nitrogen and nitrogen containg traces of water at total pressures of 0.5 - 4 torr," *Journal of Chemical Physics*, vol. 52, p. 212, 1970.

[45] J. C. Tou, T. Ramstad, and T. J. Nestrick, "Electron mobility in a plasma chromatograph," *Analytical Chemistry*, vol. 51, pp. 780–783, 1979.

[46] J. A. Stockdale, L. G. Christouphorou, and G. S. Hurst, "Capture of thermal electrons by oxygen," *Journal of Chemical Physics*, vol. 47, pp. 3267–3269, 1967.

[47] T. W. Carr, "Comparison of the negative reactant ions formed in the plasma chromatograph by nitrogen, air and sulphur hexafluoride as the drift gas with air as the carrier gas," *Analytical Chemistry*, vol. 51, p. 705, 1979.

[48] A. G. Harrison, *Chemical ionization Mass spectrometry*. 1983.

[49] F. W. Karasek and G. E. Spangler, *Theory and practice in chromatography*. 1981.

[50] A. Fick, "über diffusion," *Annales de Physique*, vol. 170, pp. 59–86, 1855.

[51] E. W. McDaniel and E. A. Mason, *The mobility and diffusion of ions in gases*. 1973.

[52] R. Zwanzig, "Time correlation functions and transport coefficients in statistical mechanics," *Ann. Rev. phys. Chem.*, vol. 16, pp. 67–102, 1965.

[53] H. E. Revercomb and E. A. Mason, "Theory of plasma chromatography/gaseous electrophoresis," *Analytical Chemistry*, vol. 47, p. 970, 1975.

[54] E. A. Mason, *Ion mobility: its role in plasma chromatography*. 1984.

[55] E. A. Mason and E. W. McDaniel, *Transport properties of ions in gases*. 1987.

[56] F. J. Knorr, R. L. Eatherton, W. F. Siems, and H. H. Hill, "Fourier transform ion mobility spectrometry," *Analytical Chemistry*, vol. 57, p. 402, 1985.

[57] W. C. Blanchard, "Control of ion tof increases performance of chemical sensor," *Research and Development*, p. 50, 1988.

[58] W. Siems, C. Wu, E. Tarver, and H. H. Hill, "Measuring the resolving power of ion mobility spectrometers," *Analytical Chemistry*, vol. 66, pp. 4195–4201, 1994.

[59] G. R. Asbury and H. H. Hill, "Evaluation of ultra high resolution ion mobility spectrometry as an analytical separation device in chromatographic terms," *Journal of Microcolumn separations*, vol. 12, pp. 172–178, 2000.

[60] B. Vautz, W Boedecker, S. Bader, and J. I. Baumbach, "Recommendation of a standard format for data sets from gc-ims with sensor controlled sampling," *International Journal for Ion mobility spectrometry*, vol. 11, pp. 71–76, 2008.

[61] B. Boedecker, W. Vautz, and J. I. Baumbach, "Visualization of mcc-ims data," *International Journal for Ion mobility spectrometry*, vol. 11, pp. 77–81, 2008.

[62] L. K. Schnackenberg and R. D. Berger, "Monitoring the health to disease continuum with global metabolic profiling and systems biology," *Pharmacogenomics*, vol. 7, pp. 1077–1086, 2006.

[63] C. Deng, J. Zhang, X. Yu, and X. Zhang, "Determination of acetone in human breath by gas chromatography-mass spectrometry and solid phase microextraction with on fibre derivatization," *Journal of Chromatography B*, vol. 810, pp. 269–275, 2004.

[64] B. Boedecker, W. Vautz, and J. I. Baumbach, "Peak finding and referencing in mcc-ims data," *International Journal for Ion mobility spectrometry*, vol. 11, pp. 83–87, 2008.

[65] B. Boedecker, W. Vautz, and J. I. Baumbach, "Peak comparison in mcc-ims data - searching for potential bio markers in human breath," *International Journal for Ion mobility spectrometry*, vol. 11, pp. 89–93, 2008.

[66] J. Aisbett, J. M. Blatt, and A. H. Opir, "General calculation of the collision integral for the linearized boltzmann transport equation," *Journal of Statistical Physics*, vol. 11, pp. 441–456, 1974.

[67] K. Tang, A. Shvartsburg, H. Lee, D. Prior, M. Buschbach, F. Li, A. Tolmachev, G. Anderson, and R. D. Simth, "High sensitivity ion mobility spectrometry/mass spectrometry using electrodynamic ion funnel inter phases," *Analytical Chemistry*, vol. 77, pp. 3330–3339, 2005.

[68] D. Davis, C. Harden, D. Shoff, S. Bell, G. A. Eiceman, and R. Ewing, "Analysis of ion mobility spectra for mixed vapours using gaussian deconvolution," *Analytica Chimica Acta*, vol. 289, pp. 263–272, 1994.

[69] P. Dugourd, R. R. Hudgins, D. E. Clemmer, and M. F. Jarrold, "High resolution ion mobility spectrometry measurements," *Reviews in scientific instrumentation*, vol. 68, pp. 1122–1129, 1997.

[70] C. Wu, W. Siems, R. Asbury, and H. H. Hill, "Electrospray ionization high resolution ion mobility spectrometry- mass spectrometry," *Analytical Chemistry*, vol. 70, pp. 4929–4938, 1998.

[71] B. Vautz, W Boedecker, S. Bader, and T. Perl, "An impeccable approach to obtain reproducible reduced ion mobilities," *International Journal for Ion mobility spectrometry*, vol. 12, pp. 47–57, 2009.

[72] M. Statherropolous, E. Sianos, A. Agapiou, A. Georgiadou, A. Pappa, N. Tzamtzis, H. Giotaki, C. Papageorgiou, and D. Kolostoumbis, "Preliminary investigation using volatile organic compounds from human expired air, blood and urine for locating entrapped people in earthquakes," *Journal of Chromatography B*, vol. 822, pp. 112–117, 2005.

[73] S. Smith, H. Burden, R. Persad, K. Whittington, B. deLacy, N. Ratcliffe, and C. Probert, "A comparative study of the analysis of human urine head space using gas chromatography-mass spectrometry," *Journal of Breath research*, vol. 2, pp. 184–193, 2008.

[74] S. Erhart, A. Amman, E. Haberlandt, G. Edlinger, A. Schmid, W. Filipiak, K. Schwarz, P. Mochalski, K. Rostasy, D. Karall, and S. Scholl, "3-heptanone as a potential new marker for valporic acid therapy," *Journal of Breath research*, vol. 3, pp. 376–381, 2009.

[75] D. Vogtland and J. I. Baumbach, "Breit-wigner-function and ims-signals," *International Journal of Ion Mobility Spectrometry*, vol. 12, pp. 109–114, 2009.

[76] G. E. Spangler, "The effects of cluster thermo chemistry on the energetics of an ion in ims," *International Journal of Ion Mobility Spectrometry*, vol. 5, pp. 42–75, 2002.

List of Publications [1]

I. Hariharan C, Baumbach J I, Vautz W (2009), Empirical prediction of reduced ion mobilities of secondary alcohols, Int. J. Ion Mob. Spec., 12:59-63

II. Hariharan C, Baumbach J I, Vautz W (2010), Linearized equations for the reduced ion mobilities of polar aliphatic organic compounds, Anal. Chem., 82:427-31

III. Hariharan C, Seifert L, Baumbach J I, Vautz W(2011) Novel design for drift tubes in ion mobility spectrometry for optimised resolution of peak clusters, Int. J. Ion Mob. Spec, 14(1):31-38

IV. Vautz W, Schwarz L, Hariharan C, Schlling M (2010) Ion Characterisation by comparison of ion mobility spectrometry and mass spectrometry data, Int. J. Ion Mob. Spec, 13:121-129

---

[1]The complete manuscripts of the publications enlisted have been attached as scanned copies in the Appendix section.

List of Figures

List of Tables

List of Symbols

IMS	Ion Mobility Spectrometer
ng·L^{-1}	nanograms per liter
ppb$_v$	parts per billion (volume)
pg·L^{-1}	picograms per liter
ppt$_v$	parts per trillion (volume)
MCC-IMS	Multi-capillary column Ion Mobility Spectrometer
GC-MS	Gas-chromatography - Mass spectrometry
V·cm^{-1}	Volts per centimeter
v$_D$	Drift velocity
l$_D$	Drift length
E	Electric field strength
K	Ion mobility
t$_D$	Drift time
cm^2·V^{-1}·s^{-1}	square centimeters per volt per second
V	Applied voltage
T$_0$	Standard temperature (273 Kelvin)
P$_0$	Standard pressure (101325 Pascals)
K$_0$	Reduced ion mobility
R$_T$	Retention time
mL·min^{-1}	milliliters per minute
MΩ	Megaohm
ms	milliseconds
^{63}Ni	Nickel 63 isotope
eV	electron volts
MALDI	Matrix assisted Laser Desorption/Ionisation
RIP	Reactant ion peak
R$_p$	Resolving power
w$_h$	Peak width at half peak intensity
R	Resolution
J	Ionic flux density
k	Boltzmann constant (1.380 e^{-23} Joules per Kelvin)
Ω$_D$	collision cross section
Mbq	Megabecquerel
m	Mass of ion
M	Mass of neutral drift gas

Appendix

Table 1: List of sixteen substances used as standards in Chapter 5

Substance	Reduced ion mobility	Retention time at 40°C
	(V·s·cm^{-1})	(s)
Acetone	0.544	2.5
2-Hexanone	0.582	7.6
2-Heptanone	0.617	15.7
2-Octanol	0.698	26.2
Limonene	0.593	28.9
1-Octanol	0.717	44.7
2-Nonanone	0.688	50.3
Isopulegol	0.682	70.0
Naphthalene	0.544	81.4
Menthol	0.602	94.7
Decanal	0.772	130.9
Carvon	0.650	155.0
1-Decanol	0.783	255.5
Thymol	0.626	296.0
2-Undecanol	0.795	313.7
Propofol	0.674	444.4

Publications from this research

ORIGINAL RESEARCH

Empirical prediction of reduced ion mobilities of secondary alcohols

Chandrasekhara Hariharan · Jörg Ingo Baumbach · Wolfgang Vautz

Abstract Ion Mobility Spectrometry is a powerful method for the rapid identification of gas-phase analytes and finds its usage in various fields including the sensitive analysis of extremely complex and humid mixtures such as human breath when additional pre-separation techniques are applied. The output data from an ion mobility spectrometer (IMS), equipped with a Multi-Capillary Column (MCC) for pre-separation, is a chromatogram of the signal intensity versus a particular retention time and a specific reduced ion mobility which are the characteristics of the detected analyte. Hence, it is important to have a database of analytes with both the values for comparison and identification of peaks in any IMS chromatogram. Commonly, such databases are collected by measurements of reference analytes. It is obvious that a prognosis of the values, without the time consuming and costly reference measurements, would be a considerable facilitation for a preliminary identification of unknowns and development of databases. In this study, a correlation between the reduced ion mobilities and the number of carbon atoms was found for secondary alcohols. The correlation was then used to predict the reduced ion mobilities of other analytes in the same homologous series. To verify the accuracy of the prognosis, the analytes were measured individually using a ^{63}Ni-MCC-IMS and compared to the predicted values. The results of the prognosis show an accuracy higher than 99.5%.

Keywords Ion mobility spectrometry · Database · Secondary alcohols · Empirical prediction · Reduced ion mobility · Homologous series

C. Hariharan (✉) · J. Ingo Baumbach · W. Vautz
ISAS — Institute for Analytical Sciences,
Bunsen-Kirchhoff-Straße 11,
Dortmund 44139, Germany
e-mail: hariharan@isas.de

Introduction

Over the past few decades, ion-mobility spectrometry has evolved into an inexpensive and powerful technique for the detection of trace compounds in the lower ng/L (ppb$_v$) down to pg/L (ppt$_v$) range, for direct monitoring of specific compound classes such as chemical warfare agents and drugs of abuse [1, 2]. However, in recent years, ion mobility spectrometers are increasingly in demand for new applications specifically on biological samples (cells, fungi, bacteria) [3–12], in medicine (diagnosis, therapy and medication control e.g. from breath analysis) [3, 4, 13, 14] and process control [15–22]. For such applications, IMS measurements faces challenges such as humid and rather complex samples, requirement of a specific sampling procedure adapted to the application, fast pre-separation techniques like multi-capillary columns and most importantly, suitable data processing techniques which include databases of relevant analytes for automatic characterisation of the signals detected in an IMS chromatogram [23–28], and different data pre-processing steps [29–32].

Till recently, IMS have been used to detect specific target analytes with known reduced ion mobility. For the analysis of complex mixtures, the reduced mobility alone will not be sufficient for the identification of analytes in the mixture. Several analytes have similar or even the same mobility [4]. Hence, additional rapid pre-separation techniques are applied. The time taken by an analyte to elute out of the MCC is termed as the retention time (t_R) of the analyte. Thus, for every analyte, there is a specific reduced ion mobility value and a retention time which are the characteristics of a particular analyte at a specific temperature, column length and flow. Providing this database of relevant analytes for every analysis enables the identification of compounds in an unknown complex mixture.

🖄 Springer

Table 1 Experimental
parameters of [63]Ni-MCC-IMS

Experimental Parameters	
Ionisation source	β radiation ([63]Ni, 550 MBq)
Grid opening time	300 μs
Spectral length / Sample interval	100 ms
Spectral resolution	40 kHz
Drift length	120 mm
Electric field intensity	310 V/cm
Drift gas & carrier gas	Synthetic air
Drift gas flow	100 mL/min
Carrier gas flow	150 mL/min
Pre-separation	MCC OV-5, 40°C (constant), 20 cm

During the analysis of complex mixtures, e.g. human breath, volatile organic compounds from bacteria etc., there are many unknown peaks in the IMS chromatogram. Identifying them is one of the major problems. There are a huge number of analytes available from which one could select, measure and identify the unknown peak. Most applicable solution is the additional sampling on adsorption materials and analysis by GC/MS. From such analysis, substances possibly responsible for the unknown signals could be proposed. This proposal has to be validated by IMS measurements of the reference analyte. Obviously, such a procedure is time consuming and expensive. Thus, additional tools for the identification of unknown analytes would be very helpful. There have been earlier attempts to calculate the ion mobility of analytes directly from the molecular structure using computational neural networks and multiple linear regression analysis [33, 34]. But, these methods are seemingly complex when compared to the prediction method proposed in this study and hence cannot be used for online characterisation of complex mixtures.

In this study, a rather simple method to see trends with the secondary alcohols between the inverse reduced ion mobility and the number of carbon atoms in the analyte is used to predict the reduced ion mobilities of other unmeasured analytes in that particular homologous series directly.

Experimental

Ion mobility spectrometry

In the drift tube—under the influence of an external electric field and with a particular drift gas—ions of different masses and /or structure reach different velocities and thus, get separated [2]. The quotient of ion velocity and electric field strength is referred to as ion mobility [35]. The mobility, K, is calculated using the measured drift time, t_D, of an ion through a specified drift length, l_D, under a known electric field, E, using the equation below [1, 2].

$$v_d = \frac{l_D}{t_D} \tag{1}$$

$$v_D = K*E \tag{2}$$

Table 2 Measured, predicted and validated inverse reduced ion mobility values of secondary alcohols

|	Analyte	No. of Carbon atoms	Measured $1/K_0$ in V.s.cm^{-2}	Measured K_0 in cm^2.V^{-1}s^{-1}	std. dev. in V.s.cm^{-2}	Predicted $1/K_0$ in V.s.cm^{-2}	Accuracy in %
Measured	2-Hexanol	6	0.6306	1.586	0.0003		
	2-Heptanol	7	0.6642	1.506	0.0003		
	2-Octanol	8	0.6988	1.431	0.0006		
	2-Undecanol	11	0.7979	1.253	0.0012		
Predicted & validated	2-Butanol	4	0.5629	1.777	0.0002	0.5639	99.82
	2-Pentanol	5	0.5957	1.679	0.0002	0.5973	99.73
	2-Nonanol	9	0.7343	1.362	0.0005	0.7309	99.54
	2-Decanol	10	0.7658	1.306	0.0004	0.7643	99.80
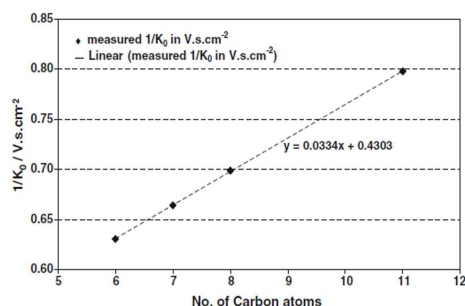
Fig. 1 Correlation of the inverse reduced ion mobility and the number of carbon atoms of the four secondary alcohols. The linear fit of the points yields the function y=0.0334x+0.4303 with a correlation coefficient of 0.9999

This ion mobility value is normalised to standard gas density, 2.687×10^{19} molecules/cm, corresponding to 273 degree Kelvin and 101325 Pascal, and reported as the reduced ion mobility, K_0 [35–37].

$$K_0 = K \left(\frac{P}{101325} \right) \left(\frac{273}{K} \right) \qquad (3)$$

At the molecular level, K is dependent on several factors and can be described by the equation,

$$K = \left(\frac{3q}{16N} \right) \left(\sqrt{\frac{2\pi}{kT}} \right) \left(\sqrt{\frac{m+M}{mM}} \right) \left(\frac{1}{\Omega} \right) \qquad (4)$$

In equation 4, q is the ionic charge (1.602×10^{-19} C), N; the number density of the drift gas, k; the Boltzmann constant (1.381×10^{-23} JK^{-1}), T; the temperature in Kelvin, m; the ion mass, M; the mass of the drift gas and Ω; the ion collision cross section [1, 34, 35, 37, 38].
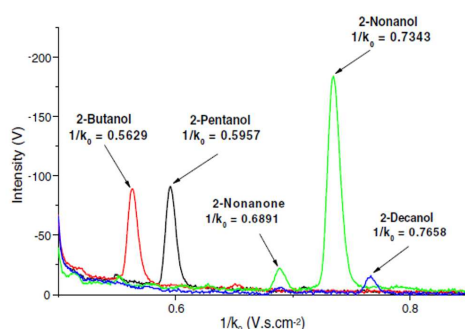

Fig. 2 Inverse reduced ion mobility values of the 4 predicted secondary alcohols together with the internal standard (2-Nonanone). The spectra were obtained at the retention time of the corresponding monomer peak maxima
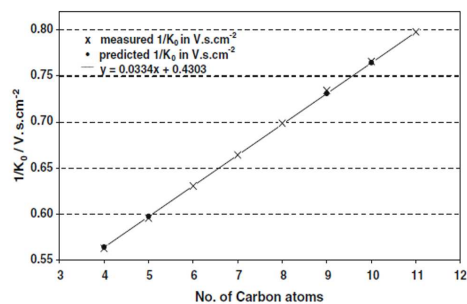

Fig. 3 Predicted and measured inverse reduced ion mobility values of measured and predicted secondary alcohols

The basic working principles of an IMS and the details of the IMS used in this study have been described in detail in previously published articles [1, 2, 5, 39, 40]. A multi-capillary column (MCC OV-5; Multichrom, Novosibirsk, Russia) was used for rapid pre-separation and was operated at a constant temperature of 40°C. The experimental parameters of the IMS used in this study are summarised in Table 1.

As the drift time t_D—which is proportional to the inverse reduced ion mobility—is the measured parameter, the inverse ion reduced mobility values (in V.s.cm^{-2}) are used in the following study for the visualisation of data and for correlation of predicted and measured ion mobilities.

All reference analytes were obtained from Sigma Aldrich (puriss. p.a.). The calibrated gases were provided by a calibration gas generator (HovaCAL 3834SO-VOC, IAS, Frankfurt, Germany). 2-Nonanone was always included in the calibration gases and was used as an internal standard for the retention time together with the reactant ion peak (RIP) for the ion mobility.

Results and discussion

From the database of analytes available at ISAS—Institute of Analytical Sciences, Dortmund, Germany, the homologous series of secondary alcohols was chosen for this study. The ion mobilities of 2-Hexanol, 2-Heptanol, 2-Octanol and 2-Undecanol were previously measured and the values are given in Table 2. From these data, the inverse reduced mobility values were plotted against the number of carbon atoms (Fig. 1). The data points were fit linearly and the corresponding equation is indicated.

Using the linear equation obtained from Fig. 1, y= 0.0334x+0.4303, the inverse reduced ion mobility values of other analytes in the same homologous series were empirically predicted as given in Table 2. To validate the quality of this empirical prediction, the analytes prognosed

were individually measured with a ^{63}Ni-MCC-IMS using the same experimental parameters given in Table 1. The reference gases were provided by the calibration gas generator stated previously. The inverse ion mobilities obtained from the spectra (Fig. 2) are given in Table 2. The measurements were carried out several times with a standard deviation of less than 0.0005 V.s.cm^{-2}. The accuracies of the empirical prediction of inverse reduced ion mobilities of the analytes, when compared to the measured ones, were greater than 99.5% (Fig. 3).

Conclusion and outlook

A linear correlation between the number of carbon atoms with the inverse reduced ion mobilities of secondary alcohols was used to predict inverse ion mobility values of other analytes in the same homologous series. This empirical prediction method proves that the inverse reduced mobilities of analytes in the IMS can be predicted very accurately from known values of the analytes in the same homologous series. More work has to be done to provide a clear insight into the reasons behind the trend within a homologous series. Furthermore, this empirical prediction will be extended to other homologous series.

Presently, this prognosis is being extended to other homologous series in order to develop a generalised equation for the prediction of the reduced ion mobility with different variables for every series depending on the molecular structure of the analyte. This would also lead to an extension of analytes' database with the predicted values from which the responsible analyte for any unknown peak in an IMS chromatogram could be identified. However, the theoretical correlation of the presented approach to the molecular structure of the analyte and to the behaviour of its ions in the drift gas under the influence of the electric field requires further investigations.

Such predictions will assist peak characterisations using Breit-Wigner-Functions and simulations of the shape of peaks in 3-D plots of IMS-chromatograms and allow forecast of peak positions within the drift time-retention time-intensity space. Furthermore, it could be helpful to reduce false alarms and to separate overlapping signals [article submitted for publication].

Springer

References

1. Louis RH, Hill HH (1990) Ion mobility spectrometry in analytical chemistry. Critical Reviews in Analytical Chemistry 21(5):321–355
2. Eiceman G. A, Karpas Z (2005) Ion Mobility Spectrometry. Taylor and Francis
3. Baumbach JI, Westhoff M (2006) Ion mobility spectrometry to detect lung cancer and airway infections. Spectroscopy Europe 18 (6):22–27
4. Vautz W, Baumbach JI (2008) Exemplar application of multi-capillary column ion mobility spectrometry for biological and medical purpose. Int. Journal of Ion Mobility Spectrometry 11:35–41
5. Ruzsanyi V, Baumbach JI, Eiceman GA (2003) Detection of the mold markers using ion mobility spectrometry. Int. Journal of Ion Mobility Spectrometry 6(2):53–57
6. Prasad S, Schmidt H, Lampen P, Wang M, Guth R, Rao JV, Smith GB, Eiceman GA (2006) Analysis of bacterial strains with pyrolysis-gas chromatography/differential mobility spectrometry. Analyst 131(11):1216–1225
7. Chaim W, Karpas Z, Lorber A (2003) New technology for diagnosis of bacterial vaginosis. European J of Obstertics & gynecology and Reproductive biology 111:83–87
8. Karpas Z, Tilman B, Gdalevsky R, Lorber A (2002) Determination of volatile biogenice amines in muscle food products by ion mobility spectrometry. 463:155–163
9. Prasad S, Pierce K, Schmidt H, Rao J, Güth R, Bader S, Synovec R, Smith GB, Eiceman GA (2007) Analysis of bacteria by pyrolysis gas chromatography–differential mobility spectrometry and isolation of chemical components with a dependence on growth temperature. Analyst 132:1031–1039
10. Snyder AP, Shoff DB, Eiceman GA, Blyth DA, Parsons JA (2002) Detection of bacteria by ion mobility spectrometry. Anal Chem 63:526–529
11. Harrington PB, Buxton TL, Chen G (2001) Classification of bacteria by thermal methylation hydrolysis by ion mobility spectrometry using SIMPLISMA and multi dimensional wavelet compression. Int. Journal of Ion Mobility Spectrometry 4(2):148–151
12. Shnayderman M, Mansfield B, Yip P, Clark HA, Krebs MD, Cohen SJ, Zeskind JE, Ryan ET, Dorkin HL, Callahan MV (2005) Species specific bacteria identification using differential mobility spectrometry and bioinformatics pattern recognition. Anal Chem 77:5930–5937
13. Westhoff M, Ruzsanyi V, Litterst P, Freitag L, Baumbach JI (2007) Ion mobility spectrometry - a new method for the fast detection of Sarkoidose in human breath? - Preliminary results of a feasibility study. J. of Physiology and Pharmacology 58(5):739–751
14. Basanta M, Koimtzis T, Thomas CL (2006) Sampling and analysis of exhaled breath on human subjects with thermal desorption gas chromatography-differential mobility spectrometry. Int. journal of ion mobility spectrometry 9:45–49
15. Baumbach JI (2006) Process analysis using ion mobility spectrometry. Anal Bioanal Chem 384:1059–1070
16. Sielemann S, Baumbach JI, Schmidt H, Pilzecker P (2002) Detection of alcohols using UV-ion mobility spectrometers. Int. Journal of Ion Mobility Spectrometry 5(3):7–10
17. Vautz W, Baumbach JI, Jung J (2006) Beer fermentation control using ion mobility spectrometry. Journal of the Institute of Brewing 112(2):157–164
18. Vautz W, Sielemann S, Baumbach JI (2004) Determination of terpenes in humid ambient air using ultraviolet ion mobility spectrometry. Anal Chim Acta 513:393–399

19. Vautz W, Zimmermann D, Hartmann M, Baumbach JI, Nolte J, Jung J (2006) Ion mobility spectrometry for food quality and safety. Food Additives & Contaminants 23(11):1064–1073

20. Walendzik G, Baumbach JI, Klockow D (2005) Coupling of SPME with MCC/UV-IMS as a tool for rapid on-site detection of ground water and surface water contamination. Anal Bioanal Chem 382:1842–1847

21. Raatikainen O, Reinikainen V, Minkkinen P, Ritvanen T, Muje P, Pursiainen J, Hiltunen T, Hyvonen P, Wright A, Reinikainen S (2005) Multivariate modeling of fish freshness index based on ion mobility spectrometry measurements. Anal Chim Acta 544:128–134

22. West C, Baron G, Minet JJ (2007) Detection of gunpowder stabilizers with ion mobility spectrometry. Forensic Science Int. 166:91–101

23. Bödeker B, Vautz W, Baumbach JI (2008) Peak Finding and Referencing in MCC/IMS-Data. Int. J. for Ion Mobility Spectrometry 11:83–87

24. Bödeker B, Vautz W, Baumbach JI (2008) Visualisation of MCC/IMS–Data. Int. J. for Ion Mobility Spectrometry 11:77–81

25. Bödeker B, Vautz W, Baumbach JI (2008) Peak Comparison in MCC/IMS - Data - Searching for potential biomarkers in human breath data. Int. J. for Ion Mobility Spectrometry 11:89–93

26. Vautz W, Bödeker B, Bader S, Baumbach JI (2008) Recommendation of a Standard Format for Data Sets from GC/IMS with Sensor-Controlled Sampling. Int. J. for Ion Mobility Spectrometry 11:71–76

27. Baumbach J, Bunkowski A, Lange S, Oberwahrenbrock T, Kleinboelting N, Rahmann S, Baumbach JI (2007) IMS2 - An integrated medical software system for early lung cancer detection using ion mobility spectrometry data of human breath. Journal of Integrative Bioinformatics 4(3):75

28. Bader S, Urfer W, Baumbach JI (2008) Preprocessing of Ion Mobility Spectra by Lognormal Detailing and Wavelet Transform. Int. J. for Ion Mobility Spectrometry 11:43–50

29. Harrington PB, Chen P (2005) Equilibrium modeling of ion mobility spectra. Int. Journal of ion mobility spectrometry 8:16–37

30. Cao LB, Harrington PB, Lui C (2004) Two-Dimensional nonlinear wavelet compression of ion mobility spectra of Chemical warfare agent simulants. Anal Chem 76:2859–2868

31. Urbas AA, Harrington PB (2001) Two-dimensional wavelet compression of ion mobility spectra. Anal Chim Acta 446:393–412

32. Harrington PD, Chen G, Urbas A (2001) Strategies for smarter chemical sensors. Int. journal for ion mobility spectrometry 4:26–30

33. Wesel MD, Jurs PC (1994) Prediction of reduced ion mobility constants from structural information using multiple linear regression analysis and computational neural networks. Anal Chem 66(15):2480–2487

34. Wesel MD, Sutter JM, Jurs PC (1996) Prediction of reduced ion mobility constants of organic compounds from molecular structure. Anal Chem 68(23):4237–4243

35. Stach J, Baumbach JI (2002) Ion mobility spectrometry - Basic elements and applications. Int. Journal of Ion Mobility Spectrometry 5(1):1–21

36. Bensch H, Leonhardt M (2002) Comparison of drift times of different IMS. Int. Journal of Ion Mobility Spectrometry 5(3):7–10

37. Xie Z, Sielemann S, Schmidt H, Li F, Baumbach JI (2002) Determination of acetone, 2-butanone, diethyl ketone and BTX using HSCC-UV-IMS. Anal Bioanal Chem 372:606–610

38. McDaniel E, Mason E (1973) The Mobility and Diffusion of Ions in Gases. John Wiley and Sons

39. Ruzsanyi V, Baumbach JI, Sielemann S, Litterst P, Westhoff M, Freitag L (2005) Detection of human metabolites using multi-capillary columns coupled to ion mobility spectrometers. J. of Chromatography A 1084:145–151

40. Baumbach JI, Eiceman GA (1999) Ion mobility spectrometry: Arriving on-site and moving beyond a low profile. Applied Spectroscopy 53(9):338–355

Linearized Equations for the Reduced Ion Mobilities of Polar Aliphatic Organic Compounds

Chandrasekhara B. Hariharan,* Jörg I. Baumbach, and Wolfgang Vautz

ISAS - Institute for Analytical Sciences, Bunsen-Kirchhoff-Strasse 11, 44139 Dortmund, Germany

Over the years, ion mobility spectrometry has evolved into a powerful technique for rapid identification of analytes in very complex sample matrixes such as human breath. Every analyte detected has a characteristic ion mobility value (and a retention time when additional preseparation techniques are employed) which is used to identify the peaks in a spectrum either by comparison with reference analytes or by simultaneous mass spectrometric measurements. In this study, the mass-mobility correlations between compounds in three different homologous series are used to predict the mobilities of the other substances in the same series in a medium of synthetic air. The results show a very high accuracy (>99.5%) of the prognosis. The linear trend equations of ion mobilities, as a function of the number of carbon atoms, obtained from the different series were then generalized into one linear equation for the reduced ion mobility for the polar aliphatic compounds and is validated by comparing it with the traditional Mason-Schamp equation. To compare the empirical equation obtained from the prognosis and the Mason−Schamp equation, the collision integral term in the latter was split into two terms to linearize it. The resulting novel ion mobility equation could be the starting step to completely describe the relationship between ion collision integral and the ion mobility for polar aliphatic compounds. The splitting of the collision integral into two terms will also give new inputs to describe the various ion models and the different forces that act on the ions and the neutral gas molecules upon which the collision integral is dependent on. This prognosis method could, furthermore, be extended to all other classes of organic compounds and could serve as a useful tool for identification of unknowns in ion mobility spectra, thereby considerably reducing the time-consuming and costly reference measurements and other coupling techniques that are currently employed.

Ion mobility spectrometry is an inexpensive and powerful analytical technique used for rapid detection of gas-phase samples in the lower ng L^{-1} (ppb$_v$) down to pg L^{-1} (ppt$_v$) levels at ambient pressures and temperatures.[1,2] Although the principles of ion motion in an electric field were explained as early as 1903 by P. Langevin, the instrumentation of an ion mobility spectrometer was developed much later in the late 1960s and early 1970s.[1,3] Ion mobility spectrometers (IMS) were initially used for direct monitoring of specific compounds classes such as chemical warfare agents, explosives, and drugs of abuse.[1−3] However, in recent years, due to its high sensitivity, information density and relatively low technical costs, they are being used for newer applications, specifically on biological samples, medical diagnosis, and process control.[4−21] These applications face challenges such as humid and rather complex sample matrixes, requirement of specific sampling procedures for each application, fast preseparation techniques, different data preprocessing steps, and most importantly, suitable data processing techniques that include reliable and accurate databases of relevant analytes for automatic identification of the signals detected in an IMS chromatogram.[22−31]

(3) Stach, J.; Baumbach, J. I. *Int. J. Ion Mobility Spectrom.* **2002**, *5* (1), 1–21.
(4) Baumbach, J. I.; Westhoff, M. *Spectrosc. Eur.* **2006**, *18* (6), 22–27.
(5) Vautz, W.; Baumbach, J. I. *Int. J. Ion Mobility Spectrom.* **2008**, *11*, 35–41.
(6) Ruzsanyi, V.; Baumbach, J. I.; Eiceman, G. A. *Int. J. Ion Mobility Spectrom.* **2003**, *6* (2), 53–57.
(7) Chaim, W.; Karpas, Z.; Lorber, A. *Eur. J. Obstet. Gynecol. Reprod. Biol.* **2003**, *111*, 83–87.
(8) Karpas, Z.; Tilman, B.; Gdalevsky, R.; Lorber, A. *Anal. Chim. Acta* **2002**, *463*, 155–163.
(9) Prasad, S.; Pierce, K.; Schmidt, H.; Rao, J.; Güth, R.; Bader, S.; Synovec, R.; Smith, G. B.; Eiceman, G. A. *Analyst* **2007**, *132*, 1031–1039.
(10) Snyder, A. P.; Shoff, D. B.; Eiceman, G. A.; Blyth, D. A.; Parsons, J. A. *Anal. Chem.* **2002**, *63*, 526–529.
(11) Harrington, P. B.; Buxton, T. L.; Chen, G. *Int. J. Ion Mobility Spectrom.* **2001**, *4* (2), 148–151.
(12) Shnayderman, M.; Mansfield, B.; Yip, P.; Clark, H. A.; Krebs, M. D.; Cohem, S. J.; Zeskind, J. E.; Ryan, E. T.; Dorkin, H. L.; Callahan, M. V. *Anal. Chem.* **2005**, *77*, 5930–5937.
(13) Westhoff, M.; Ruzsanyi, V.; Litterst, P.; Freitag, L.; Baumbach, J. I. *J. Physiol. Pharmacol.* **2007**, *58* (5), 739–751.
(14) Basanta, M.; Koimtzis, T.; Thomas, C. L. *Int. J. Ion Mobility Spectrom.* **2006**, *9*, 45–49.
(15) Baumbach, J. I. *Anal. Bioanal. Chem.* **2006**, *384*, 1059–1070.
(16) Vautz, W.; Baumbach, J. I.; Jung, J. *J. Inst. Brewing* **2006**, *112* (2), 157–164.
(17) Vautz, W.; Sielemann, S.; Baumbach, J. I. *Anal. Chim. Acta* **2004**, *513*, 393–399.
(18) Vautz, W.; Zimmermann, D.; Hartmann, M.; Baumbach, J. I.; Nolte, J.; Jung, J. *Food Addit. Contam.* **2006**, *23* (11), 1064–1073.
(19) Walendzik, G.; Baumbach, J. I.; Klockow, D. *Anal. Bioanal. Chem.* **2005**, *382*, 1842–1847.
(20) Raatikainen, O.; Reinikainen, V.; Minkkinen, P.; Ritvanen, T.; Muje, P.; Pursiainen, J.; Hiltunen, T.; Hyvonen, P.; Wright, A.; Reinikainen, S. *Anal. Chim. Acta* **2005**, *544*, 128–134.
(21) West, C.; Baron, G.; Minet, J. J. *Forensic Sci. Int.* **2007**, *166*, 91–101.
(22) Bödeker, B.; Vautz, W.; Baumbach, J. I. *Int. J. Ion Mobility Spectrom.* **2008**, *11*, 83–87.
(23) Bödeker, B.; Vautz, W.; Baumbach, J. I. *Int. J. Ion Mobility Spectrom.* **2008**, *11*, 77–81.
(24) Bödeker, B.; Vautz, W.; Baumbach, J. I. *Int. J. Ion Mobility Spectrom.* **2008**, *11*, 89–93.

* Corresponding author. E-mail: hariharan@isas.de.

(1) Louis, R. H.; Hill, H. H. *Crit. Rev. Anal. Chem.* **1990**, *21* (5), 321–355.
(2) Eiceman G. A., Karpas Z. *Ion Mobility Spectrometry*; Taylor and Francis: New York, 2005.

Ion Mobility Spectrometry. The working principle of an IMS is based on the different velocities attained by the accelerating sample ions in the drift tube. Depending on their mass and/or structure, ions under an external electric field attain different velocities in a counter-flowing neutral drift gas.[2] The average velocity attained by the accelerating ions (v_d) over a certain drift length is determined by the number of collisions made by the ion swarm with the neutral drift gas molecules and, in homogeneous low field strengths, it is directly proportional to the electric field (E).

$$v_d \propto E \tag{1}$$

The constant of proportionality between the velocity of the ions, also known as the drift velocity, and the electric field is termed as the ion mobility (K).[1,2]

$$V_d = KE$$

$$\text{(i.e.)} \quad K = v_d/E \tag{2}$$

In eq 2, the ion velocity, v_d, has the units of cm s^{-1}, the electric field E is represented in V cm^{-1}, and K, the ion mobility which is a combined property of the ion and the drift gas, is represented in cm^2 V^{-1} s^{-1}. This ion mobility value is a function of the gas density and therefore is usually normalized to the standard gas density of 2.687×10^{19} molecules cm^{-3} at standard temperature, T_0 (273 K), and pressure, P_0 (101325 Pascal), conditions and reported as the reduced ion mobility, K_0 (cm^2 V^{-1} s^{-1}).[1,3]

$$K_0 = K\left(\frac{P}{P_0}\right)\left(\frac{T_0}{T}\right) \tag{3}$$

In eq 3, P and T are the actual pressure and temperature values during the experiment. At the molecular level, the mobility of an ion is described by the Mason–Schamp equation.

$$K = \left(\frac{3q}{16N}\right)\left(\sqrt{\frac{2\pi}{kT}}\right)\left(\sqrt{\frac{m+M}{mM}}\right)\left(\frac{1+\alpha}{\Omega}\right) \tag{4}$$

where q is the ionic charge (1.602×10^{-19} C), N is the number density of the drift gas, k the Boltzmann constant (1.381×10^{-23} J K^{-1}), T is the temperature in Kelvin, m is the ion mass, M is the mass of neutral the drift gas, α is a mass-dependent correction term, and Ω is the ion collision cross-section which is derived through a series of integrations of the ion-neutral cross-sections over all possible scattering angles.[1,32]

A basic IMS consists of a sample inlet system, an ionization source, an ion gate, a drift region, and an ion collector. Additionally, a voltage supply is necessary to create the electric field. Furthermore a shutter controller, carrier and drift gases, temperature and pressure sensors, fast electrometers, and a data acquisition and analysis system are required for its complete functioning. Besides these components, the IMS may also be coupled to a gas chromatographic column (GC) or a multicapillary column (MCC) to preseparate complex and humid volatile mixtures in the sample matrix before it enters the drift tube. The details about the functionality of an IMS and the one used in this study have been described in many previously published articles.[1−3,5,33,34]

It is evident that, to identify the peaks obtained from an IMS chromatogram, we need databases of reference substances for identification. If a peak is detected by an IMS that is not included in the database, parallel measurements with other mass spectrometric methods may be carried out to explore the composition of the sample matrix. Statistical alignment tools are also used for peak identification by aligning the GC retention times to the IMS retention times and the reactant ion peak (RIP) to the reduced mobility.[22−25]

There are previous studies using computational neural networks to predict reduced ion mobilities of substances from their molecular structure.[35,36] However, these are very complex and require extensive modeling of the ion structure, resulting in an assumed ion mobility value. Hence, in a recent study by our group, the mass-mobility correlation in a homologous series of secondary alcohols was used for an empirical prediction of the ion mobilities of other compounds in the same series.[37] In this present study, a similar kind of correlation seen in other polar aliphatic organic compounds is used to predict the mobilities of other ions in the group. Later, a generalized linear ion mobility equation for polar aliphatic organic compounds is empirically derived from the different series of compounds and its plausibility is discussed by comparison with the Mason–Schamp equation.

EXPERIMENTAL SECTION

The IMS measurements in this study were carried out with a ^{63}Ni-MCC/IMS, a traditional drift tube IMS constructed at ISAS-Institute for Analytical Sciences, Dortmund, Germany. The details of the IMS used and the experimental parameters are listed in Table 1. A multicapillary column (MCC OV-5; Multichrom, Novosibrisk, Russia) was used for the rapid preseparation of the sample gases. The MCC consists of a bundle of approximately 1000 capillaries, made of 95% dimethylpolysiloxane and 5% diphenyl, aiding the fast preseparation of the sample before it enters the drift tube.

All reference substances were purchased from Sigma-Aldrich (puriss, p.a). The calibrated sample gases were provided by a calibration gas generator (HovaCAL 3834SO-VOC, IAS, Frankfurt,

(25) Vautz, W.; Bödeker, B.; Bader, S.; Baumbach, J. I. *Int. J. Ion Mobility Spectrom.* **2008**, *11*, 71–76.
(26) Baumbach, J.; Bunkowski, A.; Lange, S.; Oberwahrenbrock, T.; Kleinboelting, N.; Rahmann, S.; Baumbach, J. I. *J. Integrative Bioinf.* **2007**, *4* (3), 75.
(27) Bader, S.; Urfer, W.; Baumbach, J. I. *Int. J. Ion Mobility Spectrom.* **2008**, *11*, 43–50.
(28) Harrington, P. B.; Chen, P. *Int. J. Ion Mobility Spectrom.* **2005**, *8*, 16–37.
(29) Cao, L. B.; Harrington, P. B.; Lui, C. *Anal. Chem.* **2004**, *76*, 2859–2868.
(30) Urbas, A. A.; Harrington, P. B. *Anal. Chim. Acta* **2001**, *446*, 393–412.
(31) Harrington, P. D.; Chen, G.; Urbas, A. *Int. J. Ion Mobility Spectrom.* **2001**, *4*, 26–30.
(32) McDaniel E., Mason E. *The Mobility and Diffusion of Ions in Gases*; John Wiley and Sons: New York, 1973.

(33) Ruzsanyi, V.; Baumbach, J. I.; Sielemann, S.; Litterst, P.; Westhoff, M.; Freitag, L. *J. Chromatogr., A* **2005**, *1084*, 145–151.
(34) Baumbach, J. I.; Eiceman, G. A. *Appl. Spectrosc.* **1999**, *53* (9), 338–355.
(35) Wesel, M. D.; Jurs, P. C. *Anal. Chem.* **1994**, *66* (15), 2480–2487.
(36) Wesel, M. D.; Sutter, J. M.; Jurs, P. C. *Anal. Chem.* **1996**, *68* (23), 4237–4243.
(37) Hariharan, C.; Baumbach, J. I.; Vautz, W. *Int. J. Ion Mobility Spectrom.* **2009**, *12*, 59–63.

Table 1. Experimental Parameters of ^{63}Ni-MCC/IMS

ionization source	β radiation (^{63}Ni, 550 MBq)
grid opening time	300 μs
spectral length/sample interval	100 ms
spectral resolution	40 kHz
drift length	120 mm
electric field intensity	310 V cm^{-1}
voltage polarity	positive
drift gas and carrier gas	synthetic air (20.5% O$_2$, 79.4% N$_2$, <2 ppb$_v$ water)
drift gas flow	100 mL min^{-1}
carrier gas flow	150 mL min^{-1}
preseparation type, length	MCC OV-5, 40 °C, 20 cm
instrument temperature and pressure	ambient conditions

Germany). 2-Nonanone was always used with the reference gases as an internal standard for the retention time along with the reactant ion peak (RIP), a standard for the ion mobility, in this study.

The drift velocity, v_d, of the sample ions is a quotient of the length (l_d) of the drift tube and the drift time, t_d. The measured drift time is used to calculate the reduced mobility (K_0) at known drift length, electric field, pressure, and temperature as described in eqs 2 and 3.[1−3,5,37]

$$v_d = \frac{l_d}{t_d} \qquad (5)$$

$$v_d \propto \frac{1}{t_d} \qquad (6)$$

From eqs 2 and 6 it is seen that the drift time, which is the measured parameter, is proportional to the inverse reduced ion mobility ($1/K_0$). Hence, $1/K_0$, in V s cm^{-2}, is used as the reporting value for ion mobilities during the visualization and correlation of the IMS spectra.

From the ion mobility database available at ISAS-Institute for Analytical Sciences, Dortmund, Germany, compounds from three different homologous series were chosen for this study, namely, the primary alcohols, aldehydes, and ketones. The mobility values of the existing polar aliphatic organic compounds were plotted against the number of carbon atoms (N_c) in each compound.

From the linear trend equations obtained for the three different homologous series, the inverse reduced ion mobility values of the other substances in the same series were empirically predicted. To validate the predicted values, the predicted substances were measured individually with a ^{63}Ni-MCC/IMS using the same experimental parameters as mentioned in Table 1.

RESULTS AND DISCUSSION

The inverse reduced ion mobility values ($1/K_0$) of the different classes of the measured organic compound, listed in Table 2, were plotted against the number of carbon atoms (N_c), as shown in Figure 1. The data points were then fit linearly using Microsoft Office 2003. The linear equations obtained from the curve that had high correlation coefficient (R^2) values (eqs 7−9).

primary alcohols: $1/K_0 = 0.0355N_c + 0.4345$ ($R^2 = 1.0000$) (7)

aldehydes: $1/K_0 = 0.0333N_c + 0.4399$ ($R^2 = 1.0000$) (8)

ketones: $1/K_0 = 0.0333N_c + 0.3854$ ($R^2 = 0.9984$) (9)

From the linear equations obtained (eqs 7−9), the $1/K_0$ of the other compounds in the same series were calculated. As stated previously, the empirically predicted values were later validated by measurements with a ^{63}Ni-MCC/IMS. The results of the empirical prediction are shown in Table 2. A comparison of the predicted and measured ion mobility values is shown in Figure 2.

The high correlation coefficients seen in the complete measured ion mobilities of the compounds in all the three series indicate that three to four compounds in any series would be enough to observe the mass mobility correlation in a series (Figure 3).

In a previous study with secondary alcohols,[37] a similar trend equation was obtained for the homologous series (eq 10).

secondary alcohols: $1/K_0 = 0.0334N_c + 0.4303$ (10)

The four empirically obtained linear equations (eqs 7−10) can be written in a general form with variables as shown.

$$\frac{1}{K_0} = \varepsilon N_c + \delta \qquad (11)$$

Where, ε is the slope of the equation and δ the intercept. It is also clear that the intercept term (δ) in eq 11 is a mass-independent term and has a characteristic value for every homologous series of compounds. This ion mobility equation (eq 12) is then compared to the Mason−Schamp equation (eq 4) for detailed interpretation into this empirical prediction.

Equations 3 and 4 when combined together yield,

$$K_0 = \left(\frac{3q}{16N}\right)\left(\sqrt{\frac{2\pi}{kT}}\right)\left(\frac{1}{\sqrt{\mu}}\right)\left(\frac{1+\alpha}{\Omega}\right)\left(\frac{P}{P_0}\right)\left(\frac{T_0}{T}\right) \qquad (12)$$

where μ represents the reduced mass of the drift gas and the ion. Equation 12 when rearranged yields eq 14. In eq 13, the braced terms, marked ($1/\Psi$), are constants when the experimental and ambient conditions remain constant,

$$K_0 = \underbrace{\left(\frac{3q}{16N}\right)\left(\sqrt{\frac{2\pi}{kT}}\frac{P}{P_0}\frac{T_0}{T}\right)}_{\frac{1}{\Psi}}\left(\frac{1}{\sqrt{\mu}}\right)\left(\frac{1+\alpha}{\Omega}\right) \qquad (13)$$

Hence, eq 13 can be rewritten as

$$K_0 = \left(\frac{1}{\Psi}\right)\left(\frac{1}{\sqrt{\mu}}\right)\left(\frac{1+\alpha}{\Omega}\right) \qquad (14)$$

$$\Rightarrow \left(\frac{1}{K_0}\right) = (\Psi)(\sqrt{\mu})\left(\frac{\Omega}{1+\alpha}\right) \qquad (15)$$

Table 2. Measured, Predicted, and Validated $1/K_0$ Values of the Three Groups of Aliphatic Compounds[a]

analyte	number of carbon atoms, N_C	inverse reduced ion mobility $(1/K_0)$ V s cm^{-2}		accuracy (%)
		predicted	measured/validated	
Primary Alcohols				
$1/K_0 = 0.0355N_C + 0.4345$				
1-propanol[a]	3		0.5412	
1-butanol[b]	4	0.5765	0.5765	100.00
1-pentanol[a]	5		0.6120	
1-hexanol[b]	6	0.6475	0.6472	99.95
1-heptanol[a]	7		0.6835	
1-octanol[a]	8		0.7137	
1-nonanol[b]	9	0.7540	0.7542	99.97
1-decanol[b]	10	0.7895	0.7843	99.34
Aldehydes				
$1/K_0 = 0.0333N_C + 0.4399$				
butanal[b]	4	0.5731	0.5788	99.02
pentanal[b]	5	0.6064	0.6087	99.62
hexanal[a]	6		0.6392	
heptanal[a]	7		0.6734	
octanal[b]	8	0.7063	0.7098	99.50
nonanal[b]	9	0.7396	0.7373	99.69
decanal[a]	10		0.7726	
undecanal[b]	11	0.8062	0.7957	98.69
Ketones				
$1/K_0 = 0.0333N_C + 0.3854$				
2-butanone[a]	4		0.5212	
2-pentanone[b]	5	0.5519	0.5494	99.55
2-hexanone[a]	6		0.5823	
2-heptanone[a]	7		0.6172	
2-octanone[b]	8	0.6518	0.6529	99.83
2-nonanone[a]	9		0.6876	
2-decanone[b]	10	0.7184	0.7221	99.48
2-undecanone[b]	11	0.7517	0.7553	99.52
2-dodecanone[b]	12	0.7850	0.7899	99.34

[a] The overall accuracy of the empirical prediction is greater than 99.5%. The superscripts following the name of the compound indicates if it was used to obtain the trend (a) or if it was predicted and validated (b).

Equation 11 has been mathematically validated in this study. The two equations which now represent $1/K_0$, eqs 11 and 15, are mathematically different. Equation 11 represents a linear trend with a nonzero intercept unlike eq 15. For further insights into this divergence, eq 15 has to be written in a linear form for comparison. Linearizing eq 15 is possible by splitting a term in the numerator. The reduced mass term and the collection of constants, Ψ, are nonreducible. Hence, the collision integral (Ω) term is split into two, Ω_C and Ω_S (eq 16).

$$K = \left(\frac{3q}{16N}\right)\left(\sqrt{\frac{2\pi}{kT}}\right)\left(\sqrt{\frac{m+M}{mM}}\right)\left(\frac{1+\alpha}{\Omega_C + \Omega_S}\right) \quad (16)$$

Equation 16 when represented in form of $1/K_0$, by combining eq 3 yields,

$$\frac{1}{K_0} = \frac{(\Psi)(\sqrt{\mu})}{(1+\alpha)}(\Omega_C + \Omega_S) \quad (17)$$

$$\Rightarrow \frac{1}{K_0} = \left(\frac{\Psi\Omega_C\sqrt{\mu}}{1+\alpha}\right) + \left(\frac{\Psi\Omega_S\sqrt{\mu}}{1+\alpha}\right) \quad (18)$$

The Mason–Schamp equation, rewritten by splitting the collision integral into two terms, eq 18, can now be compared to the empirically obtained eq 11. On comparison, one of the adduct
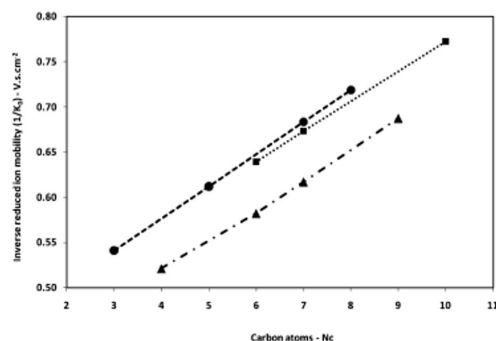
Figure 1. Inverse reduced ion mobilities against the number of carbon atoms for different homologous series ($\bullet$, primary alcohols; $\blacksquare$, aldehydes; $\blacktriangle$, ketones). Equations 7–9 give the trend equations obtained from the data points distribution and their correlation coefficient values (R^2).

terms in eq 18 should be a mass-dependent term and the second one should be a mass-independent but a series-dependent term.

The reduced mass term $\mu^{1/2}$ in the Mason–Schamp equation can be approximated to $M^{1/2}$ as $m \gg M$, is true for all the ions in this study. Hence, a valid reason for series-dependent and mass-dependent collisions taking place between the ions and neutral molecules will validate this study.
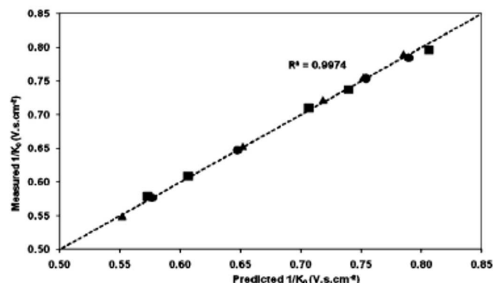
Figure 2. Comparison chart of the measured and the predicted $1/K_0$ values of all the 14 compounds from different series (●, primary alcohols; ■, aldehydes; ▲, ketones).
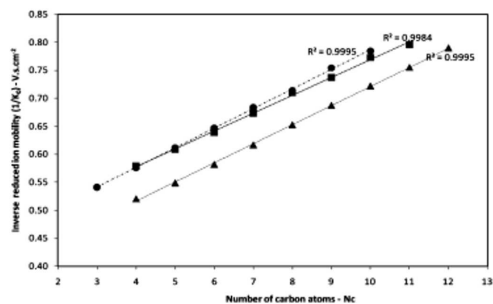

Figure 3. Linear trends seen with the measured $1/K_0$ values of the three homologous series in this study. The correlation coefficients are given on the plot. The almost linear trend implies the necessity of only few data points in a series to predict the trend for the prognosis of the mobility values of other compounds in the series.

Let us consider any class of homologous series and the ions of the compounds formed. The part of the molecule where the charge is located (the ionic head) is the same throughout the series, independent of the mass or size of the compound. This means that the neutral molecules from the drift gas that strike the ion may encounter two types of collision cross-sections: One, on the ionic head which is the same in any homologous series giving the series dependent collision (Ω_S), and the other on the tail of the ion giving rise to the mass-dependent collision integral (Ω_C).

At a more scientific level, the Boltzmann equation that is used to solve the collision cross-section of molecules is a linear differential equation used for calculations of the collision integral[38] and should, in principle, allow the collision cross-section to be broken up into linear components associated with independent force fields. Hence, by splitting the collision integral term in the Mason–Schamp equation, the empirical linear equation obtained in this study is plausible. The mass dependent term (εN_C) is due to the neutral gas collisions occurring at the non ionic part of the compound, and the series dependent term (δ) is due to the neutral gas collisions taking place in the ionic head.

(38) Aisbett, J.; Blatt, J. M.; Opie, A. H. *J. Stat. Phys.* **1974**, *2* (6), 441–456.
(39) Spangler, G. E. *Int. J. Ion Mobility Spectrom.* **2002**, *5* (2), 42–75.

CONCLUSIONS

One of the disadvantages of an IMS is the inability to directly identify the peaks detected by the instrument. With the IMS being used every day for newer applications, it is necessary to identify almost all the peaks detected by the instrument in the complex sample. The existing methods of peak identification have been stated in the previous sections of this report. An unknown sample matrix could give us alot of unknown peaks in the resultant IMS chromatogram. The prognosis of compounds performed in this study, though not helping us identify the peak directly, will considerably facilitate preliminary identification by reducing the possibility of unknown substances that could be associated with a peak in the IMS chromatogram without the costly and time-consuming reference measurements currently employed. Similar mass mobility trends are also observed in other classes of compounds such as amino acids and other groups of compounds of biological interest, and such an empirical method can be extended to these series, too. This empirical prediction method will assist peak characterisations with Breit–Wigner functions and simulations of peak shapes in 3-D plots and reduce false alarms and separate overlapping signals in an IMS chromatogram.

The splitting of the collision integral (Ω) into two terms (Ω_C, Ω_S), performed in this study, was done empirically to draw comparisons with the linear equation for reduced ion mobilities obtained from the prognosis data and the Mason–Schamp equation and to get a better understanding of the same. Even though this study has not gone deeply into the various forces that play a role during collisions, such as electrostatic and van der Waals forces, this opens up new insights into the behavioral trend seen in a homologous series. This will also give new inputs to the various models that describe the collisions taking place between the ion swarm and the neutral drift molecules in an electric field and find out if the size/volume increase in a compound/ion would have a direct relationship with the mobility data.[39] This in turn may also help in modeling the charge distribution within large organic ions and its effects on the mobility values which remains a void until now.[2,32]

ORIGINAL RESEARCH

Novel design for drift tubes in ion mobility spectrometry for optimised resolution of peak clusters

Chandrasekhara Bharadwaj Hariharan ·
Luzia Seifert · Jörg Ingo Baumbach · Wolfgang Vautz

Abstract In the past decade, Ion Mobility Spectrometry has established a very strong foot hold in medical and biological applications due to its numerous advantages including sensitivity, ruggedness and reproducibility. During the analysis of complex samples such as human breath, it is very probable that two or more analytes form peak clusters due to similar drift times and pre-separation times, thus hindering the identification of the analytes. Furthermore, such overlapping of signal makes quantification very difficult or even impossible. Resolving these peak clusters is important to enable proper identification and quantification of analytes detected for diagnosis. Hence, we designed a drift tube with variable length for investigating the influence of varying drift lengths and electric field on resolution. Peak cluster formations usually seen between acetone and the reactant ion peak, between the dimer peaks of 2-Heptanone and 4-Heptanone have been resolved with the new drift tube after optimisation. These novel drift tubes could easily negate the peak clusters often encountered when complex medical and biological samples are measured with the ion mobility spectrometer. Furthermore, the fact that these drift tubes can be altered in length thereby providing a wide range of electric fields (from 50 to 3300 V.cm^{-1}), opens up new research options in ion motions in an electric field.

Keywords Ion mobility spectrometry · Drift tube · Peak clusters · Resolution · Acetone · 2-Heptanone · 4-Heptanone

C. B. Hariharan (✉) · L. Seifert · W. Vautz
Leibniz-Institut für Analytische Wissenschaft-ISAS-e.V.,
Bunsen-Kirchhoff-Strasse 11,
44139 Dortmund, Germany
e-mail: hariharan@isas.de

J. I. Baumbach
KIST Europe Forschungsgesellschaft mbH,
Universität des Saarlandes,
Campus E 71,
66123 Saarbrücken, Germany

Introduction

The advent of the 21st century has seen Ion Mobility Spectrometry (IMS) establish itself as an inexpensive and powerful analytical technique for rapid detection of gas-phase samples in the lower ng.L^{-1} (ppb$_v$) down to pg.L^{-1} (ppt$_v$) levels at ambient pressures and temperatures. The principles underlining ion motions in an electric field were first laid down by Langevin as early as in 1890s [1]. But it took almost 70 years for the instrumentation to be first developed and used for analytical purposes [2, 3]. In the late 1960s and early 1970s, they were initially used for direct monitoring of specific compound classes such as chemical warfare agents and drugs of abuse [3–5]. Later ion mobility spectrometers were increasingly in demand for process control and security systems at airports [5]. The onset of the 21st century saw the IMS venture into the unknowns. Due to its high sensitivity, information density, relatively low costs and its functionality at atmospheric temperatures and pressures, the instrument was used for biological and medical applications [6–10]. This non target specific analysis had to face many challenges such as humid and rather complex sample matrices, requirement of a specific sampling procedure adapted to the application, fast pre-separation techniques and most importantly suitable data processing techniques which include databases of relevant analytes for automatic characterisation of the

signals detected in a chromatogram and different data pre-processing steps [11–13].

Ion mobility spectrometry

The basic working principle of an Ion Mobility Spectrometer (IMS) is based on the distinct velocities attainted by accelerating ions in an electric field. Depending on their mass and/or structure different ions reach different velocities under the influence of a constant electric field in a counter-flowing neutral drift gas [4]. The average velocity attained by the ions (v_D) over a certain drift length (l_D) is proportional to the electric field strength E (V.cm^{-1}) and the constant of proportionality is defined as the ion mobility K [4, 5]. The time spent by an ion swarm 'drifting' along the drift tube is known as the drift time t_D.

$$v_D = K*E$$
$$\text{or } \frac{l_D^2}{t_D} = K*V \tag{1}$$

While the neutral drift molecules diffuse by random Brownian motion, the ions move in a defined direction with the velocity controlled by their mobility as defined in Eq. 1 [14]. This quantity varies with the electrical field intensity E in general, but the IMS is usually run in a low-field regime where K(E) is nearly constant [4, 14]. In that limit, K depends on the ion and neutral gas cross section Ω_{av}, a first order averaged collision cross section integral. This allows separation of different ions, including structural isomers, isobars and conformers.

At the molecular level, the mobility of an ion is described by the Mason-Schamp equation.

$$K = \left(\frac{3q}{16N}\right)\left(\sqrt{\frac{2\pi}{kT}}\right)\left(\sqrt{\frac{m+M}{mM}}\right)\left(\frac{1+\alpha}{\Omega}\right) \tag{2}$$

Where, q is the ionic charge (1.602×10^{-19} C), N; the number density of the drift gas, k; the Boltzmann constant (1.381×10^{-23} J.K^{-1}), T; the temperature in Kelvin, m; the ion mass, M; the mass of the neutral drift gas, α is a mass dependent correction term and Ω; the ion collision cross section which is derived through a series of integrations of the ion-neutral cross sections over all possible scattering angles [3, 4].

A basic IMS consists of a sample inlet system, an ionisation source, an ion gate, a drift region and an ion collector. Additionally, a voltage supply is necessary to create the electric field. Furthermore a shutter controller, carrier and drift gases, temperature and pressure sensors, fast electrometers and a data acquisition and analysis system are required for its complete functioning. Besides these components, the IMS may also be coupled to a gas chromatographic column (GC) or a multi capillary column (MCC) to pre-separate complex and humid volatile mixtures in the sample matrix before it enters the drift tube [4, 11].

Since measurements with the IMS are usually made at or near atmospheric temperature and pressure conditions, comparisons between the spectra obtained require a normalisation to the standard gas density of 2.687×10^{19} molecules.cm^{-3} at standard temperature, T_0 (273 K) and pressure, P_0 (101325 Pascal) conditions and reported as the reduced ion mobility, K_0 (cm².V^{-1}.s^{-1}) [3–5].

$$K_0 = K\left(\frac{P}{P_0}\right)\left(\frac{T_0}{T}\right) \tag{3}$$

From the equations above it is seen that the drift time, which is the measured parameter, is proportional to the inverse reduced mobility ($1/K_0$). Hence $1/K_0$, in V.s.cm^{-2} is also used as the reporting value for ion mobilities alongside the drift time because it represents the real resolution of the measured data.

Generally ion mobility spectrometrists have measured separation power of the IMS by using a single peak quotient [15], called the resolving power (R_p),

$$R_p = \frac{t_D}{w_h} \tag{4}$$

Where t_D is the ion drift time and w_h is the ion pulse duration at the detector measured at the half of the maximal intensity. Mason and Revercomb developed an expression for measured peak width for IMS where only the initial pulse width and the broadening due to normal diffusion are important [16].

$$w_h^2 = t_g^2 + \left(\frac{16kT \ln 2}{Vez}\right)t_D^2 \tag{5}$$

Where t_g is the initial ion pulse width, V is the voltage potential across the drift length and z is the number of charges on the ion.

Resolution in IMS is a function of both the efficiency of the separation and the selectivity of the separation [17]. The standard two peak definition of resolution is

$$R = \left(\frac{t_{D2} - t_{D1}}{w_{b\ avg}}\right) \tag{6}$$

Where t_{D2} and t_{D1} are the drift times of the second and the first peaks and $w_{b\ avg}$ is the average base width of the two peaks.

With increasing complexity of the sample matrices, the number of substances detected by the IMS increases and hence the chances that two or more substances having very close retention times and drift times, thus resulting in peak clusters are high. Under these phenomena, identification and quantification of individual peaks can be difficult as

Int. J. Ion Mobil. Spec. (2011) 14:31–38

33

they compete against each other for protons. An optimized change in the instrument is necessary to increase the resolution without changing any influential parameters like drift gas, shutter grid size or temperature and pressure conditions. Care should also be taken to make it suitable not just for laboratorial conditions but also at clinics where the majority of the measurements take place. It is obvious that increasing the resolution of the instrument would resolve the peak cluster problems. Hence, for a higher resolution between those peaks found in human breath which lie close to one another, we constructed a drift tube whose length can be varied depending on the complexity and the demands of the sample matrix. This drift tube with variable length has a higher resolving power and resolution than the existing one which is used at ISAS for breath analysis. Studies have been carried out previously with similar kind of drift tubes but at higher pressures and temperatures [14]. In this study we present a variable length drift tube which can be used under ambient temperatures and pressure conditions. This drift tube is suitable not just under laboratorial conditions but also under clinical and commercial conditions to get better resolved peaks for clinical and medical diagnostics.

Experimental

The ion mobility spectrometers used in this study were designed and constructed at Leibniz Institut für Analytische Wissenschaft—ISAS—e.V. The detailed schematic descrip-

tion of the instrument has been described previously in many articles [3–5, 11, 18, 19]. The OV-5 multi-capillary column (MCC) used for the rapid pre-separation of the sample gases was purchased from Multichrom, Novosibrisk, Russia. The MCC consists of a bundle of approximately 1000 quartz capillaries coated with 95% dimethylpolysiloxane and 5% diphenyl. The 20 cm long MCC was maintained at a constant temperature of 40 °C using an electronic heating unit. The incoming sample from the MCC was ionised by radioactive ^{63}Ni (550 MBq). The ionised sample was sent periodically (every 100 ms) into the drift region by means of a Bradbury-Nielsen shutter gate opening for 300 µs. The reference drift tube used for the comparison in this study with the high resolution, variable length drift tube had a 12 cm drift length supplied with a voltage of 4.38 kV. Measurements were made at ambient temperature and pressure conditions and in a positive electric field.

The new drift tube presented in this study was made up of Teflon pieces, inner diameter 1.5 cm, fit externally with equally spaced brass drift rings connected by 1 MΩ resistors to provide the uniform electric field. Two 3 cm pieces, one 6 cm and one 12 cm piece of the drift tube were constructed which enabled the drift tube length to be varied up to 24 cm in 3 cm steps to suit the demands of the sample matrix. A special voltage supply unit was constructed to enable voltage supply up to 10 kV. The aperture grid and the Faraday plate at the end of the detector remained the same as in the reference IMS.

Fig. 1 Dependency of drift time of the reactant ion peak at various applied voltage with different drift lengths
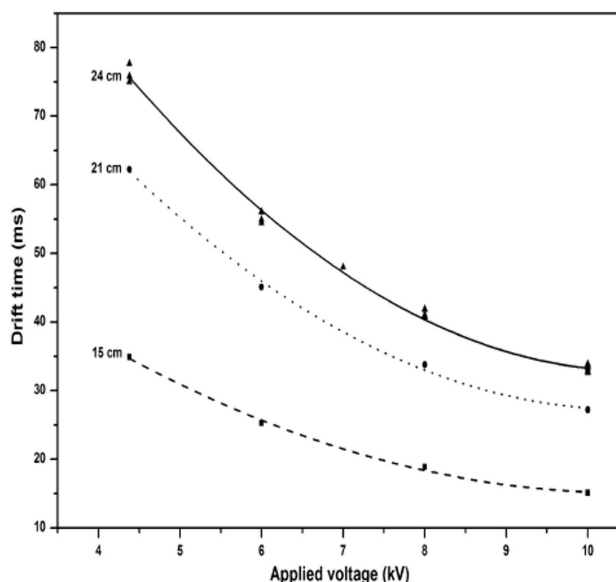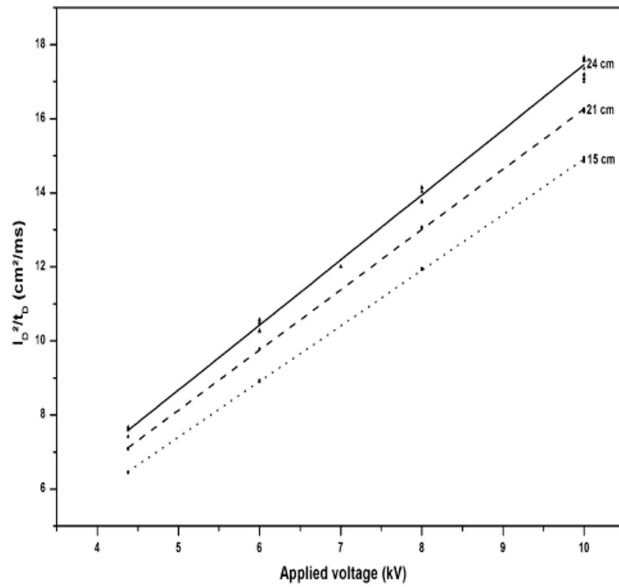
Fig. 2 Behaviour of the fraction of the squared drift length and drift time to the applied voltage at various drift lengths


Bottled synthetic air (20.5% O_2, 79.4% N_2 and <2 ppb_v water) was used as the carrier and drift gas. All other chemicals used in this study were purchased from Sigma-Aldrich (puriss, p.a). The calibrated sample gases were provided by a calibration gas generator (HovaCAL 3834SO-VOC, IAS, Frankfurt, Germany).

The reactant ion peak (RIP) obtained during all IMS measurements is the resultant of the multi-step reaction initiated by the ionisation source on the carrier and drift gas [4, 5].

In the first part of the study the peak characteristics of the RIP in the standard IMS was compared with the

Fig. 3 Variation of the full width at half maximum of the RIP with the applied electric field
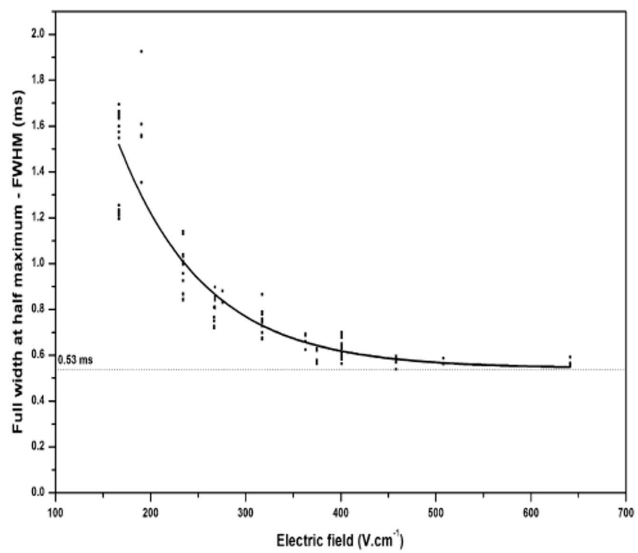
different RIPs obtained at various lengths and voltages applied on the high resolution IMS. In the second part of the study, substances which are potential markers of certain diseases found in human breath, which usually form clusters were measured with both the IMS' and their peak characteristics were compared.

Results and discussion

To test out the stability of the new drift tube constructed, measurements of the RIP were carried out at different voltages and different lengths of the drift tube and the results obtained are summarised below, Figs. 1, 2, 3.

Figure 1 shows the influence of applied voltage and drift lengths on the drift time. It is obvious that with any particular electric field, the drift time is directly proportional to the drift length (Eq. 1) and observing this tendency (Figs. 1 and 2) in the newly constructed drift tube made out of

smaller pieces proves the stability and reproducibility of the drift tube and the homogeneity of the electric field within the drift region. This initial test also shows that the drift tube can be relied upon to vary the lengths and be used for further measurements of various analytes.

In Fig. 2, we see the confirmation of Eq. 1 proving the stability of the drift tube to various drift length changes. From Figs. 1 and 2 we have the confirmation that the drift tube made up of smaller drift sections is electrically and mechanically stable to vary the lengths and carry out analytical measurements. With this confirmation, we did one more test to find out the variation of the full width half maximum (FWHM) of the RIP with the applied electric field to establish the final proof of stability of these drift tubes.

The RIP peaks obtained at various drift lengths and electric fields were fit to a Gaussian peak by the Levenberg-Marquardt algorithm and from the fit peaks, the full width at half the maximum intensity (FWHM) was hence found

Fig. 4 The RIP and the monomer peaks of acetone compared with the original IMS. The resolution (R) between the two peaks is seen shown in each spectrum alongside the corresponding electric field applied

36

Int. J. Ion Mobil. Spec. (2011) 14:31–38
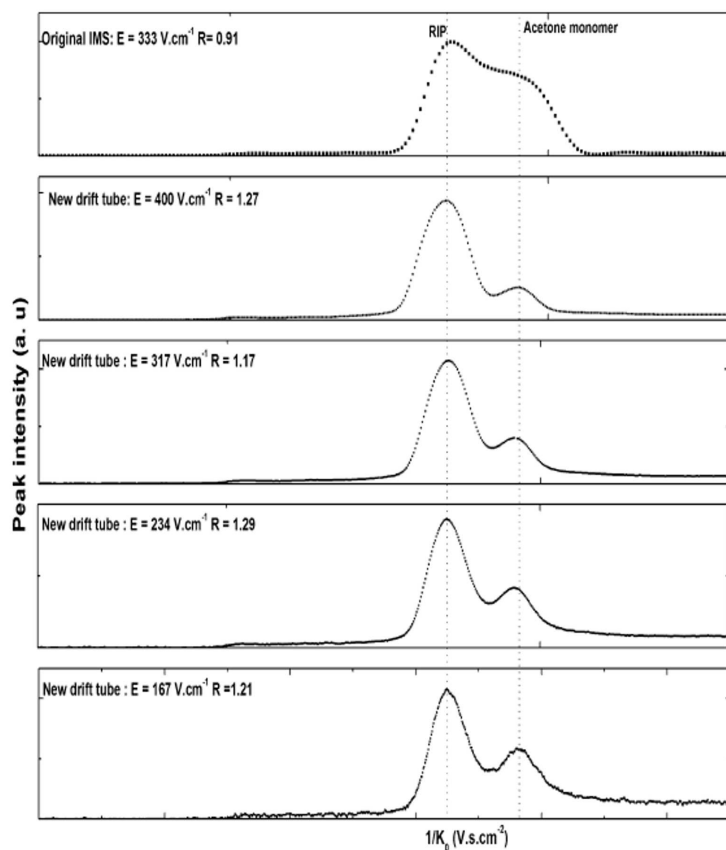
out. It is seen from Fig. 3 that the FWHM reaches a minimum (~0.53 ms) with increasing electric field for the instrument depending on the other parameters of the instrument such as the opening time of the shutter grid, response time of the pre-amplifier which remained unaltered in the new drift tube. This also depends on other factors such as broadening by Coulomb repulsion between the ions in both the reaction region and the drift channel, ion-molecule and ion-ion interactions in the drift region, gate depletion, spatial broadening by diffusion of the ion packet during the drift temperature and pressure inhomogeneities within the spectrometer and capacitive cooling between the aperture grid and the collector [20, 21].

This is mathematically derived [22] from Eq. 6 as

$$R_d \equiv \lim R\left(\frac{t_g}{t_D}\right) \to 0 = \sqrt{\frac{Vez}{16kT\ln 2}} = 0.3\sqrt{\left(\frac{Vez}{kT}\right)} \quad (7)$$

With over 200 analytes in the database with their retentions times through the MCC and their characteristic drift time, represented as $1/K_0$, to aid us identify analytes in any chromatogram, any change in the drift length would alter the database completely. But representation of drift time using $1/K_0$ for the ions in the drift channel negates this problem as the RIP is kept constant at one particular $1/K_0$ (0.4854 V.s.cm^{-2} for synthetic air and 0.4950 V.s.cm^{-2} for nitrogen) and the scale thereby calibrated which makes all the analytes retain the same $1/K_0$ though they have different drift times at various drift lengths [23].

In the next part of the study analytes usually detected in human breath and which tend to form clusters with other peaks were measured at the longest possible drift length at various voltages to find out the resolution.

Acetone (CAS Number 67-64-1), a substance commonly found in human breath in various health conditions, was our first substance of interest. The levels of acetone in a person's breath vary depending on their health condition and hence it is very important to quantify acetone found in the breath [18, 24]. The measurements carried out with the new drift tube at various electric fields are shown in Fig. 4.

Figure 4 shows that the cluster usually seen between the RIP and the monomer peak of acetone has been resolved at longer drift lengths. The resolution between the two peaks is shown besides each spectrum and the maximum resolution is at $E=234$ V.cm^{-1}. It should also be noted that the abscissa which represents $1/K_0$ has not changed for the different voltages as mentioned above, thus aiding in the retention of the existing database of substances to identify peaks in the chromatogram.

The next set of analytes used in this study was the dimer peaks of 2-Heptanone (CAS Number 110-43-0) and 4-Heptanone (CAS Number 123-19-3). The two analytes are substances in human breath that are 'signs of

Fig. 5 Dimer peaks of 2-Heptanone and 4-Heptanone comparison with a the initial IMS and b with longer drift length
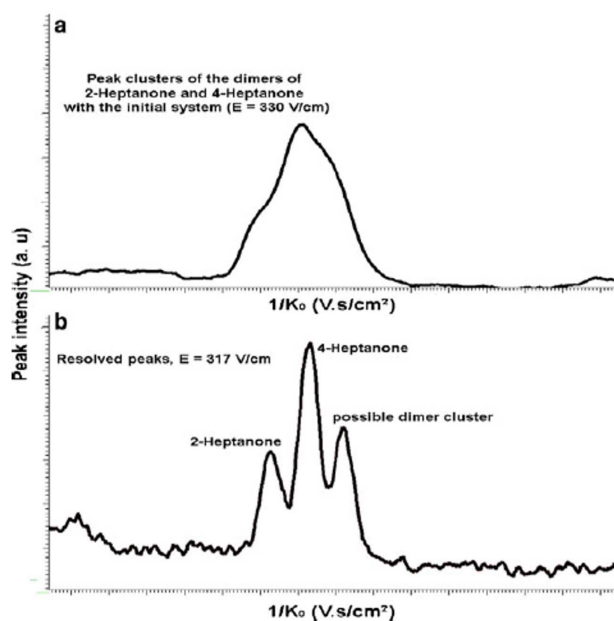
life' which help in locating trapped people. The analytes are also reported to be seen in urine samples [25, 26]. They are also used as chemical markers in petroleum products and markers for valproic acid therapy [27]. When a mixture of 2-Heptanone and 4-Heptanone is measured with the original IMS, the dimers of the two substances form a cluster which makes the identification of the two peaks almost impossible, Fig. 5a. Hence with a longer drift length but with similar electric fields, the substances were measure and the spectrum is shown in Fig. 5b.

Figure 5 shows that the peak cluster seen when a mixture of 2-Heptanone and 4-Heptanone is measured with the old IMS Fig. 5a is clearly resolved with the longer drift tube, Fig. 5b. A third peak which could be a dimer cluster of one of the analytes is also seen in the spectrum.

Conclusions

Ion mobility spectrometry, a method time tested for its sensitivity, ruggedness, reproducibility, low costs and functionality at normal temperature and pressure conditions, has established a very strong foothold in the field of medical and biological applications over the past decade. Many clinics have started using this method for breath analysis to identify markers of various health conditions and particular diseases. The requirement of a database with the mobility and retention time data to identify the peaks detected during the measurement is probably its biggest disadvantage. This gives researchers less degree of freedom to optimise the instrument as the whole database needs a makeover every time measurement parameters are changed. Changes incorporated to the pre-separation would increase the measurement time which negates the possibility of real time data acquisition.

In this study we have shown the effects of drift length and voltage changes to resolve peak clusters without altering the database by using $1/K_0$ to represent ion mobility rather than drift time. The drift tube constructed can be varied in length depending on the complexity of the substance measured and a suitable voltage supply thus being applied. The stability of drift section made up of small drift pieces, as shown in this study, could be used in research to effectively resolve clusters with a higher resolution.

Acetone is detected in every human breath at various concentration levels depending on the health condition of the subject. It is therefore very important to know the exact concentration of acetone in the human breath for any diagnosis. The monomer peak which is usually clustered with the RIP obtained when using synthetic air is resolved by using the longer drift tube. This helps us in knowing the exact intensity of the peak of acetone, hence the concen-

tration of acetone in the sample matrix to aid the correct diagnosis. Similarly, the dimer peaks of 2-Heptanone and 4-Heptanone have also been resolved and after resolution we also see a third unknown peak which could possibly be a cluster of the two substances together.

The first studies carried out in this article are just the onset of a new generation of drift tubes with variable lengths in ion mobility spectrometry. These drift tubes can be used in clinics where human breath is being measured and analysed for a multitude of markers for various diseases by tuning the drift tube suitably for the particular marker being searched for rather than having many different drift tubes/IMS for various health conditions. Further studies regarding the sensitivity of this high resolution instrument with change in drift lengths, water molecule fragments and clusters due to change in drift lengths and variation in peak parameters at constant electric fields by varying the voltage supply and length are areas which have to be studied more thoroughly to establish these drift tubes for high resolution ion mobility spectrometry in medical and biological applications.

References

1. Langevin P (1905) Une formule fondamentale de théorie cinétique. Ann de Chim et de Phys 5:245–288
2. Cohen MJ, Karasek FW (1970) Plasma chromatography—a new dimension for gas chromatography and mass spectrometry. J Chromatogr Sci 8:330–337
3. Stach J, Baumbach JI (2002) Ion mobility spectrometry—Basic elements and applications. Int J Ion Mobil Spectrom 5(1):1–21
4. Louis RH, Hill HH (1990) Ion mobility spectrometry in analytical chemistry. Crit Rev Anal Chem 21(5):321–355
5. Eiceman GA, Karpas Z (2005) Ion Mobility Spectrometry. Taylor and Francis, 2005
6. Westhoff M, Litterst P, Freitag L, Urfer W, Bader S, Baumbach JI (2009) Ion mobility spectrometry for the detection of volatile organic compounds in exhaled breath of patients with lung cancer: results of a pilot study. Thorax 64:744–748
7. Vautz W, Nolte J, Bufe A, Baumbach J, Peters M (2010) Analysis of mice's breath using gas chromatography ion mobility spectrometry. J Appl Physiol 108:697–704
8. Prasad S, Pierce K, Schmidt H, Rao J, Güth R, Bader S, Synovec R, Smith GB, Eiceman GA (2007) Analysis of bacteria by pyrolysis gas chromatography—differential mobility spectrometry and isolation of chemical components with a dependence on growth temperature. Analyst 132:1031–1039

9. Vautz W, Carstens ETH, Hirn A, Quintel M, Nolte J, Jünger M, Perl T (2010) Online determination of Plasma Propofol concentrations by expired air analysis. Int J Ion Mobil Spectrom 13 (1):37–40

10. Westhoff M, Ruzsanyi V, Litterst P, Freitag L, Baumbach JI (2007) Ion mobility spectrometry—a new method for the fast detection of Sarkoidose in human breath?—Preliminary results of a feasibility study. J Physiol Pharmacol 58(5):739–751

11. Vautz W, Baumbach JI (2008) Exemplar application of multi-capillary column ion mobility spectrometry for biological and medical purpose. Int J Ion Mobil Spectrom 11:35–41

12. Baumbach JI (2006) Process analysis using ion mobility spectrometry. Anal Bioanal Chem 384:1059–1070

13. Bödeker B, Vautz W, Baumbach JI (2008) Peak comparison in MCC/IMS—Data—Searching for potential biomarkers in human breath data. Int J Ion Mobil Spectrom 11:89–93

14. Tang K, Shvartsburg AA, Lee H, Prior D, Buschbach M, Li F, Tolmachev A, Anderson G, Smith RD (2005) High-sensitivity ion mobility spectrometry/mass spectrometry using electrodynamic ion funnel interfaces. Anal Chem 77(10):3330–3339

15. Siems WF, Wu C, Tarver E, Hill HH (1994) Measuring the resolving power of ion mobility spectrometers. Anal Chem 66 (23):4195–4201

16. Revercomb HE, Mason EA (1975) Theory of plasma chromatography/ gaseous electrophoresis—a review. Anal Chem 47(7):970–983

17. Asbury GR, Hill HH (2000) Evaluation of ultrahigh resolution ion mobility spectrometry as an analytical separation device in chromatographic terms. J Microcolumn Sep 12(3):172–178

18. Ruzsanyi V, Baumbach JI, Sielemann S, Litterst P, Westhoff M, Freitag L (2005) Detection of human metabolites using multi-capillary columns coupled to ion mobility spectrometers. J Chromatogr A 1084:145–151

19. Baumbach JI, Eiceman GA (1999) Ion mobility spectrometry: arriving on-site and moving beyond a low profile. Appl Spectrosc 53(9):338–355

20. Davis D, Harden C, Shoff D, Bell S, Eiceman G, Ewing R (1994) Analysis of ion mobility spectra for mixed vapours using Gaussian deconvolution. Anal Chim Acta 289:263–272

21. Dugourd Ph, Hudgins RR, Clemmer DE, Jarrold MF (1997) High resolution ion mobility measurements. Rev Sci Instrum 68 (2):1122–1129

22. Wu C, Siems W, Asbury R, Hill HH (1998) Electrospray ionisation high resolution ion mobility spectrometry-mass spectrometry. Anal Chem 70(23):4929–4938

23. Vautz W, Bödecker B, Bader S, Perl T (2009) An impeccable approach to obtain reproducible reduced ion mobilities. Int J Ion Mobil Spectrum 12(2):47–57

24. Deng C, Zhang J, Yu X, Zhang X (2004) Determination of acetone in human breath by gas chromatography-mass spectrometry and solid phase microextraction with on-fiber derivatization. J Chromatogr B 810(2):269–275

25. Statherropolous M, Sianos E, Agapiou A, Georgiadou A, Pappa A, Tzamtzis N, Giotaki H, Papageorgiou C, Kolostoumbis D (2005) Preliminary investigation of using volatile organic compounds from human expired air, blood and urine for locating entrapped people in earthquakes. J Chromatogr B 822:112–117

26. Smith S, Burden H, Persad R, Whittington K, de Lacy CB, Ratcliffe N, Probert C (2008) A comparative study of the analysis of human urine headspace using gas chromatography-mass spectrometry. J Breath Res 2(3):184–193

27. Erhart S, Amman A, Haberlandt E, Edlinger G, Schmid A, Filipiak W, Schwarz K, Mochalski P, Rostasy K, Karall D, Scholl S (2009) 3-Heptanone as a potential new marker for valporic acid therapy. J Breath Res 3(1):376–381

Chandrasekhara B, Hariharan

14-07-1984

Madurai, India

Curriculum Vitae

- since March 2012 - Post Doctoral research at Justus-Liebig Universität Giessen, Germany

- 2008-2012 - Ph.D research student at Leibniz-Institut für Analytische Wissenschaften - ISAS - e.V., Dortmund, Germany

- 2005-2008 - M.Sc. in Chemical Engineering, TU-Dortmund, Germany

- 2001-2005 - B.Tech. in Chemical Engineering, Anna University, Chennai, India

Conferences

- July 2011 - Invited speaker at the 20th International Society for Ion Mobility Spectrometry, *Implementation of MCC-IMS for medical and biological applications*, Edinburgh, UK

- October 2010 - Invited speaker at the International Breath Conference, *Recent advances with ion mobility spectrometry for medical and biological applications*, Barga, Italy

- July 2009 - Invited speaker at the 18th International Society for Ion Mobility Spectrometry, *Empirical prediction of reduced ion mobilities,* Thun, Switzerland

Personal details

- Nationality - Indian

- Languages - English (native) , German (fluent)

- Email - hariharan.cb@googlemail.com